THE UNIVERSITY
of EDINBURGH

The Redox Chemistry of Perrhenate and Other Anions

Danny S. Morris

Submitted for the degree of Doctor of Philosophy

The University of Edinburgh

2016

Declaration

The work described in this thesis is entirely my own, except where I have either acknowledged help from a named person or given reference to a published source. Text taken from another source will be enclosed in quotation marks and a reference given. This thesis has not been submitted, in whole or in part, for any other degree.

Signature:

Date:

Abstract

This thesis discusses reduction and oxidation reactions catalysed by the perrhenate anion and oxidation reactions catalysed by other oxo-anions i.e. sulfate and nitrate.

Chapter one introduces catalytic hydrosilylation, hydroboration, deoxydehydration and alkene epoxidation and some of their applications, with a focus on high oxidation state complexes.

Chapter two describes the synthesis of a salt of perrhenate $[N(hexyl)_4][ReO_4]$ which is highly soluble in organic solvents. The use of this salt as a catalyst for both the hydrosilylation and hydroboration of carbonyl compounds and carbon dioxide is discussed. Catalytic methylation of amines and anilines with carbon dioxide and hydrosilanes is also reported. Labelled carbon dioxide reactions and DFT calculations are conducted in order to understand the mechanism of carbon dioxide reduction using hydrosilanes.

Chapter three outlines the synthesis of a number of alkylammonium and pyridinium perrhenate salts and their application in the deoxydehydration reaction, converting vicinal diols to alkenes. The role of the counterion is discussed with pyridinium perrhenates shown to be more effective catalysts. DFT calculations are conducted to identify the most likely pathway of the catalytic cycle. Alternative reducing agents to the triphenylphosphine initially used are also studied.

Chapter four reports results of organic salts of perrhenate, sulfate and nitrate as oxidation catalysts, specifically their ability to catalyse epoxidations of alkenes. By the formation of supramolecular ion pairs (SIPs), these anions are made organic soluble which is found to significantly enhance their catalytic ability, however, the organic counterions used to form these SIPs were found to be of importance. Ionic liquids are also used for the epoxidation of alkenes. Solution studies are presented to further understanding of how these compounds interact with one another in solution.

Chapter five contains experimental conditions and characterisation for compounds discussed in this work.

Lay Summary

In our work we have shown that relatively simple compounds (perrhenate, nitrate and sulfate) act as catalysts that are capable of assisting conversion of chemicals which are abundant but with limited use, into more widely useful chemicals. For example, perrhenate can catalyse the conversion of carbon dioxide into methanol and other useful chemicals such as methylamines. The method through which this occurs is unusual for the class of chemicals to which perrhenate belongs (high oxidation state oxo compounds) and so experimental and theoretical methods were used to understand the mechanism behind these reactions. However, the significant advantages to using perrhenate for these reactions include its stability to air and water which many catalysts for these reactions cannot claim.

Perrhenate is also found to catalyse a reaction that can convert sugars into alkenes, which are an important and highly useful class of chemicals. Using model compounds rather than sugars, acids were shown to enhance this reaction and the specific source of acid was also found to be important; experimental and computational methods were also used to understand these reactions.

Additionally perrhenate is a stable catalyst for the epoxidation of alkenes, a method for converting alkenes into more useful, value-added compounds. Pleasingly, the catalyst can be recycled without loss of activity in contrast to a similar catalyst which decomposes during the reaction. In order to address the high cost of rhenium catalysts, nitrate and sulfate were used in an attempt to replace perrhenate and while not as active, did show moderate success.

Acknowledgements

I would like to thank my supervisor Jason Love for his keen interest, encouragement and guidance whilst working on this project.

Thank you to Mr. Juraj Bella, Dr. Lorna Murray, Dr. Logan Mackay and Dr. David Rogers who have all generously spent their time helping me throughout my studies.

And the Love and Arnold groups who have been fantastic to work with over the last few years and helped me get through it all with plenty of tea and chat.

Also thanks to my family and friends who have always encouraged and supported me through this.

Table of Contents

1. Introduction

The chemistry of high oxidation state metal-oxo complexes has often been strongly associated with oxidation chemistry such as oxygen transfer catalysis. Recently this has started to change with a number of reports describing the reduction chemistry of this group of compounds, notably hydrosilylation/hydroboration reactions[1] and the deoxydehydration (DODH) of vicinal diols.[2] These new methods for H-X (X = Si, B) activation were encouragingly described as a breakthrough into a new class of catalysts,[3] whereas the DODH reaction appears a promising method for the conversion of biomass into chemical feedstocks. The search for efficient oxidation catalysts using environmentally benign oxidising agents is also still on going.[4] This introduction aims to briefly describe the catalytic reactions that have been investigated in this thesis.

Hydrosilylation

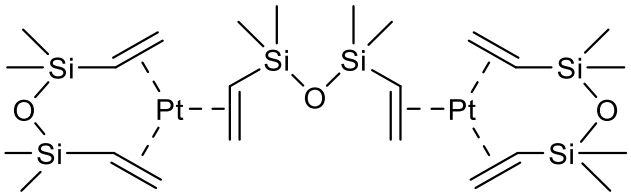

Figure 1 Karstedt's catalyst.

Amongst the first successful applications of the hydrosilylation reaction was shown by Speier with the catalyst chloroplatinic acid $[H_2PtCl_6]\cdot(H_2O)_6$ adding hydrosilanes across alkenes at very low catalyst loadings.[5] The $[H_2PtCl_6]\cdot(H_2O)_6$ has been shown to be reduced to Pt^0 and form colloids, suggesting this is the active catalyst with studies showing an induction period is present in reactions and transmission electron microscopy revealing these colloids present after a typical reaction.[6] However, studies on Karstedt's catalyst (Figure 1) showed that the colloids are produced by the deactivation of the catalyst in the presence of excess hydrosilane and the active species is monomeric two-coordinate Pt^0 complex.[7] The Chalk-Harrod mechanism[8] is outlined in Scheme 1 which shows that a Pd^0 complex undergoes oxidative addition with a hydrosilane, providing the Pt^{II} hydride. An η^2-coordinated alkene can subsequently insert into the metal hydride followed by reductive elimination of the silylalkane product.

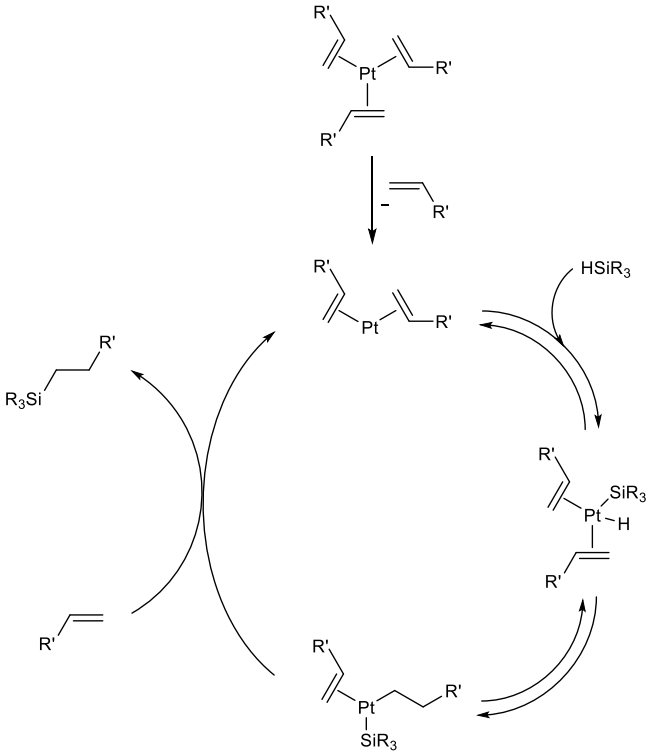

Scheme 1 Chalk-Harrod mechanism for the hydrosilylation of alkenes.

Hydrosilylation of carbonyl compounds with catalysts such as $NiCl_2$, $ZnCl_2$ or chloroplatinic acid required harsh conditions and produce byproducts.[9] For example, $ZnCl_2$ produces the silyl enol ether as a minor product and with aldehydes causes disproportionation of the product to a siloxane and ether.[10] Yet hydrosilylation was achieved using Wilkinson's catalyst [$RhCl(Ph_3P)_3$] by Nahai.[11, 12] Using catalyst loadings of between 0.1-1.0 mol %, a range of aliphatic and aromatic aldehydes and ketones were reduced to the silyl ether, often at room temperature with reaction times significantly less than 1 h. Interestingly, the analogous iridium complex undergoes irreversible oxidative addition of hydrosilanes[13] so in order to overcome this the alkene complex [$(Cyclooctene)_2IrCl$] was used in the presence of one equivalent of triphenylphosphine. If two equivalents of triphenylphosphine were used a catalytically inactive complex [$IrHCl(SiR_3)(PPh_3)_2$] was produced. Copper complexes have been shown to catalyse this reaction including $[CuH(PPh_3)]_6$ and Cu(I)Cl in the presence of bidentate phosphine ligands such as 1,2-bis(diphenylphosphino)benzene.[14, 15] However, many of the catalysts used for the hydrosilylation of carbonyl compounds tend to be low oxidation state and coodinatively unsaturated. Furthermore, these compounds are frequently air sensitive. Therefore, the report from Toste that the air

stable rhenium (V) complex $[ReI(O)_2(PPh_3)_2]$ catalyses the hydrosilylation of aldehydes and ketones was unprecedented.[16]

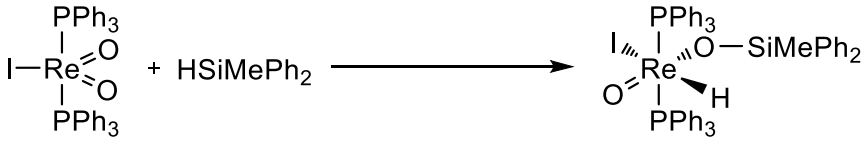

Scheme 2 Synthesis of the rhenium hydride complex $[ReHI(O)(OSiMePh_2)(PPh_2)_2]$ from $[ReI(O)_2(Ph_3P)_2]$.

$[ReI(O)_2(PPh_3)_2]$ was shown to be capable of activating the Si-H bond of $HSiMe_2Ph$ by adding the silane across one of the rhenium-oxo bonds, forming a stable rhenium (V) hydride (Scheme 2). Additionally a crystal structure of the hydride species synthesised with $HSiMePh_2$ was presented. Using catalytic quantities of $[ReI(O)_2(PPh_3)_2]$ allowed conversion of a variety of aldehydes and ketones and exhibited excellent tolerance of their functional groups. Wu and coworkers studied this system by density functional theory (DFT) calculations and agreed that a [2+2] addition of the hydrosilane was likely and further elucidated the steps of the catalytic cycle showing dissociation of one of the triphenylphosphine ligands as an initial step was favourable as it reduced steric repulsion between the two triphenylphosphine grousp and allowed coordination of the carbonyl compound (Scheme 3).[17]

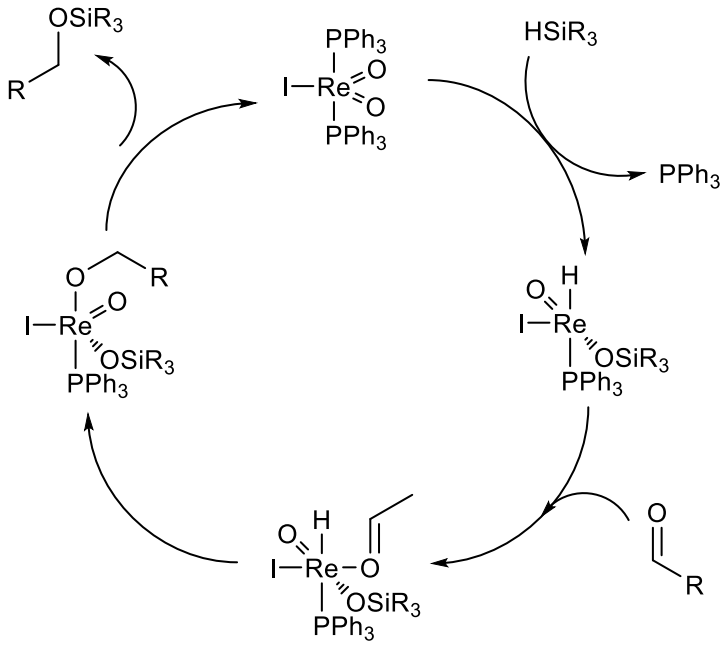

Scheme 3 Representitative scheme for the hydrosilylation of an aldehyde using $[ReI(O)_2(PPh_3)_2]$.[17]

Abu-Omar, soon after, described a rhenium (V) mono-oxo complex [ReO(hoz)$_2$][TFPB] (hoz = 2-(2′-hydroxyphenyl)-2-oxazoline(-), TFPB = tetrakis(pentafluorophenyl)borate) that was also capable of catalysing the hydrosilylation of carbonyl compounds, yet it appeared that the mechanism through which this occurred did not include a similar [2+2] addition across the rhenium-oxo bond.[18] If the stoichiometric reaction between hydrosilane and [ReO(hoz)$_2$][TFPB] is carried out, the rhenium complex is reduced to a catalytically inactive rhenium (III) complex [Re(hoz)$_2$][TFPB] with concurrent production of hydrogen and the siloxane.[19] The hydride species [ReO(hoz)$_2$H] was synthesised but shown to be a poor hydride source, approximately 70 times poorer than HSiEt$_3$. Therefore the proposed mechanism proceeded through an ionic pathway where the carbonyl compound reacts with an η^2-silane complex to afford the silylium adduct and a rhenium hydride, followed by abstraction of the hydride to provide the protected alcohol.

Mechanistic studies of rhenium oxo, imido and nitrodo complexes also found that direct involvement of the multiply bonded ligand was unlikely and investigations were consistent with an ionic mechanism as with [Re(hoz)$_2$][TFPB].[20] A number of complexes, such as the imido hydride complex, were observed during catalysis yet independent kinetic measurements for these species did not match those measured for the reaction using the parent compound. DFT calculations on related complexes also supported the ionic mechanism with the formation of an η^1-silane complex that the carbonyl compound can attack (in a backside manner) to give the silylium adduct and metal hydride products (Scheme 4).[21]

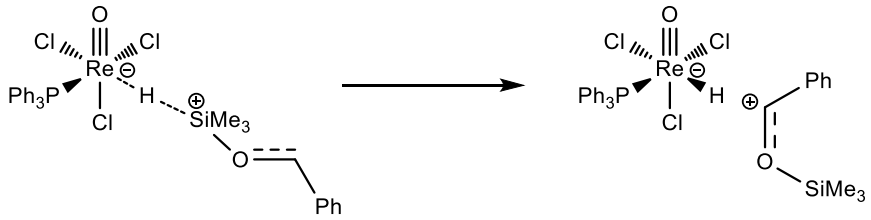

Scheme 4 Ionic activation of HSiMe$_3$ by [ReH(O)(Cl)$_3$(PPh$_3$)$_2$] and subsequent formation of the silylium adduct and metal hydride.[21]

Soon after the first report of rhenium-oxo catalysed hydrosilylation reactions, other metal-oxo complexes were also shown capable of this chemistry such as [MoO$_2$Cl$_2$].[22] Unlike the above examples, stoichiometric reaction of the catalyst with a hydrosilane

did not yield an isolable hydride and therefore the role the metal-oxo bond plays (if any) in the activation of the Si-H bond is unclear. DFT studies by Drees and Strassner showed the [2+2] addition of the silane to be much more favourable than the [2+3] addition with an activation energy of 35.8 kcal mol^{-1} compared with 46.7 kcal mol^{-1}.[23] Yet recently, Wei and co-workers have studied the ionic pathway by DFT calculations and showed the [2+2] addition of $HSiMe_3$ to $[Mo(O)_2Cl_2]$ is 29.0 kcal mol^{-1} whereas the free energy for the formation of a silane adduct is only 7.6 kcal mol^{-1} and nucleophilic attack by the substrate (an imine in this study) has an activation energy of 21.4 kcal mol^{-1} in comparison with 30.7 kcal mol^{-1} for the [2+2] mechanism.[24] Such a mechanism may explain the lack of experimental evidence for a hydride intermediate.

As briefly mentioned above, imines are also reduced using $[Mo(O)_2Cl_2]$ as are esters, amides and sulfoxides.[1] Rhenium-oxo catalysts are also capable of reducing imines and sulfoxides and in an interesting parallel to $[Mo(O)_2Cl_2]$ the simple rhenium compounds $[HReO_4]$[25] and $[Re_2O_7]$[26] were found to be the most active catalysts for the hydrosilylation of aldehydes when compared to other rhenium-oxo compounds including $[MeReO_3]$ (MTO), $[CpReO_3]$ and $[Re(O)Cl_3(PPh_3)_2]$, giving high yields of the silyl ethers in a few minutes and whilst $[Re_2O_7]$ showed no activity for ketones; $[HReO_4]$ showed similarly high yields for ketone substrates. But perhaps more interestingly $[ReI(O)_2(PPh_3)_2]$ was also shown to be able to hydrogenate alkenes to the alkane when heated at 45 °C with four equivalents of neat $HSiMe_2Ph$, giving full conversion after 20 h (Scheme 5).[27]

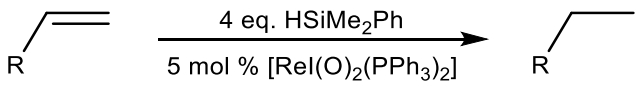

Scheme 5 Hydrogenation of an alkene with $[ReI(O)_2(PPh_3)_2]$ and $HSiMe_2Ph$.[27]

The use of hydroboranes was also shown to be effective with high oxidation state oxo complexes. Soon after the use of $[ReI(O)_2(PPh_3)_2]$ as a hydrosilylation catalyst, it was also shown to reduce sulfoxides using catecholborane (HBcat) with 4-chlorophenyl sulfoxide reduced to 4-chlorophenyl sulfide quantitatively after 1.5 h at room temperature.[28] Crystal structures were reported for the hydride species formed by the reaction of $[ReI(O)_2(PPh_3)_2]$ with both HBcat (Scheme 6) and pinacolborane (HBpin) which were analogous to the hydride formed by the reaction with $HSiMe_2Ph$.

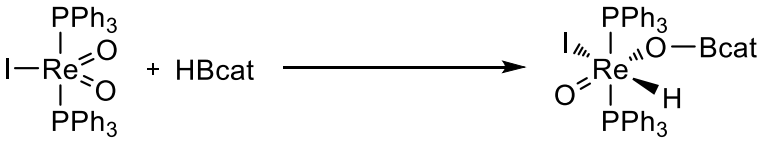

Scheme 6 Synthesis of the rhenium hydride complex [ReHI(O)(Bcat)(PPh_2)$_2$] from [ReI(O)$_2$(Ph_3P)$_2$].

CO_2 Reduction by Hydrosilanes

Utilisation of CO_2 is desirable as it is an inexpensive, plentiful, non-toxic and non-flammable C_1 carbon source. Whilst the reduction of CO_2 with H_2 is a difficult process often requiring high pressures, the use of hydrosilanes and hydroboranes offers a milder method for its conversion.[29, 30] A variety of useful chemicals can be synthesised from this method including formic acid, formaldehyde and methanol.

$RuCl_3{\cdot}(H_2O)_n$ was studied using HSi(hexyl)$_3$ and $HSiMe_2Ph$ as reducing agents in acetonitrile by Pitter and coworkers.[31] After *in situ* conversion to the ionic salt [RuCl(MeCN)$_5$][$RuCl_4$(MeCN)$_2$], the hydrosilylation of CO_2 was catalysed producing the silylformates in high yields. Studies on the related species [$RuCl_2$(MeCN)$_4$] showed that the presence of the chlorosilane $ClSiMe_2Ph$ promoted the reaction. It is present during reactions from the *in situ* reduction of [$RuCl_3$(MeCN)$_3$] with the hydrosilane but there is a clear promoting effect when added to reactions where [$RuCl_2$(MeCN)$_4$] is used and no further reduction is required to generate the active catalyst.[32]

DFT calculation on the mechanism show that rather than adding to the ruthenium centre through oxidative addition, the activation of the Si-H bond produces a weakly bound chlorosilane ligand and the ruthenium hydride (Scheme 7).[32] As this ligand is only weakly bound, a resting state produced from the substitution of the chlorosilane with acetonitrile and therefore the promoting effect of the chlorosilane is rationalised by its ability to reactivate the resting state. Analogous compounds with bromide ligands proved to be poorer catalysts with calculations showing higher activation energies for the bromosilane ligand and transfer of the silane onto CO_2.

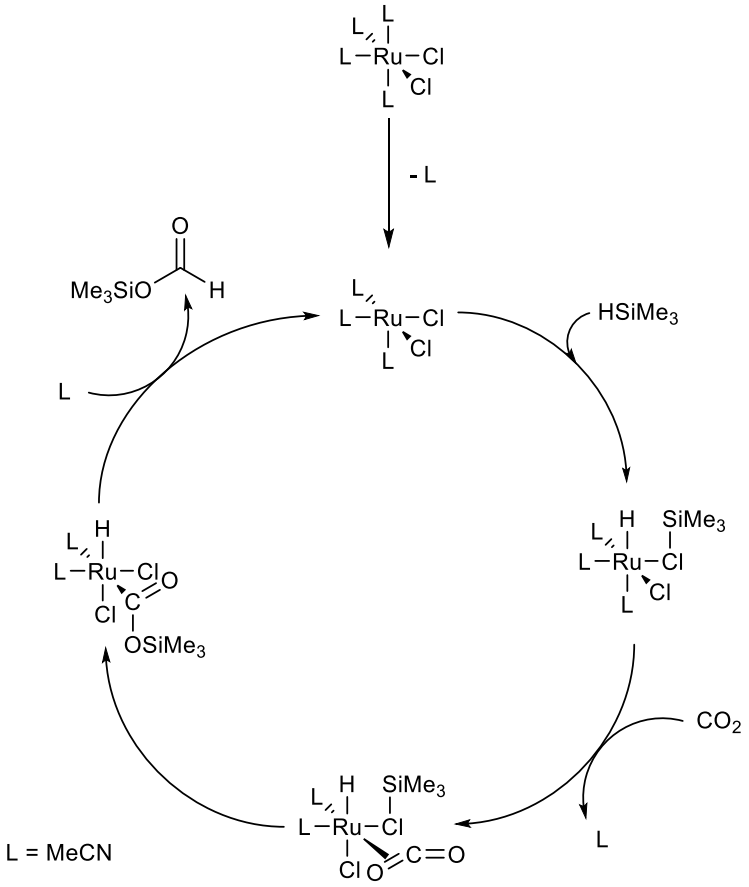

Scheme 7 Hydrosilylation of CO_2 with $HSiMe_3$ catalysed by $[RuCl_2(MeCN)_4]$ proposed by DFT calculations.[32]

The iridium complex [Ir(CN)(CO)dppe] (dppe = (1,2-bis(diphenylphosphino)ethane) was shown to slowly convert silanes such as $HSiMe_3$ to the formate $HC(O)OSiMe_3$ (Scheme 8) which was observed in the ^1H NMR spectrum after 1 d at 40 °C; $[IrH(CO)_2dppe]$ and $[Ir(H)_2(CN)(CO)dppe]$ were identified as the major hydride complexes present.[33] Whilst this reaction is reversible with equilibrium reached after 7 d at 60 °C, further heating at 40 °C saw reduction of the formate products to the acetal and after 14 d significant production of the methoxide product $MeOSiMe_3$ was observed. The secondary silane H_2SiMe_2 gave quicker conversion to silylacetal products after 1 d at 40 °C and as with $HSiMe_3$ further heating gave methoxide products.

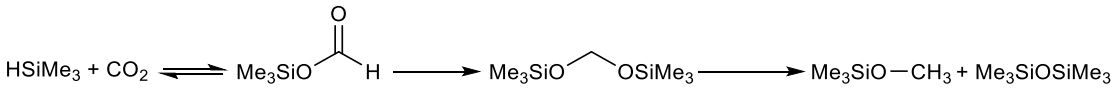

Scheme 8 Reversible formation of the silyl formate with $HSiMe_3$ and subsequent reduction to the methoxysilyl product.

More selective iridium complexes have been subsequently reported, for example [Ir(SiMe{OSiMe$_2$}$_2$)(CF$_3$SO$_3$)(NSiN)(CH$_3$CN)] (NSiN = bis(pyridine-2-yloxy)methylsilyl) enables solvent free conversion of the silane HSiMe(OSiMe$_3$)$_2$ with 90 % selectivity for the formate after 6 d at room temperature under modest pressures of CO_2 (3-8 bar).[34] Using the precursor to this catalyst, [IrH(CF$_3$SO$_3$)(NSiN)COE], as a precatalyst similar yields of the silylformate were obtained yet the siloxane byproduct O(SiMe{OSiMe$_3$}$_2$) was also produced in 10-15 % yields.[35] Reactions conducted in toluene-d_8 also show this byproduct as well as traces of the methoxide CH$_3$OSi(OSiMe$_3$)$_2$. DFT calculations on [Ir(SiMe{OSiMe$_2$}$_2$)(CF$_3$SO$_3$)(NSiN)(CH$_3$CN)] show the most favourable pathway proceeds through initial dissociation of acetonitrile and η^2-silane coordination to the iridium centre (Scheme 9). Similarly to the ruthenium chloride catalysts, transfer of silyl group onto the triflate ligand and hydrogen onto the iridium forms a hydride complex to which CO_2 approaches and in one step transfers both the hydride and silyl group onto the carbon and oxygen respectively.[34]

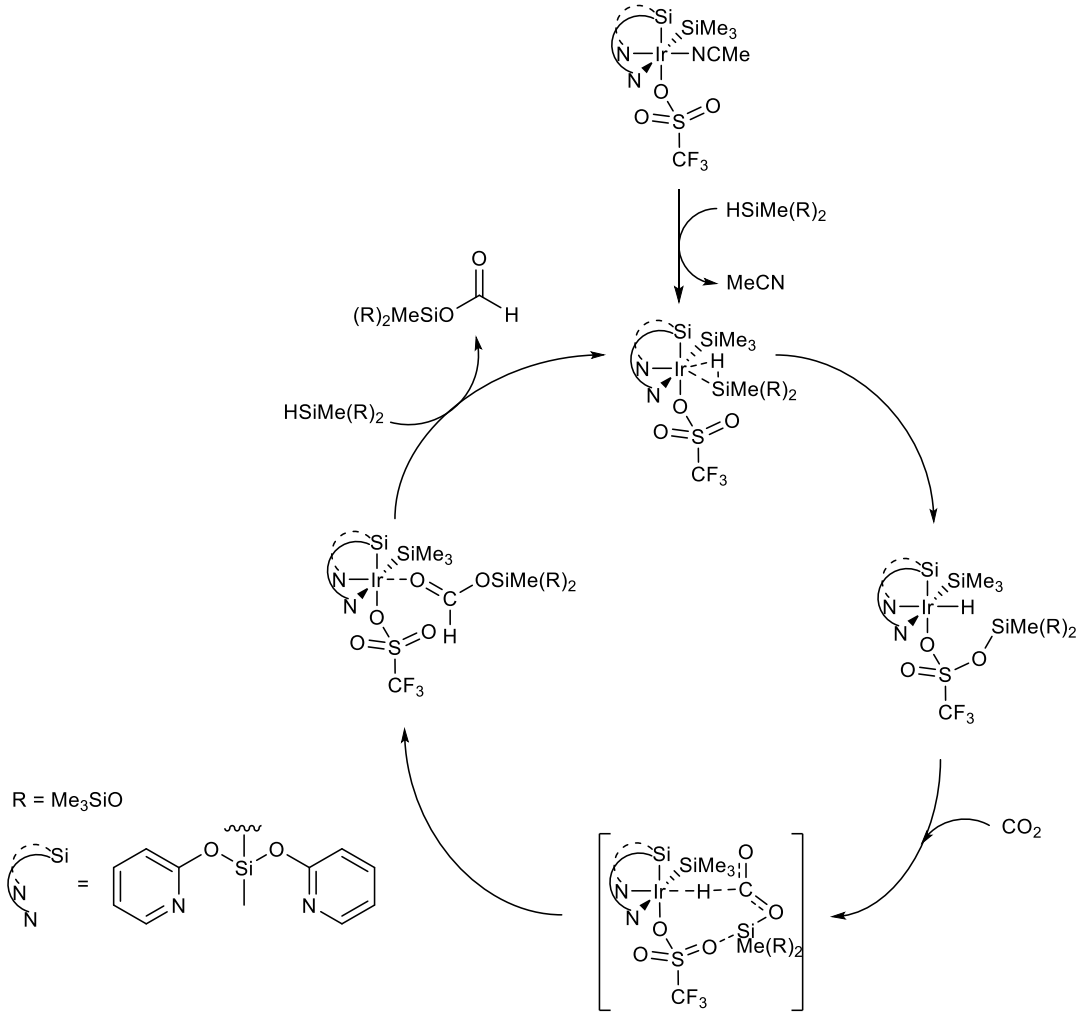

Scheme 9 Mechanism for the hydrosilylation of CO_2 with $HSiMe(OMe)_2$ and $[IrH(CF_3SO_3)(NSiN)COE]$, based on intermediates and transition states from DFT calculations.[34]

The rhenium hydride $[ReHBr(NO)(P^iPr_3)_2]$ does not react with CO_2 on its own but in the presence of $B(C_6F_5)_3$ the η^2-CO_2 adduct can be observed with the borane bound to the CO_2 unit.[36] This dimerises in solution to give the poorly soluble $[\{Re(\mu\text{-}Br)(NO)(\eta^1\text{-}OCH{=}O\text{-}B(C_6F_5)_3)(P^iPr_3)_2\}_2]$ but the μ-Br ligands can easily be split by placing under 1 bar of H_2 at 60 °C giving the compressed dihydride $[ReBrH_2(NO)(\eta^1\text{-}OCH{=}O\text{-}B(C_6F_5)_3)(P^iPr_3)_2]$, where the hydride ligands resemble an extreme elongation of a dihydrogen ligand but are essentially non-bonding (Scheme 10). Both the dimer and its hydrogen complex were competent catalysts for the hydrosilylation of CO_2 with $HSiEt_3$ at 80 °C to the acetal in 87 % and 89 % yields respectively, with only traces of the methoxide product. From stoichiometric reactions it was suggested that replacement of the coordinated $B(C_6F_5)_3$ with $[SiEt_3]^+$ (and formation of

$[HB(C_6F_5)_3]^-$ weakens the formate ligand's rhenium-oxygen bond an allows further reaction with $HSiEt_3$ to give the acetal.

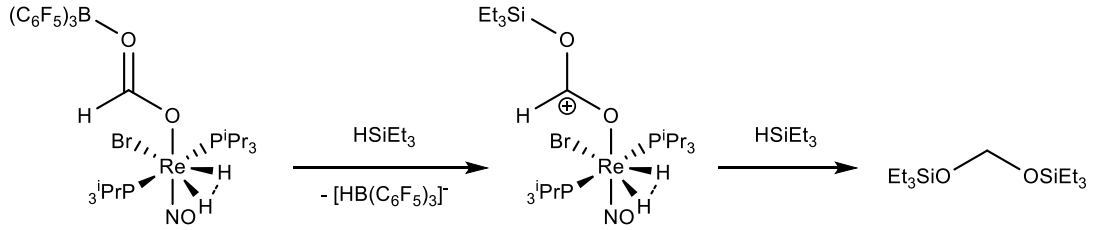

Scheme 10 Formation of the silylacetal from the stoichiometric reaction of $HSiEt_3$ with $[ReBrH_2(NO)(\eta^1\text{-}OCH{=}O\text{-}B(C_6F_5)_3)(P^iPr_3)_2]$. Ommited are two rhenium complexes observed in the product mixture.[36]

A related system using nickel bis(phosphino)boryl [Ni(PBP)H] (Scheme 11) reacts with CO_2 to give the formate ligated product yet no reaction with $HSiEt_3$ was observed at room temperature and heating resulted in decomposition of the complex.[37] Yet stoichiometric reactions showed by adding an equivalent of $B(C_6F_5)_3$ releative to the complex, full conversion of the silane occurred after 0.5 h at 70 °C giving exclusively the acetal product and a new complex [Ni(PBP)(OCHO)]. This new compound was a competent hydrosilylation catalyst with conversions of 91 % after 34 h at 70 °C with 0.1 mol % catalyst loading. In a further experiment, after the $^{13}CO_2$ substrate had largely been consumed, four equivalents of $B(C_6F_5)_3$ were added which caused quantitative conversion of the acetal to methane after an additional 3.75 h at 70 °C.

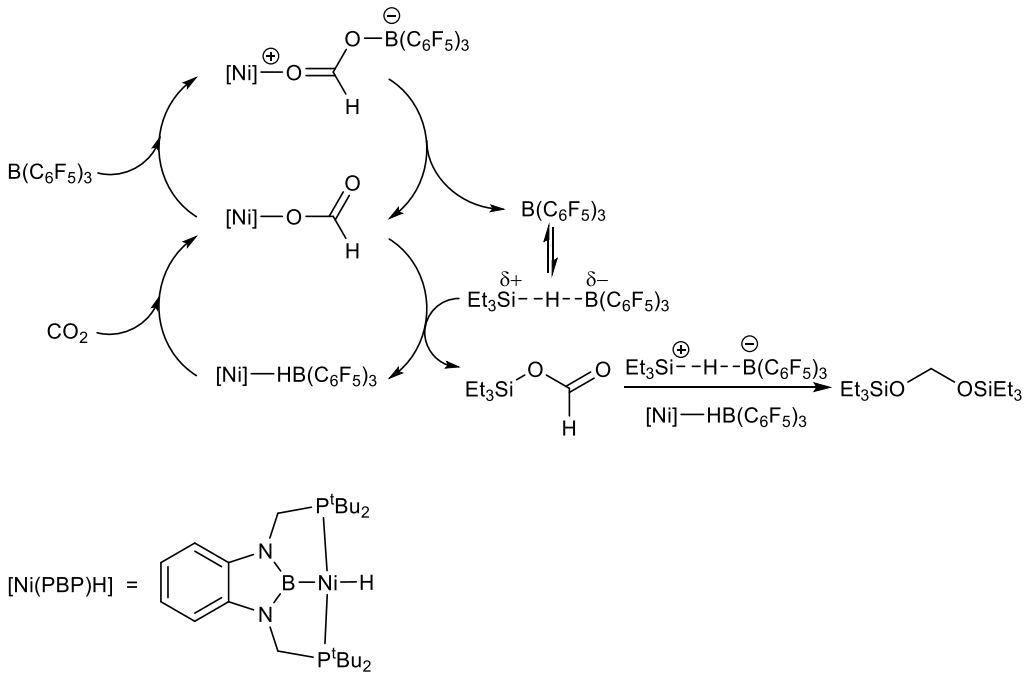

Scheme 11 Proposed mechanism for the selective hydrosilylation of CO_2 with $HSiEt_3$ to the silylacetal using the [Ni(PBP)(OCHO)] catalyst.[37]

CO_2 Reduction with Hydroboranes

Conversion of CO_2 to methoxyboryl species is also possible, with the first example from Guan and coworkers using a nickel PCP pincer complex [NiH(^{t}BuPCP)] (Scheme 12).[38] CO_2 underwent reversible insertion into the nickel-hydride bond to give a formate complex that reverted to the hydride when heated at 60 °C under vacuum. The hydride could also be reformed by the addition of one equivalent of catecholborane (HBcat) at room temperature which also produced the formoxyboryl HC(O)OBcat, with excess HBcat giving MeOBcat. This reaction was also successful using catalytic amounts of [NiH(^{t}BuPCP)] (0.2 mol %) under 1 bar CO_2, with 61 % yield of methanol after hydrolysis of the product. The reaction also formed $O(Bcat)_2$ as a byproduct.

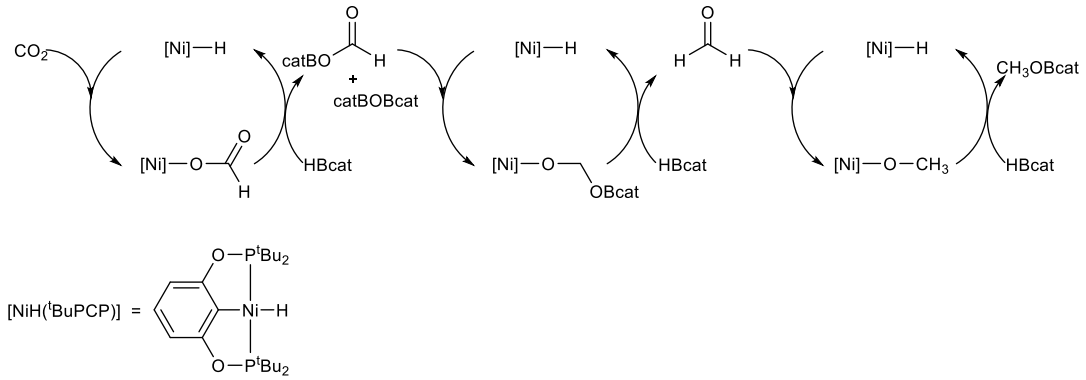

Scheme 12 Proposed catalytic cycle for the [NiH(^{t}BuPCP)] mediated reduction of CO_2 with HBcat to CH_3OBcat.[38]

Investigations into the mechanism by DFT calculations support the formation of HC(O)OBcat by the coordination of HBcat to the terminal formate oxygen and formation of a six-membered ring organised so the borane hydride transfers onto the nickel centre and releases HC(O)OBcat.[39] Reduction of this product to formaldehyde was shown to be energetically unfavourable unless mediated by the nickel catalyst with reduction by HBcat calculated to be +40.0 kcal mol^{-1}. Inserting HC(O)OBcat into a Ni-H bond was significantly lower at +27.6 kcal mol^{-1} and formed an ethoxide product [Ni]OCH_2OBcat that expelled formaldehyde to give the [Ni]OBcat complex (Scheme 13). Addition of another HBcat reformed the catalyst and produced the $O(Bcat)_2$ observed in experimental studies. Finally a similar process occurs for the reduction of formaldehyde with the initial formation of a nickel methoxy ligand [Ni]OMe after insertion into the Ni-H bond and then reformation of [Ni]H by addition of HBcat and expulsion of MeOBcat.

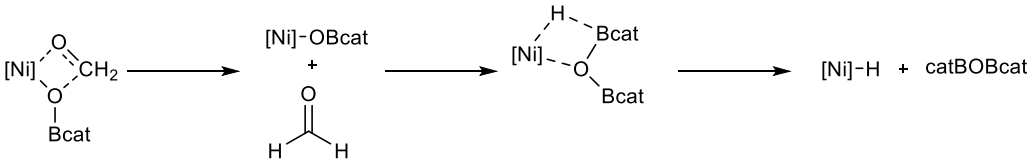

Scheme 13 Process through which formaldehyde and $O(Bcat)_2$ are produced.[39]

Bontemps and Sabo-Etienne reported the reduction of CO_2 with HBpin using a ruthenium polyhydride complex [$RuH_2(H)_2(PCy_3)_2$] to a variety of C_1 and C_2 compounds including the formate, acetal and methoxide products.[40] Whilst HBpin was fully consumed after 0.5 h at room temperature with 10 mol % catalyst loading, the true end point was after 22 d when only $O(Bpin)_2$ and MeOBpin were observed. Of particular interest was the formation of the unexpected $HC(O)OCH_2$OBpin, the first evidence of direct reductive coupling of two CO_2 units. By adding formaldehyde to

the mixture of products observed after consumption of HBpin, HC(O)OBpin was converted to $HC(O)OCH_2OBpin$.[41] This was also synthesised separately from HC(O)OBpin and formaldehyde in the absence of catalyst. These results show the origin of these C_2 compounds is from formaldehyde produced during the experiment and with an interest in trapping formaldehyde, CD_3OD was added which converted both $HC(O)OCH_2OBpin$ and the acetal $CH_2(OBpin)_2$ to CD_3OCH_2OD.

Deoxydehydration

The deoxydehydration (DODH) reaction converts vicinal diols to the corresponding alkene with the aid of a reducing agent.[2] This transformation is of current interest due to the search for new methods of generating useful chemicals, in particular the conversion of biomass to feedstocks. However, biomass such as sugars are highly oxygenated and require reduction of this oxygen content to be used as feedstocks or even fuels. One polyol that has become of interest of late is glycerol which, due to the increase in production of biofuels of which it is a byproduct, has been in over production since 1995.[42] With the wide variety of polyol substrates available including the waste product glycerol, the development of this transformation has recently become of significant interest.

Cook and Andrews reported the reduction of phenyl-1,2-ethanediol (styrene diol) to styrene with PPh_3 as the reducing agent and 2 mol % $[Re(Cp^*)O_3]$ as the catalyst (Scheme 14).[43] Initial reduction of the catalyst with PPh_3 to give $[Re(Cp^*)O_2]$ was proposed which allowed coordination of styrene diol with release of water to form the glycolate. This compound could then expel the alkene to reform the catalyst. However, they also suggested deactivation by over-reduction of the catalyst producing a Re^{III} compound. In efforts to combat this they found *p*-toluenesulfonic acid (pTSA) acted as a promoter, suggested to encourage the formation of the glycolate in order to prevent over reduction of the catalyst. Coordinating solvents had a detrimental effect, although with 22 mol % of pTSA this effect was minimised with a 91 % conversion of styrene diol after 13 h in THF, a solvent shown to give poor yields in the absence of pTSA. The sugar alcohol erithritol was also studied exhibiting 80 % yield of the diene and a combination of 2-butene-1,4-diol and 3-butene-1,2-diol after 28 h at 135 °C.

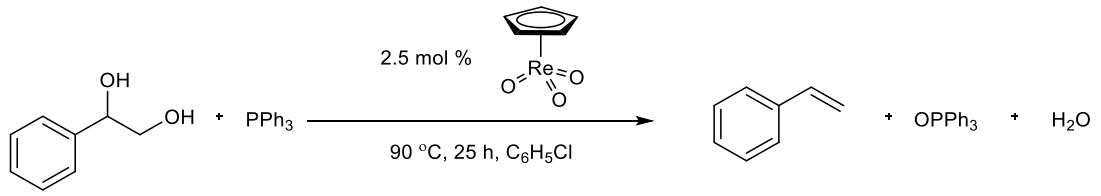

Scheme 14 DODH of styrene diol with [Cp*ReO_3].[43]

Gebbink subsequently reported the more sterically congested 1,2,4-tri(^{t}butyl)cyclopentadienyl (^{ttt}Cp) rhenium oxide complex [^{ttt}CpReO$_3$] which, under similar conditions to [Cp*ReO_3] catalyst discussed above, gave 99 % conversion of styrene diol after 40 h at 135 °C.[44] However the more "biomass-like" 1,2-octanediol was reduced to 1-octene after only 15 h with 94 % selectivity (Scheme 15). The catalyst also exhibited good stability with turnover numbers of 1400 observed for this reaction at 180 °C. Modification of the ^{ttt}Cp ring showed that the bulkier ^{i}Pr and ^{t}Bu substituted Cp ligands provided more selectively 1-octene with little isomerisation to cis- or trans-2-octene whereas peralkylated Cp ligands generally gave a much higher proportion of the isomers (19-29 % at 180 °C).[45] Reaction of 1-octene with [Cp*ReO_3] (2 mol %) showed isomerisation only in the presence of PPh_3, indicating the reduced rhenium species is responsible for observed isomerisation.

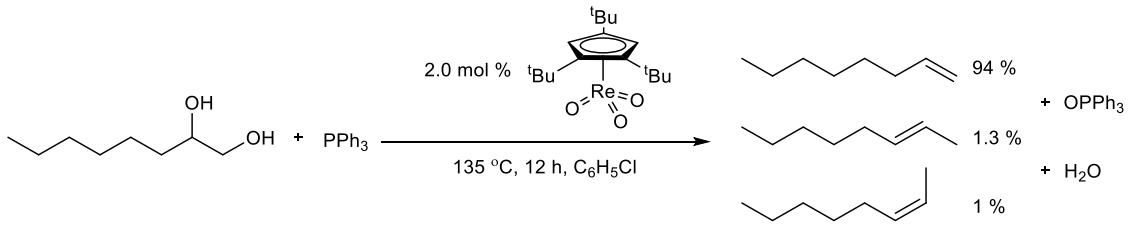

Scheme 15 DODH of 1,2-octandiol with PPh_3 and [^{ttt}CpReO$_3$] as the catalyst.[44]

As an alternative to the rhenium catalysts, the use of more economic metals has been explored. A vanadium dioxo complex [Bu_4N][VO_2(dipic)] (dipic = 2,6-pyridinedicarboxylate) was shown effective for the DODH of a number of diols using PPh_3 as the reductant.[46] Styrene diol was reduced to styrene using 10 mol % [Bu_4N][VO_2(dipic)] with 95 % yield at 150 °C in benzene. An increase in temperature to 170 °C yielded 87 % of 1-octene from 1,2-octanediol and 85 % *E*-diethyl fumarate from (+)-diethyl tartrate.

Recently this reaction has been studied by DFT calculations by both Galindo[47] and Fu.[48] Both authors note that triplet state intermediates provide a lower energy

pathway, however Galindo concluded that the reaction proceeds through initial reduction of $[VO_2(dipic)]^-$ with PPh_3, whereas Fu found the glycolate formation preferable. Fu identified an alternate mechanism for the extrustion of the alkene where for the triplet glycolate complex rather than the two C-O bonds cleaving in a concerted fashion, only one C-O bond cleaved to give a carbon radical that recoordinated to the vanadium centre after spin crossover to the singlet state. Concerted cleavage of the V-C/O-C bond then proceeds to eliminate the alkene (Scheme 16). The mechanisms also differ in that initial coordination and deprotonation of the diol is considerably more favourable in Fu's calculations (free energy of the transition state = +13.7 kcal mol^{-1}) than Galindo's (+39.8 kcal mol^{-1}). In both studies of this cycle (initial condensation) reduction of the vanadium glycolate with PPh_3 is the main rate determining step although much lower in Fu's study (+34.3 kcal mol^{-1}) than Galindo's (+52.8 kcal mol^{-1}), making the initial condensation route more plausible. While no transition state for the initial reduction of the catalyst was found by Fu, estimates were made that suggested it was significantly higher than condensation of the diol (~ +40 kcal mol^{-1}).

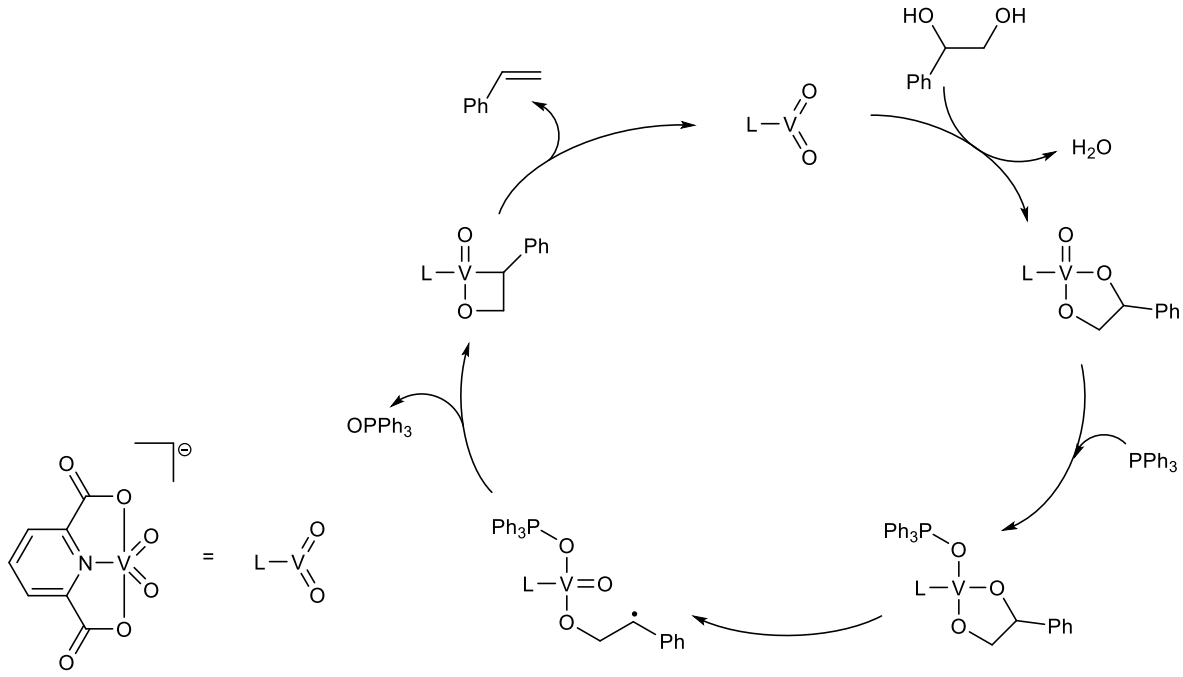

Scheme 16 Mechanism for the DODH of styrene with PPh_3 and $[V(O)_2dipic)]^-$ catalyst, based on Fu's DFT calculations.[48]

Seeking more economic metals for the DODH reaction is an important target, as is the use of economic and environmentally friendly reducing agents. Nicholas has pioneered the use of sodium sulfite as the reducing agent with a variety of rhenium-

oxo complexes.[49] MTO catalysed reactions (8 mol %) of a concentrated styrene diol solution in benzene afforded 59 % of styrene (90 % conversion) after 4 h at 150 °C, although small amounts of dimeric ethers were also identified in this reaction. Addition of 15-crown-5 and the higher boiling chlorobenzene to the heterogeneous reaction mixture sped the conversion of 1,2-octanediol to 21 h from 40 h in the absence of crown ether. Increased solubility of sodium sulfite (which is very poor in the apolar solvents this reaction required; THF and acetonitrile gave poor conversion and water none) is clearly an important consideration when choosing reducing agents.

Notably, [Na][ReO_4] was first reported to be capable of catalysing the DODH reaction by Nicholas,[49] although conversions and yields were poor in the absence of crown ether, even with 10 mol % of catalyst. Therefore in the presence of 15-crown-5 a 30 % yield of 1-octene (100 % conversion) was detected after 100 h at 150 °C and by inclusion of the dehydrating agent sodium sulphate the yield was increased to 38 % after only 42 h. The more soluble [Bu_4N][ReO_4] was also applied successfully with 68 % yield of 1-octene (100 % conversion) after 100 h.[50] A number of pyridine additives (10 mol %) were tested but in all cases conversion and yield were supressed.

Investigation into the mechanism showed that reaction of styrene diol with MTO to give the glycolate (in a 3:1 reactant to product ratio) and conversion to an unidentified but presumably reduced rhenium species by heating with sodium sulfite were both possible.[50] Later DFT calculations aided in the understanding of the mechanism showing initial reduction of MTO by [Na][SO_3]$^-$ is preferred,[51] although loss of free [Na][SO_4]$^-$ is not viable (+45.9 kcal mol^{-1}) until the end of the catalytic cycle. Indeed, the calculations show that the anion is non-innocent during the reaction with coordination of the diol initially forming a coordinated sodium bisulfate (Scheme 17). This rearranges to form the expected hydroxide ligand but the second diol proton transfers to form the sodium bisulfate again, followed by formation of the hydrogen bonded aquo complex. Extrusion of the alkene can occur from either this or the dehydrated product with activation energies of +33.0 or +32.0 kcal mol^{-1} respectively. Dissociation of [Na][SO_4]$^-$ is endergonic with the product MTO +16.1 kcal mol^{-1} above the [Na][SO_4]$^-$ coordinated complex.

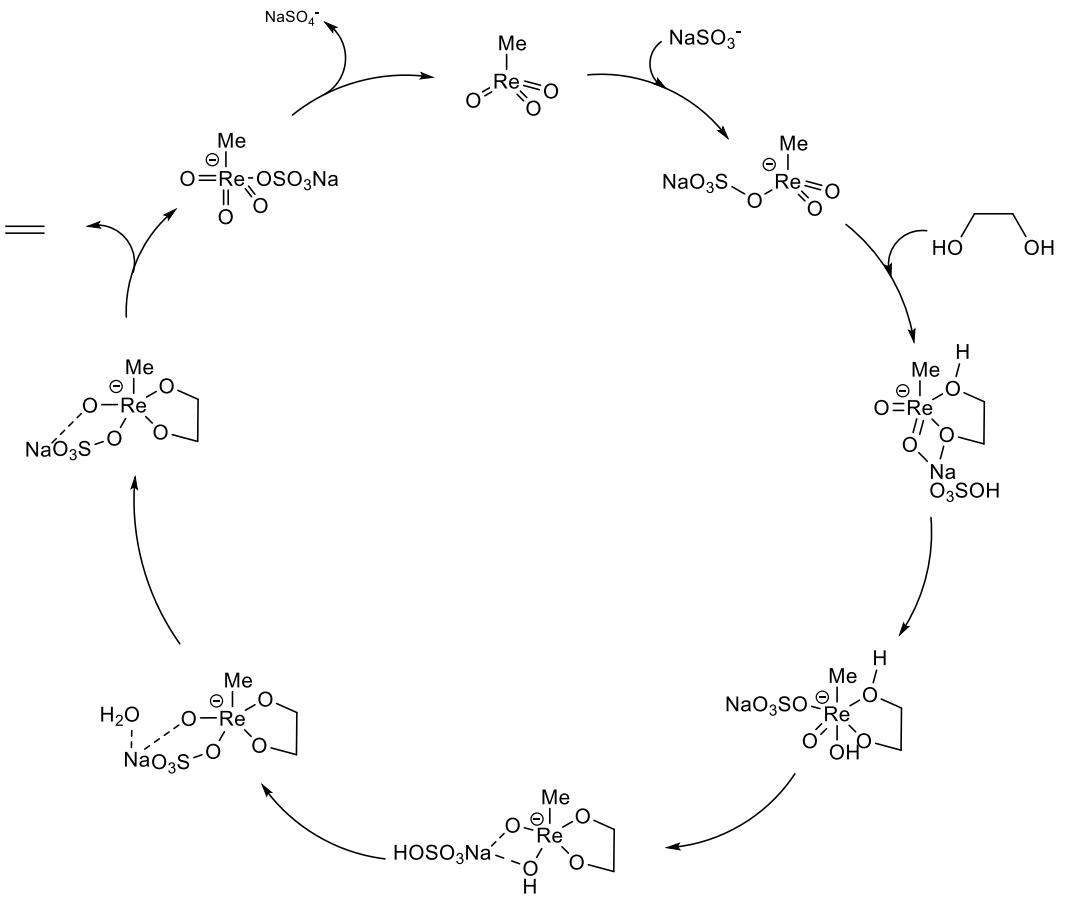

Scheme 17 Mechanism for the DODH of ethandiol with $NaSO_3^-$ as reducing agent. Intermediates are from DFT calculations.[51]

Alcohols have also been identified as promising reducing agents for the DODH reaction after observations that diols such as octane-4,5-diol is capable of acting as both the substrate and reducing agent when catalysed with $Re_2(CO)_{10}$ under air (no conversion was seen when conducted under N_2).[52] Alcohols would be a desirable reducing agent as their oxidised products can be reduced back to the alcohol thereby being recyclable. This observation of substrate self-reduction led Bergman to use a number of long chained alcohols as reducing agents (and solvent) for the DODH of 1,2-tetradecanediol with 2.5 mol % of either $Re_2(CO)_{10}$ or $BrRe(CO)_5$. For example 5-nonanol gave yields of 83 % of the alkene after 3.5 h at 180 °C and 3-octanol gave 82 % yield after 4 h at 170 °C. As with Cook and Andrews, a catalytic amount of acid (in this case TsOH or H_2SO_4) promoted the reaction so that lower temperatures could be used. Addition of 5 mol % TsOH gave 74 % of the alkene (100 % conversion) after 2.5 h at the reduced temperature 155 °. This is an important factor as many polyols will decompose at high temperatures. These examples also show a marked improvement on reaction times, likely due to the high reaction temperatures possible

in the non-volatile alcohol solvents and using the reducing agent in great excess (as the solvent).

Toste reported the conversion of several polyols to linear polyenes and even aromatic compounds using this methodology and MTO as catalyst.[53] Erythritol was fully converted using MTO (2.5 mol %) with 3-octanol as the reductant at 170 °C in 1.5 h. The major product was 1,3-butadiene although 11 % of 2,5-dihydrofuran was also present. With modification of the method using instead 3-pentanol at 200 °C, D-sorbitol and D-manniol were reduced to (*E*)-hexatriene, both in 54 % yield after 1 h and 1.5 h respectively. Inositols, cyclic C_6 polyols, gave high 60-96 % yields of benzene and phenol after 0.5 h under the same conditions. Furan was also produced from the sugars D-erythrose and D-threose (60 % and 47 % respectively) after 1.25 h at 155 °C, particularly interesting due to the direct availability from biomass feedstocks (Scheme 18).

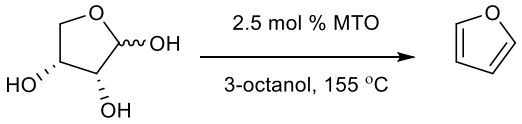

Scheme 18 Conversion of D-erythrose by 3-octanol with MTO.[53]

A reduced Re^{V} product from heating MTO with 3-pentanone in the presence of 3-hexyne was isolated as the η^2-alkyne product (Scheme 19).[53] This underwent condensation with the diol 1,4-anhydroerythritol at room temperature and heating of the glycolate extruded the alkene from the complex. These observations led the authors to suggest a catalytic cycle with initial reduction of MTO followed by diol condensation and finally extrusion of the alkene product. Mechanistic studies from Fristrup on the alcohol reductant DODH reaction with MTO using *in situ* IR spectroscopy found the Re^{v} and Re^{VII} glycolates were present in solution, although determined that the Re^{VII} glycolate was reversibly formed and existed as a deactivated form of the catalyst.[54] Therefore, if the Re^{VII} glycolate is not reduced to allow elimination of the alkene, the mechanism likely proceeds through initial reduction of MTO. DFT calculations studying this mechanism from Wang also agree that reduction occurs first, with the reduced species $[MeReO(OH)_2]$ providing the most favourable pathway rather than $[MeReO_2]$.[55] It was also suggested that the alcohol reductant also has a role as a proton shuttle, facilitating proton transfers from the diol to the OH ligands.

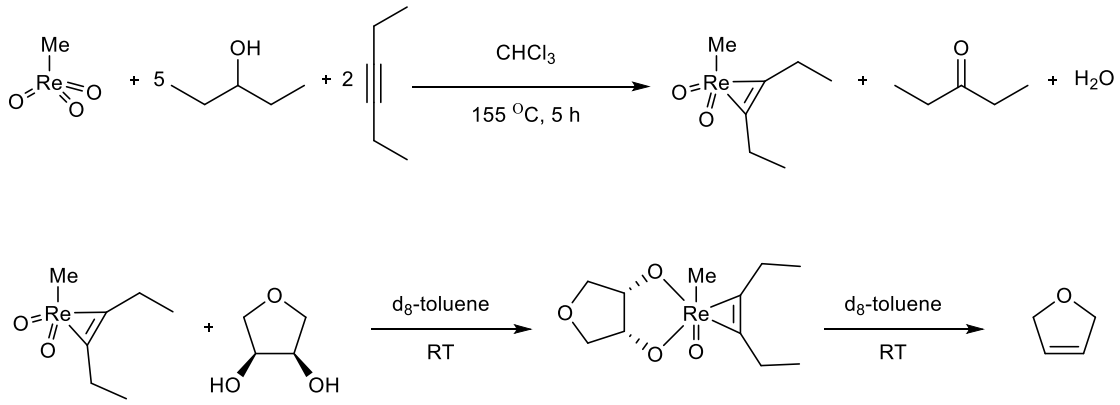

Scheme 19 Reduction of MTO and "trapping" the Re^{V} complex with 3-hexyne. Below this, synthesis of the glycolate followed by extrusion of the alkene by thermolysis.[53]

Epoxidation of Alkenes

The epoxidation of alkenes is a highly utilised transformation in industry. Estimates suggest that more than 10 % of propene produced is converted to propene oxide, an important precursor to a number of polymers.[56] With the large amount of this product required, there is a constant striving to implement economic processes without a large environmental impact. Currently, the hydroperoxide process is used which involves the peroxidation of an alkane such as ethylbenzene to ethylbenzene hydroperoxide (Scheme 20) which acts as an epoxidation agent for propene to produce propene oxide and 1-phenylethanol. (The byproduct 1-phenylethanol can be dehydrated to styrene in order to produce a second value added product.) Use of a heterogeneous catalyst (titanium supported on silica)[57] aids in the separation of products.

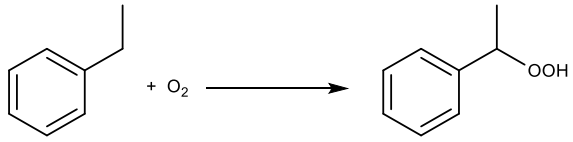

Scheme 20 Oxidation of ethylbenzene to ethylbenzene hydroperoxide.[56]

Hydrogen peroxide is an attractive oxidising agent due to its strength and the only byproduct being water. Due to its high cost it has not been utilised in the epoxidation of propene, although processes involving the *in situ* production of hydrogen peroxide are being developed to reduce the cost of hydrogen peroxide.[56] This oxidant has been used successfully with molecular homogenous catalysis. Venturello employed a tungstate catalyst with phase transfer agents to epoxidise a range of alkenes, although

ring opening of the epoxide was a significant problem and efforts to decrease this involved short contact times with the acidic aqueous phase and use of an excess of alkene.[58] This inevitably led to poor conversions. While the tungstate-phosphate containing $[N(hexyl)_4]_3[PO_4\{WO(O_2)_2\}_4]$ was shown to be both a stoichiometric epoxidation agent and a catalyst for epoxidation with aqueous hydrogen peroxide, the same requirements of short contact time and excess substrate were needed to prevent ring opening.[58] Use of trialkylammonium hydrogensulfates as phase transfer agents for sodium tungstate by Noyori was important for the high reactivity reported in their system (sodium chloride was shown to slow the reaction).[59] Using this method terminal alkenes were epoxidised in high yields using 2 mol % of sodium tungstate after 2-4 h at 90 °C, although some substrates such as styrene were susceptible to ring-opening due to the acidic aqueous phase.

MTO has also proven to be capable of using hydrogen peroxide for epoxidation reactions and exhibits high activity even below room temperature.[60] The peroxo and bisperoxo intermedieates (Figure 2) have been identified as the products of the reaction of MTO with hydrogen peroxide, with the bisperoxo complex being the major species when concentrations of hydrogen peroxide are in excess.[61] Interestingly the crystal structure of the bisperoxo complex was obtained as an adduct with water. DFT calculations have attributed an increase in stability of the adduct compared with the anhydrous form, reporting that ΔE for the hydration of the bisperoxo product is -16.3 kcal mol^{-1}.[62]

Figure 2 Mono- and bisperoxo complexs of MTO.[64]

Sharpless noted that ring opening of the epoxide was still observed with MTO, particularly in aqueous hydrogen peroxide but the addition of pyridine not only supressed this process but also promoted the epoxidation reaction itself.[63] Addition of 1 mol % of pyridine (0.5 mol % MTO) saw conversion of cyclooctene halt at 40 % after 5 min, yet 12 mol % of pyridine saw conversion at 90 % after 5 min and continued to more than 95 % after 15 min. The pyridine adduct prevents the acidic water adduct

from forming and acting as a proton source which causes ring opening of the epoxide, yet also helps slow the decomposition of MTO by preventing attack of HOO^-.[64, 65]

However, despite the high activity and selectivity possible with MTO, decomposition of the catalyst to methanol and perrhenate is observed.[64] The catalyst is more stable at high pH and the presence of base aids in decomposition to methane and perrhenate (in the absence of hydrogen peroxide). This adds to the cost of the catalyst as it cannot be recycled and as rhenium is an expensive metal, the application of this reaction is limited.

Other methods for epoxidation exist, however due to the high activity of the MTO catalyst substantial efforts have been made to optimise the reaction and prevent catalyst decomposition. Recently modified conditions saw turn over frequencies of 39000 h^{-1} in the presence of fluorinated solvents (which are also capable of activating hydrogen peroxide in the absence of a metal catalyst)[66] and 5000 equivalents of pyrazole additive, which exhibits a stronger promoting effect than pyridine.[67]

Aims of this Thesis

The wide range of catalysis possible with high oxidation state complexes outlined in the introduction has led us to investigate the systems using the perrhenate anion, arguably the simplest form of a high oxidation state rhenium compound. Therefore, this thesis aims to use a number of perrhenate salts as the catalyst for hydrosilylation reactions, deoxydehydration reactions and epoxidation reactions. While there is some information in the literature for each of these reactions using perrhenate, little is known about the effect of the counterion on the activity of the catalyst. During our investigations activity of perrhenate is studied both through experimental work and computational modelling, including any observed effects of the counterion. Additionally, evidence presented for the mechanism through which perrhenate acts as an epoxidation agent led to attempts to replace the perrhenate anion with similar oxo-anions.

References

1. S. C. A. Sousa, I. Cabrita and A. C. Fernandes, *Chemical Society Reviews*, 2012, 41, 5641-5653.
2. C. Boucher-Jacobs and K. M. Nicholas, in *Selective Catalysis for Renewable Feedstocks and Chemicals*, ed. M. K. Nicholas, Springer International Publishing, Cham, 2014, pp. 163-184.
3. W. R. Thiel, *Angewandte Chemie International Edition*, 2003, 42, 5390-5392.
4. S. A. Hauser, M. Cokoja and F. E. Kuhn, *Catalysis Science & Technology*, 2013, 3, 552-561.
5. J. L. Speier, J. A. Webster and G. H. Barnes, *Journal of the American Chemical Society*, 1957, 79, 974-979.
6. L. N. Lewis, *Chemical Reviews*, 1993, 93, 2693-2730.
7. J. Stein, L. N. Lewis, Y. Gao and R. A. Scott, *Journal of the American Chemical Society*, 1999, 121, 3693-3703.
8. B. Marciniec, in *Hydrosilylation: A Comprehensive Review on Recent Advances*, ed. B. Marciniec, Springer Netherlands, Dordrecht, 2009, pp. 3-51.
9. B. Marciniec, *Comprehensive Handbook on Hydrosilylation*, Elsevier Science, 2013.
10. I. Ojima, in *Organic Silicon Compounds (1989)*, John Wiley & Sons, Ltd, 1989, pp. 1479-1526.
11. I. Ojima, M. Nihonyanagi and Y. Nagai, *Journal of the Chemical Society, Chemical Communications*, 1972, 938a-938a.
12. I. Ojima, M. Nihonyanagi, T. Kogure, M. Kumagai, S. Horiuchi, K. Nakatsugawa and Y. Nagai, *Journal of Organometallic Chemistry*, 1975, 94, 449-461.
13. M. A. Bennett, R. Charles and P. J. Fraser, *Australian Journal of Chemistry*, 1977, 30, 1201-1211.
14. B. H. Lipshutz, W. Chrisman and K. Noson, *Journal of Organometallic Chemistry*, 2001, 624, 367-371.
15. B. H. Lipshutz, C. C. Caires, P. Kuipers and W. Chrisman, *Organic Letters*, 2003, 5, 3085-3088.
16. J. J. Kennedy-Smith, K. A. Nolin, H. P. Gunterman and F. D. Toste, *Journal of the American Chemical Society*, 2003, 125, 4056-4057.
17. L. W. Chung, H. G. Lee, Z. Lin and Y.-D. Wu, *The Journal of Organic Chemistry*, 2006, 71, 6000-6009.
18. E. A. Ison, E. R. Trivedi, R. A. Corbin and M. M. Abu-Omar, *Journal of the American Chemical Society*, 2005, 127, 15374-15375.
19. E. A. Ison, R. A. Corbin and M. M. Abu-Omar, *Journal of the American Chemical Society*, 2005, 127, 11938-11939.
20. G. Du, P. E. Fanwick and M. M. Abu-Omar, *Journal of the American Chemical Society*, 2007, 129, 5180-5187.
21. L. Huang, Y. Zhang and H. Wei, *European Journal of Inorganic Chemistry*, 2014, 2014, 5714-5723.
22. A. C. Fernandes, R. Fernandes, C. C. Romao and B. Royo, *Chemical Communications*, 2005, 213-214.
23. M. Drees and T. Strassner, *Inorganic Chemistry*, 2007, 46, 10850-10859.
24. Y. Wang, P. Gu, W. Wang and H. Wei, *Catalysis Science & Technology*, 2014, 4, 43-46.
25. P. c. M. Reis and B. Royo, *Catalysis Communications*, 2007, 8, 1057-1059.
26. B. Royo and C. C. Romão, *Journal of Molecular Catalysis A: Chemical*, 2005, 236, 107-112.
27. R. G. de Noronha, C. C. Romão and A. C. Fernandes, *Tetrahedron Letters*, 2010, 51, 1048-1051.

28. A. C. Fernandes, J. A. Fernandes, F. A. Almeida Paz and C. C. Romao, *Dalton Transactions*, 2008, 6686-6688.
29. F. J. Fernandez-Alvarez, A. M. Aitani and L. A. Oro, *Catalysis Science & Technology*, 2014, 4, 611-624.
30. C. C. Chong and R. Kinjo, *ACS Catalysis*, 2015, 5, 3238-3259.
31. A. Jansen, H. Görls and S. Pitter, *Organometallics*, 2000, 19, 135-138.
32. P. Deglmann, E. Ember, P. Hofmann, S. Pitter and O. Walter, *Chemistry – A European Journal*, 2007, 13, 2864-2879.
33. T. C. Eisenschmid and R. Eisenberg, *Organometallics*, 1989, 8, 1822-1824.
34. R. Lalrempuia, M. Iglesias, V. Polo, P. J. Sanz Miguel, F. J. Fernández-Alvarez, J. J. Pérez-Torrente and L. A. Oro, *Angewandte Chemie International Edition*, 2012, 51, 12824-12827.
35. A. Julian, E. A. Jaseer, K. Garces, F. J. Fernandez-Alvarez, P. Garcia-Orduna, F. J. Lahoz and L. A. Oro, *Catalysis Science & Technology*, 2016, 6, 4410-4417.
36. Y. Jiang, O. Blacque, T. Fox and H. Berke, *Journal of the American Chemical Society*, 2013, 135, 7751-7760.
37. P. Rios, N. Curado, J. Lopez-Serrano and A. Rodriguez, *Chemical Communications*, 2016, 52, 2114-2117.
38. S. Chakraborty, J. Zhang, J. A. Krause and H. Guan, *Journal of the American Chemical Society*, 2010, 132, 8872-8873.
39. F. Huang, C. Zhang, J. Jiang, Z.-X. Wang and H. Guan, *Inorganic Chemistry*, 2011, 50, 3816-3825.
40. S. Bontemps, L. Vendier and S. Sabo-Etienne, *Angewandte Chemie International Edition*, 2012, 51, 1671-1674.
41. S. Bontemps and S. Sabo-Etienne, *Angewandte Chemie International Edition*, 2013, 52, 10253-10255.
42. J. Yi, S. Liu and M. M. Abu-Omar, *ChemSusChem*, 2012, 5, 1401-1404.
43. G. K. Cook and M. A. Andrews, *Journal of the American Chemical Society*, 1996, 118, 9448-9449.
44. S. Raju, J. T. B. H. Jastrzebski, M. Lutz and R. J. M. Klein Gebbink, *ChemSusChem*, 2013, 6, 1673-1680.
45. S. Raju, C. A. M. R. van Slagmaat, J. Li, M. Lutz, J. T. B. H. Jastrzebski, M.-E. Moret and R. J. M. Klein Gebbink, *Organometallics*, 2016, 35, 2178-2187.
46. G. Chapman and K. M. Nicholas, *Chemical Communications*, 2013, 49, 8199-8201.
47. A. Galindo, *Inorganic Chemistry*, 2016, 55, 2284-2289.
48. Y.-Y. Jiang, J.-L. Jiang and Y. Fu, *Organometallics*, 2016, 35, 3388-3396.
49. S. Vkuturi, G. Chapman, I. Ahmad and K. M. Nicholas, *Inorganic Chemistry*, 2010, 49, 4744-4746.
50. I. Ahmad, G. Chapman and K. M. Nicholas, *Organometallics*, 2011, 30, 2810-2818.
51. P. Liu and K. M. Nicholas, *Organometallics*, 2013, 32, 1821-1831.
52. E. Arceo, J. A. Ellman and R. G. Bergman, *Journal of the American Chemical Society*, 2010, 132, 11408-11409.
53. M. Shiramizu and F. D. Toste, *Angewandte Chemie International Edition*, 2012, 51, 8082-8086.
54. J. R. Dethlefsen and P. Fristrup, *ChemCatChem*, 2015, 7, 1184-1196.
55. S. Qu, Y. Dang, M. Wen and Z.-X. Wang, *Chemistry – A European Journal*, 2013, 19, 3827-3832.
56. T. A. Nijhuis, M. Makkee, J. A. Moulijn and B. M. Weckhuysen, *Industrial & Engineering Chemistry Research*, 2006, 45, 3447-3459.
57. J. K. F. Buijink, J. J. M. van Vlaanderen, M. Crocker and F. G. M. Niele, *Catalysis Today*, 2004, 93–95, 199-204.

58. C. Venturello and R. D'Aloisio, *The Journal of Organic Chemistry*, 1988, 53, 1553-1557.
59. K. Sato, M. Aoki, M. Ogawa, T. Hashimoto and R. Noyori, *The Journal of Organic Chemistry*, 1996, 61, 8310-8311.
60. W. A. Herrmann, R. W. Fischer and D. W. Marz, *Angewandte Chemie International Edition in English*, 1991, 30, 1638-1641.
61. W. A. Herrmann, R. W. Fischer, W. Scherer and M. U. Rauch, *Angewandte Chemie International Edition in English*, 1993, 32, 1157-1160.
62. P. Gisdakis, S. Antonczak, S. Köstlmeier, W. A. Herrmann and N. Rösch, *Angewandte Chemie International Edition*, 1998, 37, 2211-2214.
63. J. Rudolph, K. L. Reddy, J. P. Chiang and K. B. Sharpless, *Journal of the American Chemical Society*, 1997, 119, 6189-6190.
64. M. M. Abu-Omar, P. J. Hansen and J. H. Espenson, *Journal of the American Chemical Society*, 1996, 118, 4966-4974.
65. S. M. Nabavizadeh, A. Akbari and M. Rashidi, *Dalton Transactions*, 2005, 2423-2427.
66. K. Neimann and R. Neumann, *Organic Letters*, 2000, 2, 2861-2863.
67. P. Altmann, M. Cokoja and F. E. Kühn, *European Journal of Inorganic Chemistry*, 2012, 2012, 3235-3239.

2. Hydrosilylation and Hydroboration with Perrhenate

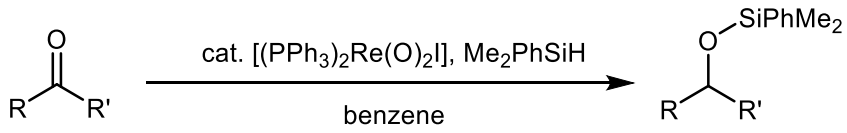

Scheme 21 Hydrosilylation of carbonyls using Toste's catalyst.[1]

The simple rhenium-oxo complex $[(PPh_3)_2Re(O)_2I]$ has been reported by Toste to catalyse the reduction of aldehydes and ketones with hydrosilanes (Scheme 1) through addition of the silane across the rhenium-oxygen bond,[1] forming a rhenium-hydride into which a carbonyl can insert. Work from Abu-Omar showed that the mono-oxo compound $[(hoz)_2Re(O)][TFPB]$ (hoz = 2-(2′-hydroxyphenyl)-2-oxazoline(-), TFPB = tetrakis(pentafluorophenyl)borate) is also capable of acting as a hydrosilylation catalyst,[2] although results from kinetic studies were not compatible with the formation of a hydride.[3] It is not only Re^{V} oxo compounds that are capable of this chemistry as $[Re_2O_7]$, $[MeReO_3]$ (Re^{VII}) and even $[MoCl_2O_2]$ have also been used successfully.

Amongst the advantages of using high oxidation state complexes as catalysts is their stability towards air and moisture, which simplifies their handling. Given the importance of the metal-oxo in this class of catalysts, we began to investigate whether the simple perrhenate anion was also capable of acting as a hydrosilylation catalyst. As with many metal-oxo complexes, perrhenate is more strongly associated with oxidation catalysis, although one previous report does show that perrhenic acid is capable of reducing sulfoxides using H_3SiPh and catecholborane (HBcat).[4]

Synthesis of $[N(hexyl)_4][ReO_4]$

In order to study the perrhenate anion as a hydrosilylation catalyst it was necessary to synthesise an organic soluble perrhenate. The tetrahexylammonium cation was chosen in order to maximise the solubility in a variety of solvents but also to prevent interactions between the counterion and catalyst. $[N(hexyl)_4][ReO_4]$ was made by stirring an aqueous solution of ammonium perrhenate with a chloroform solution of tetrahexylammonium bromide and isolating the product from the organic phase, as a colourless solid. Crystals suitable for X-Ray diffraction were grown from the slow evaporation of hexane into a concentrated benzene solution.

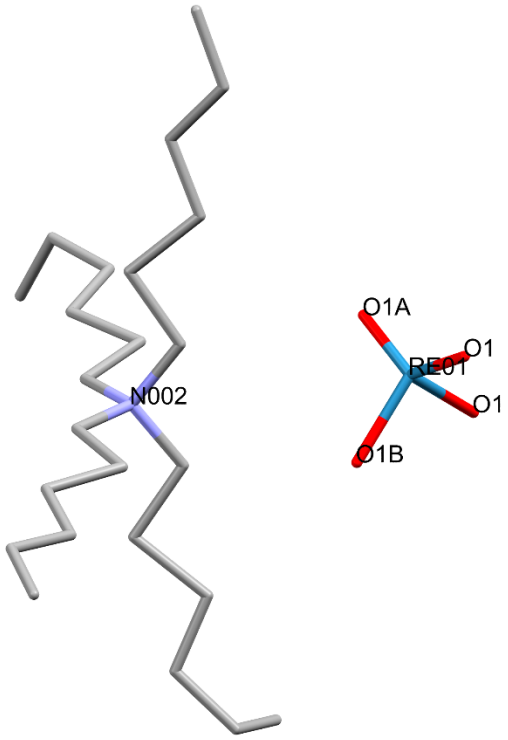

Figure 1 Solid state structure of $[N(hexyl)_4][ReO_4]$, (displacement ellipsoids are drawn at 50 % probability). For clarity, hydrogen atoms and disordered atoms have been omitted.

This new perrhenate salt was initially used to study the hydrosilylation catalysis of aldehydes and ketones.

Reduction of Aldehydes and Ketones

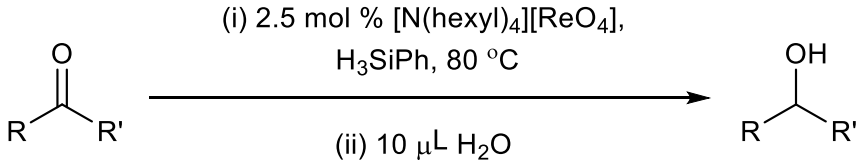

Scheme 2 Hydrosilylation and hydrolysis of carbonyl compounds using $[N(hexyl)_4][ReO_4]$.

With a loading of 2.5 mol % $[N(hexyl)_4][ReO_4]$ and H_3SiPh (0.24 mmol) in C_6D_6, 98.3 % benzaldehyde (0.2 mmol) was consumed after 1.5 h. The major product in the ^1H NMR spectrum is $PhHSi(OCH_2Ph)_2$ with the C*H*$_2$ visible at 4.74 ppm and Si*H* at 5.33 ppm, as reported in the literature.[5] Only a small amount of $PhSi(OCH_2Ph)_3$ can be seen, identified by the C*H*$_2$ at 4.85 ppm. Thirdly, resonances at 5.21 and 4.60 ppm can be assigned to $PhH_2Si(OCH_2Ph)$. Of course, with the majority of the silylether product being $PhHSi(OCH_2Ph)_2$, only 63.1 % of the silane was consumed. Addition of an excess of water (2.8 eq.) and further heating for 1 h resulted in the hydrolysis of the

silyl-ethers to give benzyl alcohol in 98.3 % yield by ^{1}H NMR spectroscopy and their identities confirmed by their ^{1}H and ^{13}C NMR spectra.

Table 1 Hydrosilylation of benzophenone using 2.5 mol % [N(hexyl)$_4$][ReO$_4$], 0.2 mmol hydrosilane, heated at 80 °C for 1.5 h.

Entry	Hydrosilane	Solvent	Conversion (%)	Yield (%)
1	$PhSiH_3$	C_6D_6	98.3	98.3
2	Ph_2SiH_2	C_6D_6	1.8	0
3	$PhSiH_3$	CD_3CN	100	98.5
4	Ph_2SiH_2	CD_3CN	97.4	85.1

The reactivities of the hydrosilanes H_3SiPh and H_2SiPh_2 in both C_6D_6 and CD_3CN were compared (Table 1). Whilst the results for H_3SiPh are only negligibly different between the two solvents, the large increase in consumption of benzaldehyde and yield of the benzyl alcohol in CD_3CN compared with C_6D_6 for H_2SiPh_2 led to the use of CD_3CN for all further reactions. H_3SiPh was used as the hydrosilane due to the high conversion of substrate regardless of solvent.

Hydrosilylation of a range of carbonyl compounds, including substrates with additional functional groups for which the catalyst proved to be tolerant was carried out (Table 2). Reduction of ketones proved to be significantly slower than aldehydes and in all cases except benzophenone did not achieve full conversion even after 10 h, probably due to the less polar carbonyl bond in ketones due to electron donation from the methyl substituents.

Table 2 Hydrosilylation of carbonyl compounds using 2.5 mol % $[N(hexyl)_4][ReO_4]$, 1.2 eq H_3SiPh in CD_3CN, heated at 80 °C for 10 h.

Entry	Substrate	Conversion (%)	Yield (%)
1	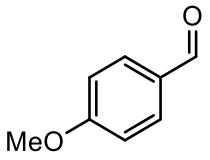	100	93.4
2	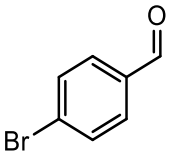	100	95.1
3	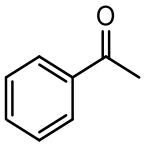	42.4	24.1
4	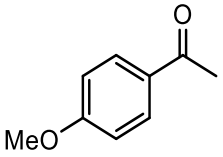	20.0	15.4
5	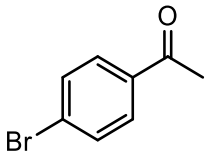	40.4	33.1
6	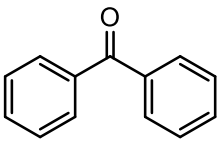	100	100

The possible hydrosilylation mechanism is investigated in the next section with respect to CO_2 reduction. However, the successful activation of the Si-H bond by perrhenate to achieve reduction of a variety of carbonyl compounds has been achieved. Unfortunately, the results for reduction of ketones was not as successful as for aldehydes. With this in mind, these encouraging preliminary results prompted the study on the hydrosilylation of CO_2.

Reduction of CO_2 to Methanol

A number of reports of reduction of CO_2 with hydrosilanes have been published where, despite the stability of CO_2, the reaction proceeds exothermically due to the formation of strong Si-O bonds.[6] Due to these strong driving forces, the reaction can often be conducted using mild conditions, typically 1 bar CO_2 and at room/low temperature. There are three main products observed in these reactions, the simplest being the silylformate, which was first observed as the end product by Koinuma using ruthenium phosphine complexes as catalysts.[7] Examples, including work from Pitter, now exist where only the silylformate is produced and no further reduction takes place.[8] Silyl acetals afforded from the further reduction of silylformates have been observed by Kawaguchi,[9] although subsequent reduction to methane is seen. Piers recently observed the selective conversion of CO_2 to silyl acetals by preventing pathways to the more highly reduced products.[10] Finally, reduction of CO_2 to a methoxysilyl ether is seen unselectively by Eisenberg[11] but appears as the major product in the carbene catalysed reduction of CO_2 by Ying.[12]

Given this precedent for reduction of CO_2 with hydrosilanes, a similar reaction was attempted using perrhenate as the catalyst and which soon became the focus of this work. The reaction between CO_2 (1 bar), $PhSiH_3$ (0.2 mmol) and $[N(hexyl)_4][ReO_4]$ (2.5 mol %) in C_6D_6 at 80 °C shows that the silane is 95 % consumed after 12 h by ^1H NMR spectroscopy. The ^1H NMR spectrum contains a broad region between 3.70 and 3.25 ppm with multiple peaks and also between 5.80 and 5.05 ppm. It is in these regions that $Si\text{-}OCH_3$ groups and Si-H protons would be expected to be found, respectively. The numerous resonances in these regions indicate that the product of this reaction may be oligomeric. Once water is added (2.8 eq) and the reaction once again heated to 80 °C for 1 h, these resonances disappear to give a sharp singlet at 3.06 ppm corresponding to methanol in a 42.4 % yield.

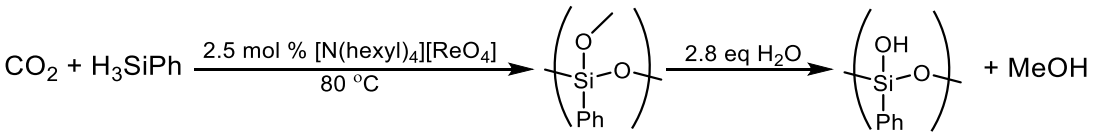

Scheme 3 Hydrosilylation of CO_2 forming polymeric methoxysilane products.

The secondary hydrosilane H_2SiPh_2 was also effective for this reaction with full conversion after 12 h under the same conditions. The ^1H NMR spectrum in C_6D_6 after

4 h shows there are two major products containing a Si-H bond at 5.91 and 5.62 ppm both showing ^{29}Si satellites, confirming that the products in this region are silane byproducts. The reaction was heated for a further 8 h and showed a similar set of resonances to the reaction with H_3SiPh between 3.60 and 3.25 ppm corresponding to Si-OCH_3 groups and 6.20 to 5.70 ppm corresponding to Si-H byproducts. After addition of water (2.8 eq) and heating for 1 h, as with the previous example, a sharp peak corresponding to methanol at 3.07 ppm was seen giving a yield of 28.7 %.

CD_3CN was found to be a more suitable solvent for this reaction, where the silane was 95.5 % depleted within 4 h when using H_3SiPh and fully converted for H_2SiPh_2 after 3 h. The conversion was further accelerated in d_7-DMF, taking 1 h for full conversion for either silane. Whilst no conversion of $HSiPh_3$ was observed after 29 h at 80 ° in CD_3CN, use of d_7-DMF allowed heating of the solution to 150 °C. At this temperature full conversion of $HSiPh_3$ was achieved after 8 h with 12.7 % of the silylformate also present at this point. Table 3 shows the results of the reaction with various hydrosilanes in a range of solvents.

Table 3 Hydrosilylation of CO_2 catalysed by 2.5 mol % $[N(hexyl)_4][ReO_4]$, 0.2 mmol hydrosilane, 1 bar CO_2. Heated at 80 °C. ([a] 150 °C).

Entry	Hydrosilane (0.2 mmol)	h	Solvent	Conversion (%)	Yield CH_3OH (%)
1	H_3SiPh	4	CD_3CN	95.5	30.9
2	H_2SiPh_2	3	CD_3CN	100	28.8
3	H_3SiPh	16	CD_3CN	100	40.0
4	H_2SiPh_2	16	CD_3CN	100	36.4
5	H_3SiPh	12	C_6D_6	95	42.4
6	H_2SiPh_2	12	C_6D_6	100	28.7
7	H_2SiPh_2	1.5	d_5-Pyr	100	43.5
8	H_3SiPh	9	d_7-DMF	100	60.0
9	H_2SiPh_2	9	d_7-DMF	100	50.7
10	$HSiPh_3$[a]	8	d_7-DMF	100	10.0
11	H_2SiMe_2Ph	8	d_7-DMF	100	32.0

These differences in rate of reaction between the solvents would appear to be due to the solubility of CO_2 in the respective solvent. For example CO_2 is five times as

soluble in DMF as it is in CH_3CN.[13] This is supported by the observation that at higher pressures the reaction proceeds in a shorter period of time. For example a reaction of H_2SiPh_2 and CO_2 (2 bar) in CD_3CN shows the silane is more than 97 % consumed within 1.5 h.

In order to confirm that CO_2 is involved in this reaction, H_2SiPh_2 and 2.5 mol % $[N(hexyl)_4][ReO_4]$ were heated in CD_3CN at 80 °C in the absence of CO_2 where, after 1 h, a negligible amount of silane was consumed (< 3 %). A resonance corresponding to hydrogen is visible at 4.59 ppm as well as a small resonance at 5.58 ppm, which can be identified as a product containing a Si-H bond due to ^{29}Si satellites. It is possible that in the absence of a CO_2 that the silane has reacted with water present in the solvent but clearly a suitable substrate must be present for significant consumption of the silane.

Use of ^{13}C labelled CO_2, gave some insights into the mechanism of the reaction with H_2SiPh_2 when monitored by ^1H and ^{13}C NMR spectroscopy at room temperature, hourly up to 10 h and then every 4 h (Figures 2 and 3). Immediately, a small doublet can be seen at 8.29 ppm in the ^1H NMR spectrum with a corresponding doublet in the ^{13}C NMR spectrum at 162.98 ppm, both with a coupling constant of 214 Hz. A doublet in this region is consistent with that of a silyl-formate. This doublet grows over the next 2 h before becoming broader and shifting downfield to 8.51 ppm after 5 h. At this point another two doublets appear at 3.73 ppm (J_{HC} 144 Hz) and 5.28 ppm (J_{HC} 168 Hz) in the ^1H NMR spectrum and a quartet at 51.87 ppm (J_{CH} 144 Hz) and 85.59 ppm (J_{CH} 168 Hz) in the ^{13}C NMR spectrum. These two sets of resonances show the formation of $SiOCH_3$ and silyl acetal $Si\text{-}OCH_2O\text{-}Si$ groups, the product and intermediate in the sequential reduction of CO_2.

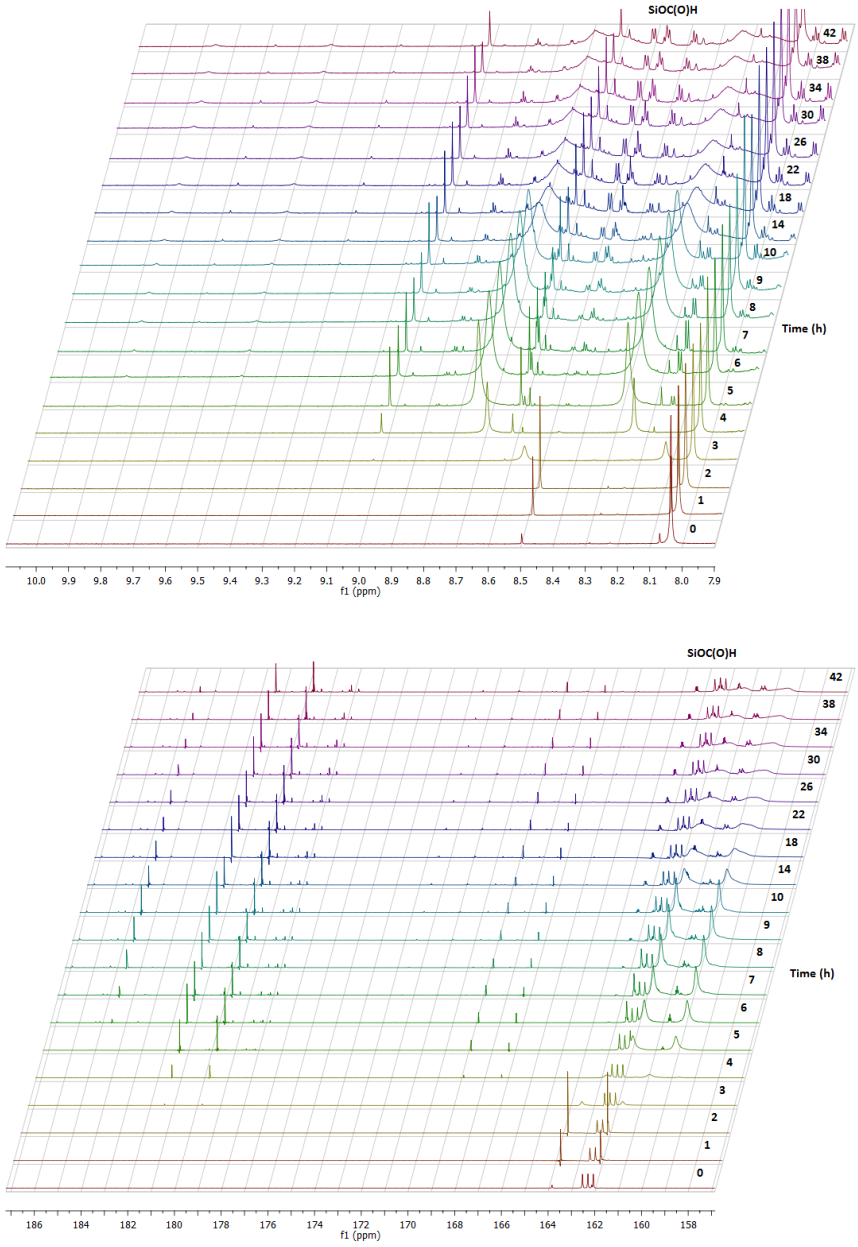

Figure 2 ^{1}H and ^{13}C NMR spectra showing growth of silylformate products over time.

As the reaction progresses the silyl-formate resonances become increasingly broad and additional doublets are seen in this region in both the ^{1}H and ^{13}C NMR spectra. This supports the formation of an oligomeric product. Certainly by the end of the reaction it is clear that there are several environments in which Si-OCH_3 groups are present from the overlapping quartets in the ^{13}C NMR spectrum. Additionally the byproducts with Si-H resonances arise due to the production of oligomers and their continued presence after the silane has been consumed indicates that these Si-H bonds are more difficult to activate; in a reaction with unlabeled CO_2 the resonances in the silane

region appear to be consumed completely if the reaction is heated for an additional 9 h.

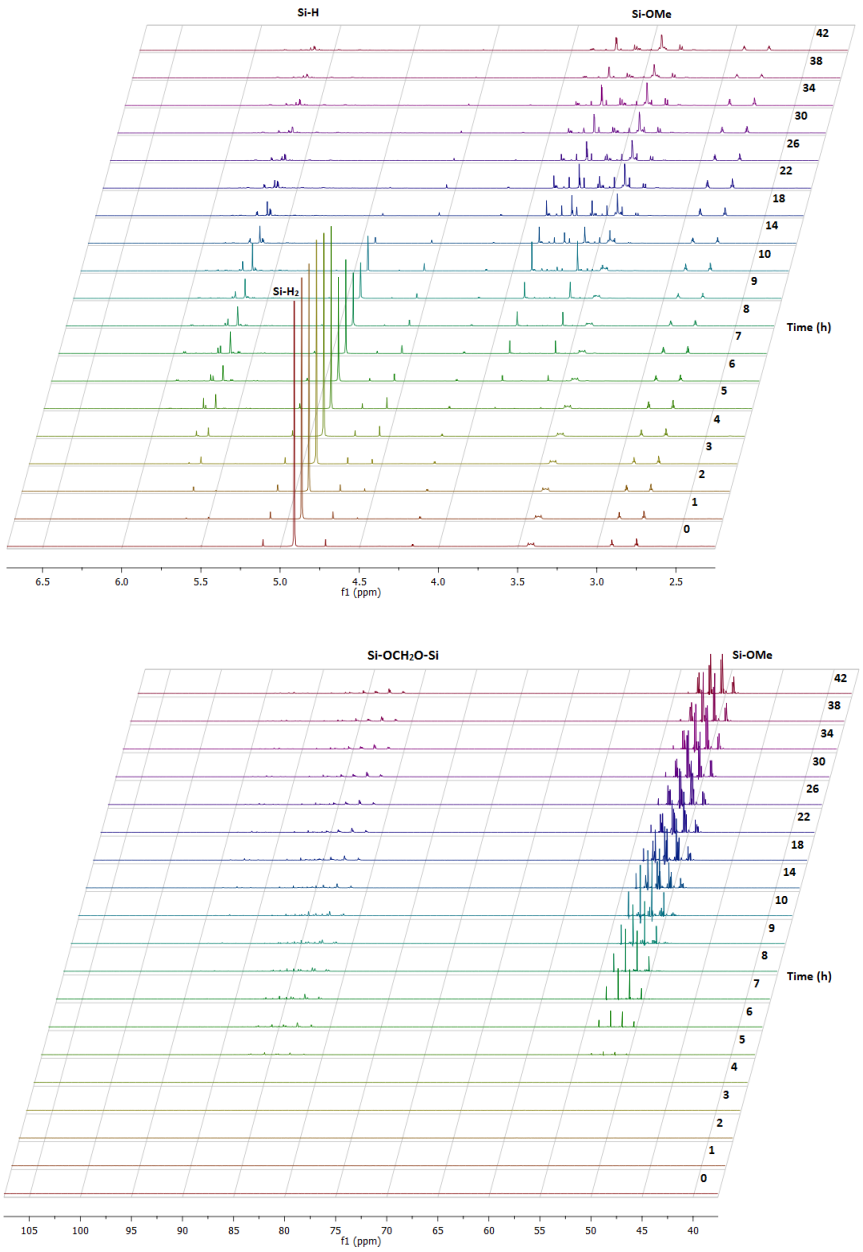

Figure 3 ^{1}H and ^{13}C NMR spectra showing growth of methoxysilane products and consumption of H_2SiPh_2 over time.

Hydrolysis of the $^{13}CO_2$ reaction gives doublets at 8.33 ppm (J_{HC} 210 Hz), 4.79 ppm (J_{HC} 159 Hz) and 3.31 ppm (J_{HC} 139 Hz) in the ^{1}H NMR spectrum. The ^{13}C NMR shows a corresponding doublet at 163.69 ppm (J_{CH} 210 Hz), a triplet at 83.01 ppm (J_{CH} 159 Hz) and quartet at 49.07 ppm (J_{CH} 139 Hz). The latter two resonances support the formation of both formaldehyde and methanol. While it might be expected that the silylformate would hydrolyse to formic acid, the chemical shift is not consistent with

literature values and therefore suggests that the silylformate is not hydrolysed. The product, however, can be assigned as $Ph_2Si(OCHO)_2$ which was reported by Chong and Kinjo,[14] and which is observed in a perrhenate catalysed reaction conducted in CD_3CN.

Another two multiplets in the ^{13}C NMR spectrum show the presence of an unusual additional product with the structure H_3COH_2COSi- (Figure 4). At 90.29 ppm, a triplet of doublets of quartets is related to the quartet of triplets of doublets at 54.02 ppm. To explain the multiplets a $^{13}CH_2$ and $^{13}CH_3$ couple to their own protons to give the overall triplet and quartet. Further coupling to the protons either side of the ether through a three bond coupling gives the quartet and triplet multiplets respectively. Finally these are split again by ^{13}C-^{13}C coupling. This product is only clearly visible after hydrolysis and therefore is $H_3COH_2COSi(OH)Ph_2$.

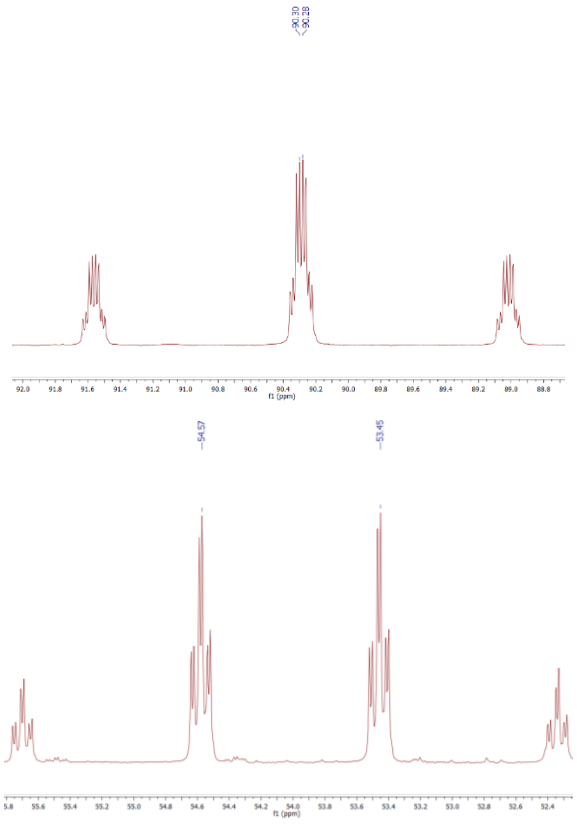

Figure 4 Multiplets in the ^{13}C NMR spectrum for the $SiOCH_2OCH_3$ product.

It is not completely clear how this product forms. One possibility shown by Bontemps and Sabo-Etienne in their work reducing CO_2 with HBpin was the reaction of formaldehyde with the formate OHCOBpin to give the analogous product $OHCOCH_2OBpin$.[15] This reaction occurs in the absence of catalyst and was used to

help prove that formaldehyde is formed in the reaction through the decomposition of $CH_2(OBpin)_2$ which also gave $O(Bpin)_2$ as a byproduct. Considering the similarities, this raises questions as to whether $CH_2(OSiHPh_2)_2$ decomposes to give formaldehyde and the siloxane. Any formaldehyde formed during the reaction would quickly be reduced to give the methoxysilyl, as seen by the rapid reduction of aldehydes by the same system. Furthermore this has been predicted by Wang and coworkers in their computational study of the reduction of CO_2 with hydrosilanes using NHCs as catalysts, describing the formation of formaldehyde as inevitable.[16] This would also explain why no silyl acetal products are observed in the NMR spectra. Using these experimental observations, a proposed catalytic cycle for the hydrosilylation of CO_2 through the formation of a rhenium hydride is presented below (Scheme 4).

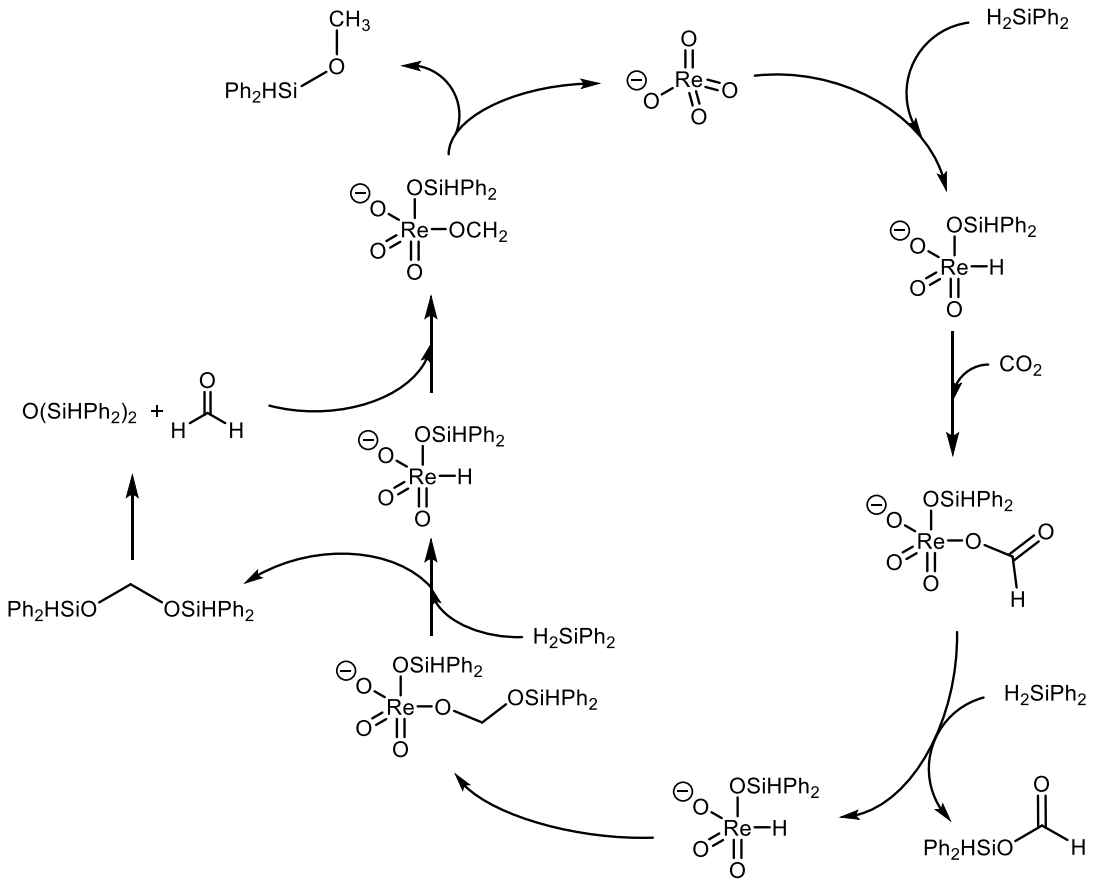

Scheme 4 Proposed catalytic cycle for the hydrosilylation of CO_2 with [N(hexyl)4][ReO4] and H_2SiPh_2.

From several reactions in acetonitrile, after the product has been hydrolysed large crystals form and are characterised by X-ray crystallographic unit cell analysis, showing the major byproduct is the cyclic tetramer $(Ph_2SiO)_4$. Reactions involving $HSiPh_3$ give the siloxane $O(SiPh_3)_2$ (Scheme 5), which grew as large crystals as the

reaction solution cooled but before water was added, proving that the siloxane is produced during the reaction and not only after hydrolysis.

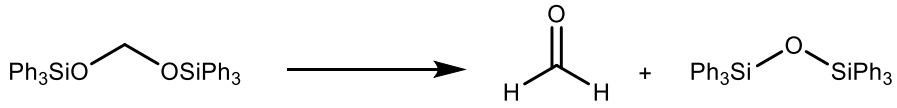

Scheme 5 Decomposition of the acetal $CH_2(SiPh_3)_2$ to formaldehyde and corresponding siloxane.

One side reaction that occurs is the production of hydrogen. This suggests that a process where either hydrogen is reductively eliminated from an intermediate or that the silane is being coupled to itself. No evidence of the latter of these two processes is found as when the silane is heated to 80 °C with perrhenate in the absence of CO_2 for 1 h, only negligible consumption of silane (< 3%) is seen. In order to determine whether the catalyst remains active at the end of the reaction, an experiment in d_7-DMF was recharged with H_2SiPh_2 and CO_2 three times after the initial run and heated again at 80 °C. Each run was complete within 1 h and showed a large increase in methoxysilane products. After hydrolysis the yield of methanol reached 75.9 %.

As these reactions are conducted in solvents that are not pre-dried, another possible source of the hydrogen is water present in the solvent reacting with the hydrosilane (or rhenium hydride species). However, for reactions in CD_3CN, water is still visible at the end of the reactions for both H_3SiPh and H_2SiPh_2, showing reduction of CO_2 by hydrosilanes is favoured over reacting with water. When CD_3CN is dried over 4 Å molecular sieves for 24 h showing a reduction in water content by 90 % (by ^1H NMR spectroscopy), the yield of CH_3OH (using H_2SiPh_2) increases from 28.8 % to 38.9 %. Unfortunately this still does not explain why the yield is so much lower than the expected yield and cannot be explained by the presence of water in entirety as water will only consume a stoichiometric amount of the hydrosilane.

Noting that a strong amine-like odor was released at the end of reactions in d_7-DMF, the possibility of reduction of the solvent was investigated. Indeed at 2.09 ppm a 1:1:1 triplet showing H-D coupling is found which has previously been reported as $CDH_2N(CD_3)_2$ (Figure 5).[17] Unfortunately, due to the low boiling point of trimethylamine, an accurate yield cannot be calculated for this reaction although it is clear that at least 9.5 % of the silane was consumed in this reaction. A similarly strong smell was evolved by reactions in CD_3CN, but in this case only a small doublet at 2.78

ppm can be seen. This has been reported previously as $CD_3CH_2NH_2$, a product from the reduction of CD_3CN.[18] It is unlikely that the yield of this side reaction is as high as that in d_7-DMF because, as mentioned above, there is minimal consumption of hydrosilane when the reaction is heated for 1 h in the absence of CO_2.

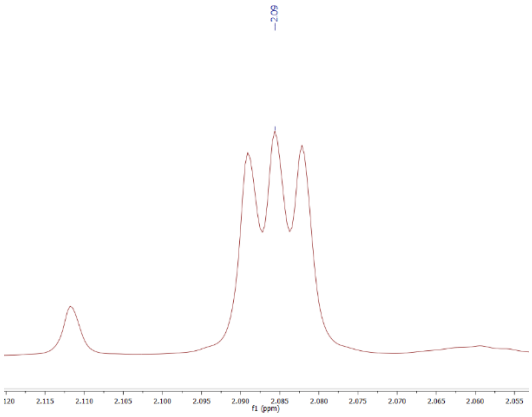

Figure 5 Triplet at 2.09 ppm for $CDH_2N(CD_3)_2$ in d_7-DMF.

The most likely explanation for the lower than quantitative yield is a result of the oligomeric products formed before hydrolysis of the solution. Any remaining Si-H bonds on the oligomers are attached to products that significantly reduce the ease of activation of the Si-H bond. This is seen with other silanes (e.g. $HSiPh_3$) where not all hydrosilanes are able to react unless much harsher conditions are used. As further heating of the Si-H byproducts seen in the ^1H NMR spectra for both H_3SiPh and H_2SiPh_2 reactions in order to achieve complete conversion is necessary, this sensitivity of perrhenate to the source of the Si-H bond can be observed.

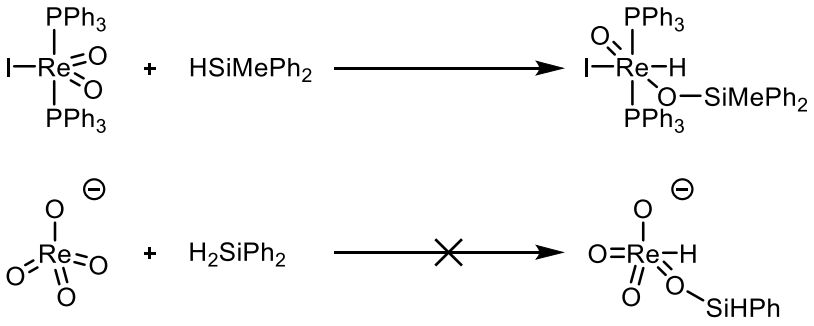

Scheme 6 Formation of a hydride intermediate.

From the rhenium-oxo complex $[Re(PPh_3)_2(O)_2I]$, a stable hydride can be synthesised by the addition of a large excess of silane (Scheme 6).[19] The resulting complex, confirmed by X-ray crystallography, shows that the silane adds across one of the rhenium-oxo bonds. When a similar reaction is attempted with $[N(hexyl)_4][ReO_4]$

using H_2SiPh_2, no evidence suggesting the formation of a rhenium-hydride is found after 5 d at room temperature. Heating $[N(hexyl)_4][ReO_4]$ with 2 eq. H_2SiPh_2 over 26 h does result in the partial consumption of silane and a shift of the tetrahexylammonium resonances, yet no obvious product that can be attributed to a hydride is seen by ^1H NMR spectroscopy. In the aromatic region of the spectrum a product can be assigned to the tetramer $(Ph_2SiO)_4$, although the baseline in this region is broad suggesting that oligomeric products are also formed with $(Ph_2SiO)_4$ being the stable end product. The shift of the tetrahexylammonium suggests that the rhenium compound is no longer perrhenate, and this would explain the presence of $(Ph_2SiO)_4$. Furthermore, the region -7 to -11 ppm which is typical of hydrides, does show a number of very weak resonances. This implies that transfer of the hydride to the rhenium is possible but it is likely that the presence of several silane species is not unrelated to the presence of numerous resonance in the hydride region. It should be noted, however, that such species are not seen in catalytic reactions, the chemical shift of the counterion does not change and the reaction seen on a stoichiometric scale is not seen otherwise. As no clear product was produced from this reaction and due to the lack of similarities seen on a catalytic scale, no attempts to characterise the mixture by IR spectroscopy.

Another possibility is the formation of a rhenium carbonate. Such a species is known for the molybdate anion $[PPN]_2[MoO_4]$ (PPN^+ = bis(triphenylphosphine)iminium) which reversibly binds to up to two molecules of CO_2 to form $[PPN]_2[MoO_3(\kappa^2\text{-}CO_3)]$ (Scheme 7) and at low temperatures the dicarbonate $[PPN]_2[MoO_2(\kappa^2\text{-}CO_3)_2]$ can also be acessed.[20] Addition of $HSiEt_3$ to $[PPN]_2[MoO_3(\kappa^2\text{-}CO_3)]$ generates [PPN][OCHO] and $[PPN][MoO_3(OSiEt_3)]$. However, when $[N(hexyl)_4][ReO_4]$ is observed under an atmosphere of CO_2, no change is seen in the ^{13}C NMR spectrum; i.e. no resonances in the region of 165 ppm, which would indicate a carbonate bound to the rhenium centre, even when the spectrum is measured at 70 °C. Noting that $[PPN]_2[MoO_3(\kappa^2\text{-}CO_3)]$ converts back to $[PPN]_2[MoO_4]$ in the presence of water, the NMR study of $[N(hexyl)_4][ReO_4]$ was repeated using anhydrous solvent but still failed to show evidence of a carbonate. From this it was concluded that it is unlikely that the carbonate is involved in the mechanism.

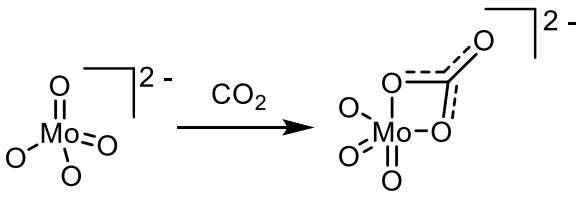

Scheme 7 Formation of a molybdenum carbonate.

Methylation of Amines with CO_2

Another area that has been explored recently is the methylation of amines using CO_2 and hydrosilanes. A so called "diagonal approach" towards CO_2 reduction, this directly uses CO_2 as a C_1 building block without isolation of one of the tradition C_1 building blocks such as formaldehyde or formic acid. Cantat and Cazin have both reported the catalytic methylation of amines with zinc and copper carbene complexes respectively using CO_2 as the C_1 feedstock and H_3SiPh as the reducing agent. Cantat suggested a mechanism based on experimental observation showing reaction of a silylformate (visible by ^1H NMR spectroscopy) with an amine to produce a formamide, which was subsequently reduced to the methyl group.[21] No reduction of CO_2 was observed in the absence of the amine, therefore ruling out transfer from methoxysilyl groups. Cazin's proposed catalytic cycle, which was supported by DFT calculations,[22] again showed initial formation of silylformate which reacted with the amine to produce a formamide. Using these processes both aliphatic and aromatic amines were methylated.

Given the success of the $[N(hexyl)_4][ReO_4]$ catalyst in converting CO_2 into CH_3OH through a mechanism involving silylformates, its activity was tested for the conversion of several amines to methylamines. The reaction between CO_2 (2 bar), H_2SiPh_2 (4 eq) and diisopropylamine at 80 °C in CD_3CN shows a yield of 78.4 % of MeN^iPr_2 after two hours (Table 4). However, even with further heating, no increase in product yield was seen after this point. Other amines such as isopropylamine and pyrrolidine are also converted to the dimethylamine and methylamine respectively; attempts to use aromatic amines as substrates were unsucessful.

Table 4 Methylation of amines with 2.5 mol % [N(hexyl)4][ReO4], 2 bar CO_2 in CD_3CN heated at 80 °C.

Entry	Amine	Hydrosilane (eq)	Conversion (%)	Yield (%)
1	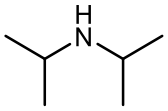	4	100	73.7
2		8	88.2	42.5
3	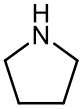	4	65.5	51.6

As the reactions in the perrhenate catalysed reduction of CO_2 show that a silylformate is formed as the first product, it can be assumed that the silylformate reacts with the amine in a similar way as seen by both Cantat and Cazin (Scheme 8). Additionally, as -SiOMe products are observed in all perrhenate catalysed reactions but conversion often does not reach 100 % and stalls after 2 hr, it is clear that transfer of the methyl onto the amine nitrogen does not occur. Evidently, in these reactions there is a competition between reaction of the silylformate with the amine or further reduction of the silylformate to produce the –SiOMe byproducts. As such, reaction with aromatic amines is disfavoured due to their poorer nucleophilic properties. However, if this competition can be tipped in favour of reaction with the amine, the scope of the reaction can be increased.

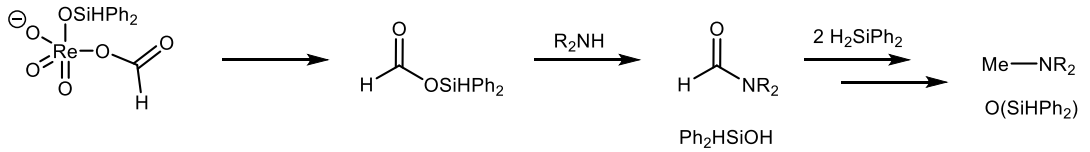

Scheme 8 Proposed reaction of silylformate with amine.

To test this hypothesis, using H_3SiPh (0.2 mmol), CO_2 (2 bar) and $[N(hexyl)_4][ReO_4]$ in CD_3CN, the methylation of N-methylaniline (0.2 mmol) was attempted at room temperature in order to slow the further reduction of the silylformate. Full conversion of the starting material was observed after 98 h, although product yields continue to rise up to 144 h, and production of N,N-dimethylaniline was evident with a new resonance at 2.91 ppm for the two methyl groups in 36.6 % yield. The reaction, however, does not only give the expected product. Two resonances are also found at

2.86 ppm (2 H) and 4.78 ppm (6 H). This corresponds to two N-methylaniline molecules linked together with a CH_2 group to afford the aminal $CH_2(PhNH)_2$ in 52.1 % yield; the chemical shifts are similar to those reported in the literature.[23] Furthermore, this is not a minor product but higher yielding than N,N-dimethylaniline.

The aminal $CH_2(PhNH)_2$ can be synthesised by the condensation reaction of N-methylaniline with formaldehyde at room.[23] Its formation in the catalysed reaction is therefore explained by the formation of formaldehyde in the reaction, as proposed in calculations by Wang and coworkers,[16] by the decomposition of $CH_2(OSiH_2Ph)_2$, giving formaldehyde and siloxane byproducts. As formaldehyde is not seen in the NMR spectra, it must be quickly reduced by silane under normal conditions (as seen previously, aldehydes are quickly reduced using this system) but clearly here it is consumed by the aniline. This also provides strong evidence that formaldehyde is an intermediate in the reaction. It should be noted that aminals have previously been generated from CO_2 by Beller and Cantat, who both used H_3SiPh as their reducing agents.[24, 25]

Certainly methylation of aromatic amines can be achieved, yet under the current conditions not only the expected products are produced. However the ability to react the anilines with formaldehyde opens up a new class of reactions where, for example, imines could be synthesised from the formaldehyde produced in the reaction. This has already been reported by Sabo-Etienne and Bontemps for their reduction of CO_2 with HBpin in the presence of 2,6-diisopropylaniline, which produced the imine.[26]

What is particularly interesting about using perrhenate as the catalyst for this type of reaction is its aforementioned stability towards both air and water. All the reactions here are conducted using solvent without any drying procedures (including the hygroscopic amines) and yet the product is obtained in high yield. Other methodologies require dry solvents, an inert atmosphere[21, 22, 27] and occasionally high pressures of CO_2.[24] Also, since the non-coordinating tetrahexylammonium counterion is only present to increase solubility in solvents such as benzene, it is probable that the commercially available $[N(butyl)_4][ReO_4]$ can also produce similar results.

DFT Mechanism Studies

In order to understand the reaction in greater detail, several mechanisms have been studied using density functional theory (DFT) calculations. Since the addition of HMe_2SiPh to $[(PPh_3)_2Re(O)_2I]$ yields a stable hydride, thought to be through a [2+2] addition,[19, 28] it is reasonable to suppose that a similar [2+2] addition occurs with $[N(hexyl)_4][ReO_4]$. However, a [3+2] mechanism has also been suggested for the activation of silanes and while this was found to be an unfavourable mechanism for $[(PPh_3)_2Re(O)_2I]$, a computational study on the activation of both silane and methane showed that metal tetroxide complexes were found to be more likely to react by a [3+2] mechanism.[29] The hydroxide ligand produced by a [3+2] addition may also tautomerise quickly to give the metal-hydride species, and was therefore also considered.

As the reaction was strongly silane specific, H_3SiPh was used in the calculations rather than a model hydrosilane such as silane, which has been used in some previous hydrosilylation DFT studies.[29, 30] The simpler tetramethylammonium cation was used, however, as a model for the counterion and appeared to be necessary because energies for the solvation were found to unreliable in its absence. All calculations were ran with Gaussian09 using the B3LYP functional, the 6-311++G(d,p) basis set was used for all atoms except Re for which the SDD basis set was used and the GD3BJ empirical dispersion correction. Solvent effects were estimated using the SMD solvation model as single point energy calculations on the optimised structures for both benzene and DMF. All energies discussed are free energies.

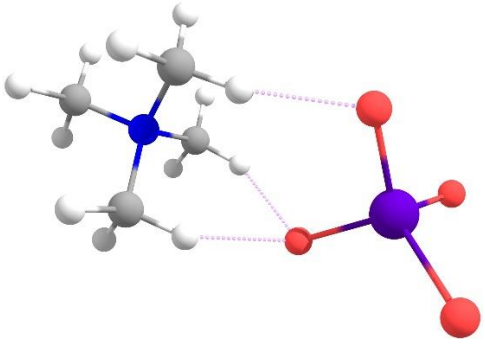

Figure 6 Interactions between $[NMe_4]^+$ and $[ReO_4]^-$.

In most cases the tetramethylammonium cation is located near a rhenium-oxo with a bifurcated hydrogen bond between two of the C-H bonds and the rhenium-oxo with

distances of approximately 2 Å, as in $[NMe_4][ReO_4]$ (Figure 6). While the $[NMe_4]^+$ may be interacting more strongly than $[N(hexyl)_4]^+$ might be expected to, this does not appear to be strong enough to effect the reactivity of the rhenium complexes or the geometry in any significant way. Resultantly, in all figures $[NMe_4]^+$ has been omitted for clarity.

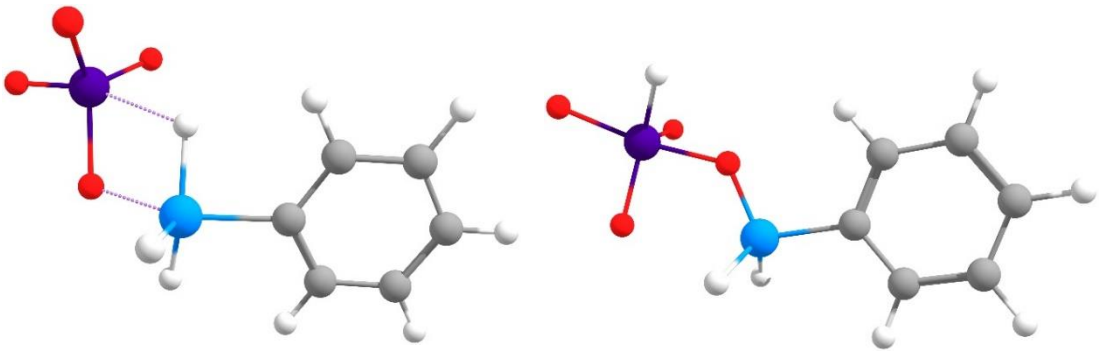

Figure 7 a. TS for [2+2] reaction of perrhante and H_3SiPh b. [2+2] product.

Firstly the [2+2] addition of the silane across the rhenium-oxo bond to give a rhenium-hydride was considered. Nucleophilic attack of a rhenium-oxo leads to a 4-membered ring transition state with a trigonal bipyramidal silicon centre with the activated silicon-hydrogen bond elongated to 1.59 Å (Figure 7a). This has a solvent dependent activation energy of $\Delta G_{benzene}$ = +16.5 kcal mol^{-1}/ ΔG_{DMF} = +21.6 kcal mol^{-1}. Forming the distorted trigonal bipyramidal geometry of $[ReH(O)_3(OSiH_2Ph)]^-$ is favourable with $\Delta G_{benzene}$ = -6.4 kcal mol^{-1}/ ΔG_{DMF} = -0.5 kcal mol^{-1} (Figure 7b). The rhenium-oxo bonds have lengths ranging between 1.80-1.72 Å; however, the variation in these lengths appears to be due to the presence of the counterion, in the absence of which they range between 1.75-1.74 Å. If the two complexes are compared to perrhenate, both in the absence of $[NMe_4]^+$, it can be seen that there is only a slight decrease from 1.76 Å for perrhenate. This is not as significant as the shortening of the rhenium-oxo bond in the di-oxo complexes studied by Wu and coworkers where after [2+2] addition of a silane, the remaining oxo bond was reduced from 1.73 Å to 1.66 Å due to a reduction in the competition for the bonding with the rhenium centre which resulted in triple bond character.[28] As there are three oxo ligands remaining these effects are minimalised in the rhenium hydride $[ReH(O)_3(OSiH_2Ph)]^-$.

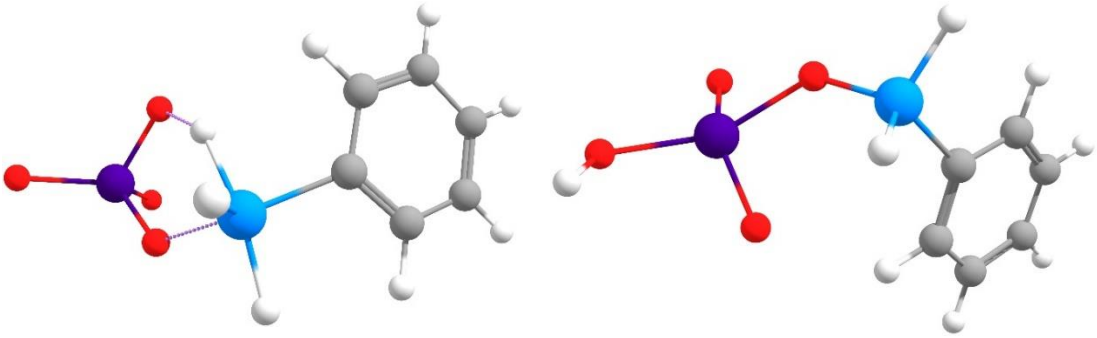

Figure 8 a. TS for [3+2] reaction of perrhenate and phenylsilane b. [3+2] product.

An alternative activation of the silicon-hydrogen bond can be achieved through a [3+2] mechanism in which the perrhenate oxo abstracts a proton from the H_3SiPh to produce a hydroxide ligand (Figure 8). This also occurs through a five coordinate silicon transition state where the silicon hydrogen bond is elongated to 1.67 Å and where $\Delta G_{benzene}$ = +19.2 kcal mol^{-1}/ ΔG_{DMF} = +25.4 kcal mol^{-1} (Figure 8a). Unusually, the geometry of the product is of a strongly distorted tetrahedral geometry at Re with angles O(2)-Re-O(5) = 142.5° and O(3)-Re-O(4) = 147.4° (Figure 8b). Formation of this hydroxide product is slightly less favourable than the rhenium-hydride with $\Delta G_{benzene}$ = -5.1 kcal mol^{-1}/ ΔG_{DMF} = +1.6 kcal mol^{-1}.

Noting that a rhenium-hydride is not seen experimentally, it might be expected that the [2+2] product and [3+2] products tautomerise which is a known reaction of hydroxide ligands; for example, in $[Re(OH)(EtC{\equiv}CEt)_3]$ the hydrogen migrates intramolecularly to the rhenium.[31] Yet for $[NMe_4][ReH(O)_3(OSiH_2Ph)]$, the activation energy of this process is +22.3 kcal mol^{-1} in benzene and +29.4 kcal mol^{-1} for DMF, therefore as the free energies for the [2+2] and [3+2] transition states are lower than that for tautomerisation, it is not likely process. This is similar to calculations for the hydrosilylation catalyst $[MoO_2Cl_2]$ where the energy for such a hydrogen transfer was found to be higher than the formation of the products either side of the transition state.[29]

In spite of a lack of experimental evidence to support a rhenium-hydride for $[N(hexyl)_4][ReO_4]$, we still considered this mechanism as a similar case can be seen with the related catalyst $[MoO_2Cl_2]$. When Royo and coworkers reported $[MoO_2Cl_2]$ as a catalyst for the hydrosilylation of aldehydes and ketones, it was also noted that they were unable to observe any intermediates or hydrides by ^1H NMR spectroscopy.[32] A previous DFT study on $[MoO_2Cl_2]$ by Calhordra and coworkers attempted to explain

this by the possibility of a radical mechanism but were unable to distinguish whether it was more favourable than the [2+2] mechanism using the 6-31G(d,p) basis set. However, as mentioned above, work by Drees and Strassner using the 6-311++G(d,p) basis set ruled out the [3+2] mechanism and tautomerisation between the two. Formation of radicals was not studied in this later work but using the same methodology (where the intermediates were identified but no transition states) in this work the formation of radicals can be shown to be unfavourable with the homolytic cleavage of the rhenium-hydride bond being +41.2 and +41.5 kcal mol^{-1} in benzene and DMF respectively.

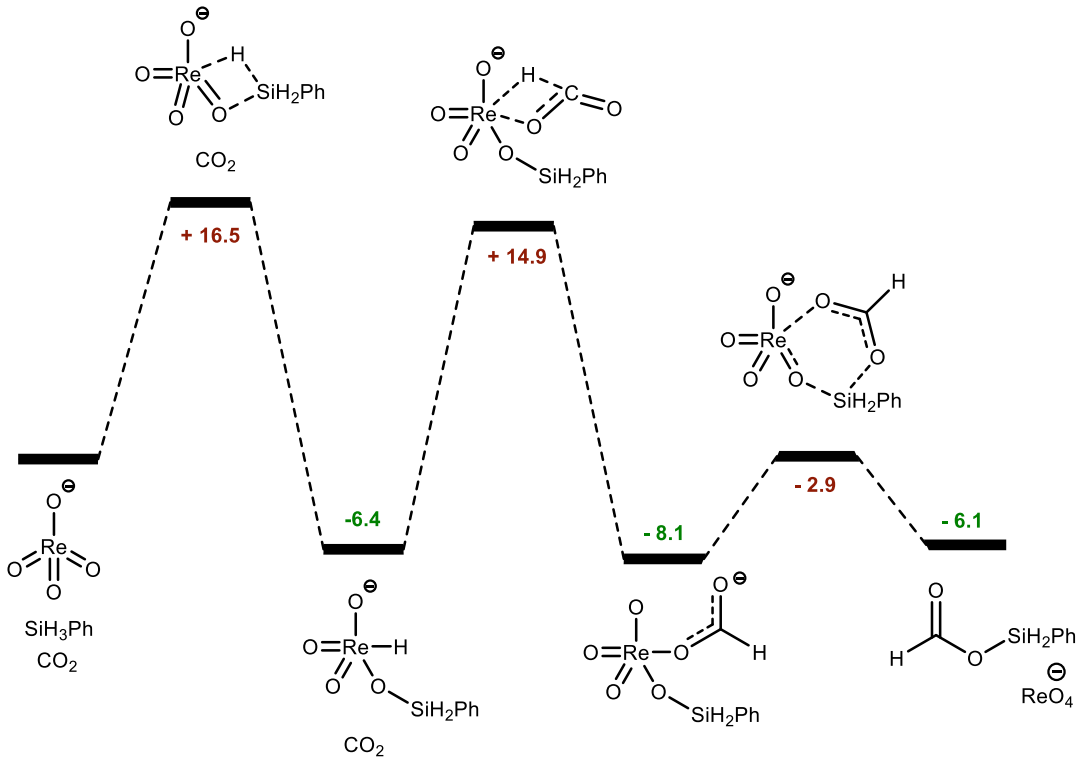

Scheme 9 Energy profile for mechanism starting with [2+2] addition of H_3SiPh to perrhenate in benzene.

Insertion of CO_2 into the rhenium-hydride bond leading to the metal formate can occur directly without initial coordination of CO_2 to the rhenium. In the transition state, H-Re-O bond angle increases from 109.4° to 134.1° in order for rhenium to coordinate to the proximate oxygen of the CO_2, while the substrate itself is bent with and O-C-O angle of 145.2° and a strong carbon-hydride interaction with a C-H distance of 1.37 Å (Figure 9). This step requires a change in free energy to +14.9 kcal mol^{-1} in benzene and +20.8 kcal mol^{-1} in DMF. Whilst lower than the activation energy for formation of the hydride in benzene, this is slightly higher than the same step in DMF, suggesting

that the solvent can affect the rate determining step. Interestingly, this step contrasts Wu's study of Toste's catalyst where coordination of the substrate occurred in advance of reduction.

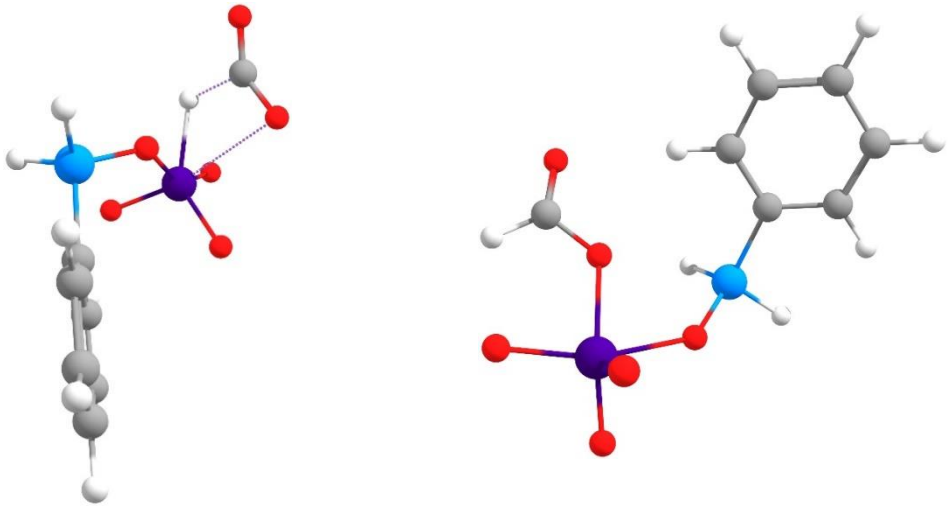

Figure 9 a. TS for insertion of CO2 into Re-H bond and b. rhenium-formate product.

Transfer of the hydride to CO_2 in order to produce free formate was also considered and has a slightly lower barrier: $\Delta G_{benzene}$ = +11.7 kcal mol^{-1}/ ΔG_{DMF} = +19.1 kcal mol^{-1}. It is unclear whether the formate is ever "free" as the energies for the formation of formate and a neutral rhenium complex are much larger than the transition state. Additionally, further re-organisation of the formate would be necessary for coordination yet no evidence or additional transition states for this have been located. Based on this evidence, the direct insertion of CO_2 into the rhenium-hydride bond appears a more likely candidate.

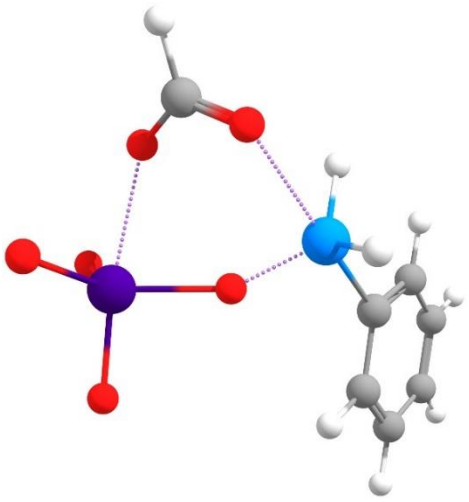

Figure 10 TS for the attack of the formate ligand on the silicon centre to form perrhenate and silyl formate.

The formate ligand then attacks the silicon with the uncoordinated oxygen through a six-membered cyclic transition state rather than through a retero-[2+2] addition through the coordinated oxygen (Figure 10) as seen in some computational mechanisms for the reduction of aldehydes.[28, 29] This step releases the silylformate product and reforms the perrhenate catalyst. For this step the transition state is very low; $\Delta G = +5.2$ kcal mol^{-1} in both benzene and DMF showing that once the metal-formate is produced, the formate is quickly transferred to the silicon with little difficulty.

The distorted geometry of the [3+2] mechanism appears to be a logical starting point for the CO_2 reduction, where it has essentially opened up a coordination site on the rhenium. The transition state for this process shows a bent CO_2 coordinated with a O-C-O angle of 117.4° and the carbon 1.47 Å from the hydrogen. However, the process is relatively high in energy with an increase in free energy $\Delta G_{benzene} = +24.8$ kcal mol^{-1}/ $\Delta G_{DMF} = +32.8$ kcal mol^{-1} (Scheme 10).

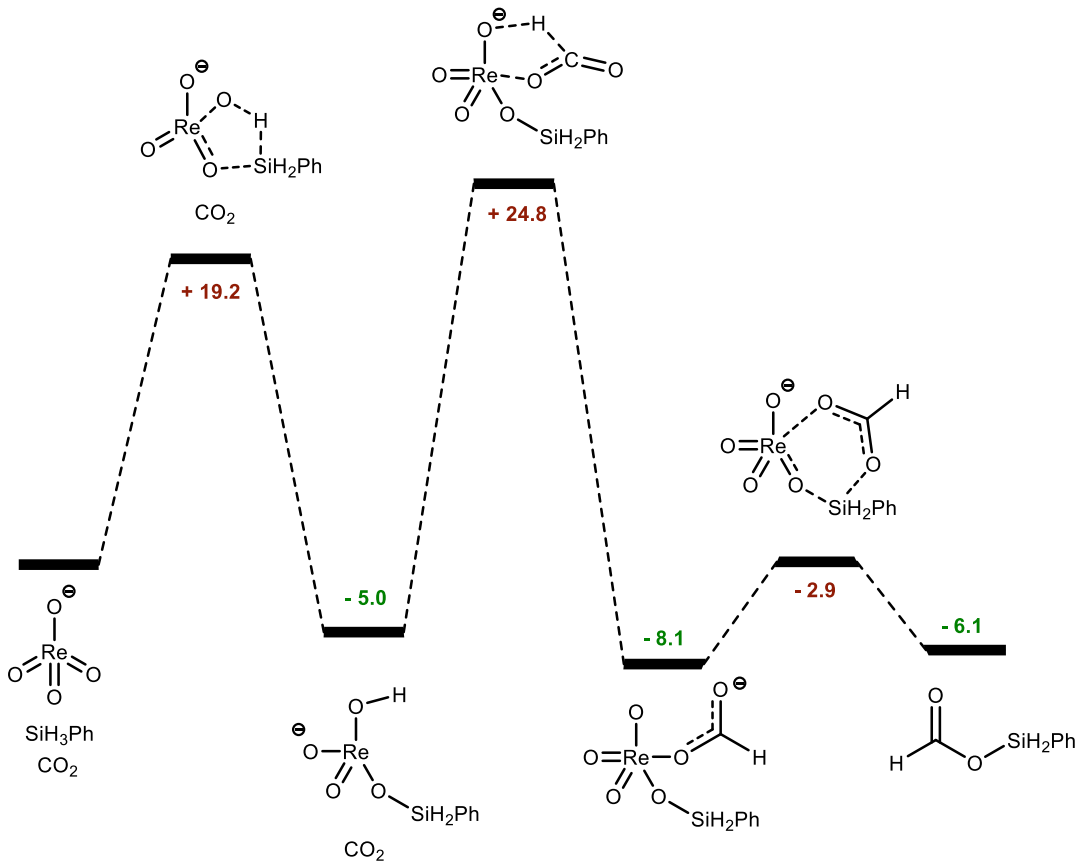

Scheme 10 Scheme for the reduction of CO_2 starting from the [3+2] addition product of phenylsilane to perrhenate in benzene.

Previously it was noted that the rhenium-carbonate was sought experimentally and while it was not identified in the reaction mixtures, its formation was studied by DFT calculations which help clarify why it was not seen by NMR spectroscopy. The transition state for the formation of $[ReO_3(\kappa^2\text{-}CO_3)]^-$ shows a strong interaction between the rhenium-oxo and carbon atom (Figure 11a), pulling the second oxygen atom close to the rhenium centre to which it eventually coordinates (Figure 11b). The carbonate ligand in the product is not symmetrically bound due to the *trans* influence of an oxo ligand. With rhenium-oxygen bonds of 2.01 Å and 2.21 Å, these are significantly longer than that of perrhenate (average 1.76 Å). The carbon-oxygen bonds are also elongated from 1.16 Å in the free CO_2 to 1.32 Å, 1.37 Å, and 1.20 Å. These results are very similar for those found both computationally and experimentally for $[MoO_3(\kappa^2\text{-}CO_3)]^{2-}$.[20]

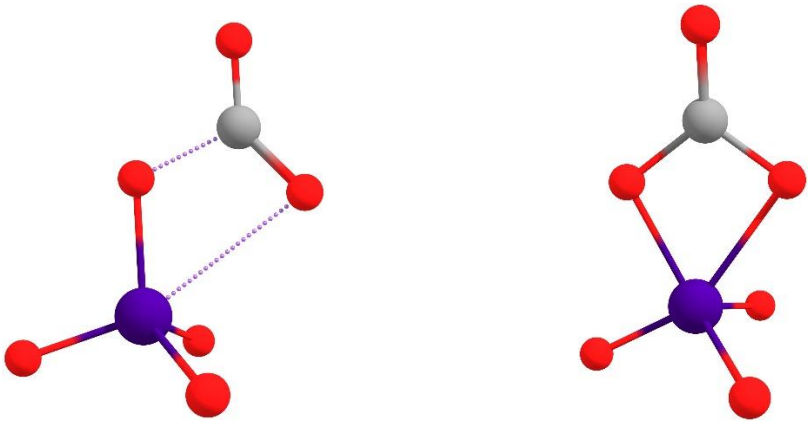

Figure 11 a. TS for coordination of CO_2 to perrhenate to form $[ReO_3(\kappa^2\text{-}CO_3)]^-$ b. $[ReO_3(\kappa^2\text{-}CO_3)]^-$.

Unlike the formation of $[MoO_3(\kappa^2\text{-}CO_3)]^{2-}$ which was exergonic and exothermic, for $[ReO_3(\kappa^2\text{-}CO_3)]^-$ the formation is both endergonic and endothermic (Scheme 11). In benzene the transition state has a change in free energy of $\Delta G_{benzene}$ = +15.6 kcal mol^{-1}/ ΔG_{DMF} = +18.3 kcal mol^{-1}, with the products resting only slightly below this at +10.5 kcal mol^{-1}/ 12.3 kcal mol^{-1} respectively. Whilst these energies are more favourable than either the [2+2] or [3+2] mechanisms, the product is not stable as the activation energy for the reformation of the perrhenate anion and CO_2 is only +5.1 kcal mol^{-1}.

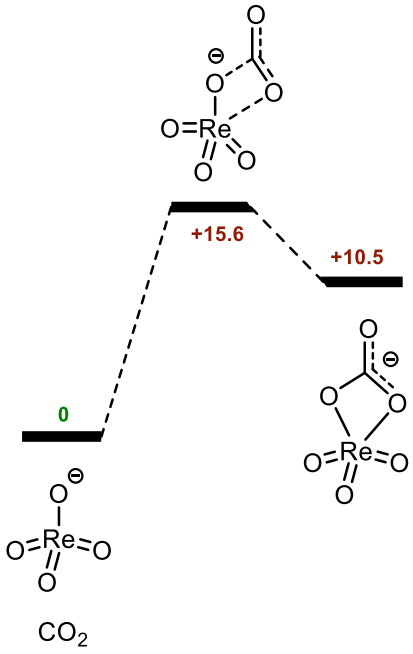

Scheme 11 Energy profile for the formation of $[ReO3(\kappa^2\text{-}CO_3)]^-$.

In addition to the apparently unstable carbonate product, no transition state was found for the its reaction with H_3SiPh, with relaxed potential energy surface scans ran varying the distance between oxygen and silicon for all three oxygens of the carbonate. Inability to find a transition state for the formation of a silylformate combined with unstable product suggests that this is not the correct intermediate in the catalytic cycle.

From these calculations it is seen that starting from the hydride is the more favourable mechanism for CO_2 reduction, which is a reactivity similar to other metal-oxo complexes. This matches the propensity of rhenium to form hydrides. However, it is unfortunate that while the hydride route has been shown to be energetically possible, there is currently no experimental evidence to prove this mechanism and therefore the results should be taken with caution. Throughout these studies, the energies for the reactions in DMF have been higher than those in benzene, yet experimentally the reactions proceed more rapidly in DMF. This is interesting as it suggests benzene is the better solvent for the reaction therefore if the concentrations of CO_2 in solution can be increased to match that of DMF (by increasing the pressure of CO_2 in the reaction), the reaction can be improved upon without the need for expensive or potentially interfering solvents (for example reduction of the carbonyl group on DMF). This is supported by the experimental evidence that the reactions do indeed proceed faster at 2 bar of CO_2.

Hydroboration of Aldehydes and Ketones

Using $[(PPh_3)_2Re(O)_2I]$, Fernandes expanded on the work of Toste, activating the B-H bonds of pinacolborane (HBpin) and catecholborane (HBcat) in order to catalyse the reduction of sulfoxides.[33] The rhenium-hydride complex $[(PPh_3)_2ReH(O)(OBpin)I]$, analogous to that synthesised from $HSiMe_2Ph$ was isolated and characterised crystallographically, suggesting that hydroboranes may react very similarly to hydrosilanes with metal-oxo catalysts.

As such, the perrhenate $[N(hexyl)_4][ReO_4]$ was tested as a catalyst for this reaction. Immediately upon addition of 1.2 equivalents of pinacolborane to a solution of benzaldehyde with a 2.5 mol % catalyst loading, the colourless solution turns brown and the ^1H NMR spectrum shows that the boronic ester has formed in 39.1 % yield. Allowing the reaction to sit at room temperature the yield increased to 71.9 % after 12 h. In addition to this, the substrate is not fully consumed due to the apparent consumption of pinacolborane by a side reaction. To illustrate this another reaction with 2 equivalents of pinacolborane showed complete conversion of the benzaldehyde immediately yielding 73.6 % of the boronic ester.

The complete consumption of substrate is repeated with acetophenone giving a yield of 61.5 % with 1.2 equivalents of pinacolborane after 12 h but 99.8 % with 2 equivalents afte 5 min. Furthermore, benzophenone gives 67.9 % and 97.9 % with 1.2 equivalents and 2 equivalents, respectively. (The lower yield for benzaldehyde appears to be due to the production of an unidentified byproduct when 2 equivalents are used. This is not, however, typical of the reactions presented below in Table 5.)

Table 5 Hydroboration of carbonyl compounds using 2.5 mol % $[N(hexyl)_4][ReO_4]$, 1.2 eq HBpin in C_6D_6 at room temperature for 12 h.

Entry	Substrate	Conversion (%)	Yield (%)
1	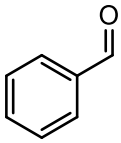	73.7	71.9
2	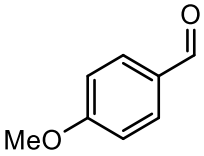	84.0	82.1
3	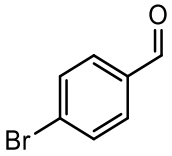	100	98.9
4	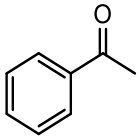	64.9	61.5
5	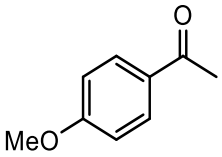	66.9	66.6
6	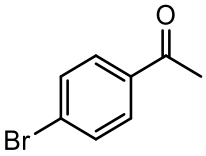	76.7	72.8
7	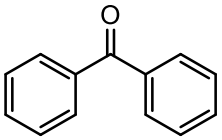	68.7	67.9

This method is applicable to a number of functionalised aldehydes and ketones (Table 5). Noticeably higher yields are achieved in carbonyl reduction with HBpin than H_3SiPh and furthermore no heating is required. While more pinacolborane is needed for full conversion to compensate for side reactions, this presents a promising alternative to reduction of carbonyl compounds with hydrosilanes.

Hydroboration of CO_2

As reduction of carbonyl compounds was observed with pinacolborane as well as hydrosilanes, some preliminary reactions with CO_2 were carried out. Using CO_2 (1 bar) and pinacolborane (0.2 mmol) with 2.5 mol % $[N(hexyl)_4][ReO_4]$ in C_6D_6, the reaction appeared to start immediately with several new resonances forming in the ^{1}NMR spectrum, notably, all of which were similar to those reported by Bontemps and Sabo-Etienne in their report of the reduction of CO_2 by HBpin using the ruthenium hydride $[(PCy_3)_2Ru(H)_2(H_2)_2]$.[15] At 3.51 ppm a resonance assigned to MeOBpin is present and another at 5.48 ppm for $CH_2(OBpin)_2$. A resonance at 9.17 ppm is in the region expected for a formate, although this differs from that reported previously for HC(O)OBpin is 8.13 ppm. In our eye it is possible that the formate resonance is shifted due to the presence of HOBpin, formed by reaction with water present in the solvent; the published study used dry solvents for this reaction. Finally a product assigned as $HC(O)OCH_2OBpin$ can be seen at 5.39 ppm with the corresponding formate proton visible at 7.41 ppm which is, again, slightly shifted from the published values. As previously mentioned, this compound is synthesised from the reaction of *in situ* generated formaldehyde with HC(O)OBpin (Scheme 12).

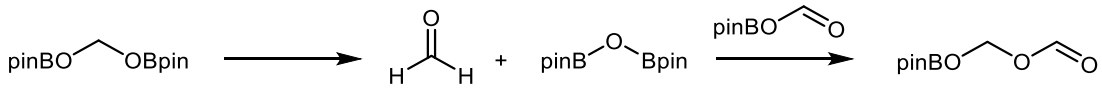

Scheme 12 Production of $OHCOH_2COBpin$ by reaction of OHCOBpin with transient formaldehyde.

When allowed to sit for 16 h, the resonances for both HC(O)OBpin and MeOBpin grow with the latter being the major product. The reaction was left for 16 h and seen to slowly proceed at room temperature but heating for 1 h at 80 °C significantly increased the MeOBpin product, whilst the other two products remained present in the same quantities. Heating for another 2 h slightly increased the yield of MeOBpin and with HBpin still visibly present in the reaction; presumably the catalyst is significantly less active at this point (HBpin is the limiting reagent).

While these are only preliminary results, they do point towards a similar mechanism to that of the hydrosilylation of CO_2, in which CO_2 is first reduced to the formate, then to the transient boronic acetal which produces formaldehyde, which is then swiftly reduced to the boronic ester. Also similarly, when the $[N(hexyl)_4][ReO_4]$ was reacted on a stoichiometric scale with two equivalents of HBpin, no hydride or discrete product

could be identified; a number of multiplets from − 6.2 to −7.4 ppm are observed which is similar to the stoichiometric reactions of perrhenate with hydrosilanes. Hydrogen gas can be seen at 4.47 ppm. A reaction conducted in d_7-DMF with only 2.5 mol % catalyst showed such rapid consumption of the HBpin that CO_2 was not able to be added. During this rapid reaction a gas was evolved, presumably hydrogen which is visible in the ^{1}H NMR spectrum at 4.56 ppm. It is unclear what process is occurring here, although the catalytic dehydrocoupling of boranes to make diboranes is known which would explain the generation of hydrogen without catalyst decomposition. However, no attempts to identify by products of this reaction were made. Furthermore no $CHD_2C(CD_3)_2$ is seen in this reaction ruling out significant reduction of the solvent as cause of HBpin consumption. However, considering that two equivalents of HBpin are required for full conversion of aldehyde and ketone substrates, it is clear that there is a second route in which the borane is consumed.

When the reaction is conducted in CD_3CN, the same products can be observed in the spectrum, apart from $OCHOCH_2OBpin$ which appears to have been reduced further to H_3COCH_2OBpin with resonances at 5.15 and 2.99 ppm. (There is no formate resonance present that can be assigned to $OCHOCH_2OBpin$.) To this reaction an excess of water (2.8 eq) was added which showed the conversion of the MeOBpin, after brief heating, to MeOH although quantification of this has not yet been attempted. Surprisingly the acetal appears to be tolerant of the water, possibly requiring longer heating times to release formaldehyde. This may in fact be beneficial if the acetal is to be used as a CH_2 synthon because predrying of reactants should not be necessary.

Bontemps and Sabo-Etienne identified this reaction as a source of C_1 building blocks and later found the *in situ* generated formaldehyde was able to react with primary amines to produce the imine,[26] much in the same way as the formaldehyde generated in the perrhenate hydrosilylation of CO_2 reacted with methylaniline to give $CH_2(MeNPh)_2$. The perrhenate catalyst has been shown to reduce CO_2 to very similar products, and previously capable of functionalising alkyl and aromatic amines with the similar hydrosilane system. Following this, the HBpin route should also be capable of functionalising amines and further using CO_2 as a C_1 building block, adding a new set of reactions to the already versatile perrhenate catalyst.

Conclusions

The high oxidation state ammonium perrhenate proves to be a capable catalyst for the reduction of various substrates containing C=X multiple bonds (X = O, N) in a host of solvents. As with many other high oxidation state catalysts, it is tolerant of air and moisture even in reaction conditions that are often studied under rigorously anaerobic conditions.[1] In addition the simple synthesis of the catalyst from commercial precursors allows the multigram synthesis of a product that is highly soluble in many organic solvents, in a matter of hours.

That a 6 electron reduction of CO_2 can be achieved with such mild reducing agents as hydrosilanes and boranes using the simple perrhenate anion shows the strengths of the metal-oxo activation of Si-H and B-H bonds. Indeed, as Oestriech notes, reduction to methoxysilanes is not a common product from hydrosilane reactions.[34] However, the ability to convert CO_2 into various C_1 synthons is perhaps more interesting as it facilitates additional uses for the abundant and cheap feedstock as reagents for important transformations with a versatile and easy to handle catalyst. Production of the $H_3COH_2COSi(OH)Ph_2$ product demonstrates an additional production of C_2 compounds from CO_2.

Based on previous reports of high oxidation state hydrosilylation and hydroboration catalysts, a mechanism beginning with a metal hydride is proposed. While unfortunately (and despite significant efforts) the hydride could not be isolated or seen by ^{1}H NMR spectroscopy, DFT calculations showed that $[HReO_3(OSiH_2Ph)]^-$ is not only a possible intermediate, but that its formation is more favourable than $[(HO)ReO_2(OSiH_2Ph)]^-$ or $[ReO_3(\kappa^2\text{-}CO_3)]^-$. As such, this shows similarities with findings from other studies high oxidation state hydrosilylation catalysts and includes perrhenate in this unique set of catalysts which make use of the metal-oxo bond for reductive chemistry.

References

1. J. J. Kennedy-Smith, K. A. Nolin, H. P. Gunterman and F. D. Toste, *Journal of the American Chemical Society*, 2003, 125, 4056-4057.
2. E. A. Ison, E. R. Trivedi, R. A. Corbin and M. M. Abu-Omar, *Journal of the American Chemical Society*, 2005, 127, 15374-15375.
3. G. Du, P. E. Fanwick and M. M. Abu-Omar, *Journal of the American Chemical Society*, 2007, 129, 5180-5187.
4. I. Cabrita, S. C. A. Sousa and A. C. Fernandes, *Tetrahedron Letters*, 2010, 51, 6132-6135.
5. C. Ghosh, T. K. Mukhopadhyay, M. Flores, T. L. Groy and R. J. Trovitch, *Inorganic Chemistry*, 2015, 54, 10398-10406.
6. F. J. Fernandez-Alvarez, A. M. Aitani and L. A. Oro, *Catalysis Science & Technology*, 2014, 4, 611-624.
7. H. Koinuma, F. Kawakami, H. Kato and H. Hirai, *Journal of the Chemical Society, Chemical Communications*, 1981, 213-214.
8. P. Deglmann, E. Ember, P. Hofmann, S. Pitter and O. Walter, *Chemistry – A European Journal*, 2007, 13, 2864-2879.
9. T. Matsuo and H. Kawaguchi, *Journal of the American Chemical Society*, 2006, 128, 12362-12363.
10. F. A. LeBlanc, W. E. Piers and M. Parvez, *Angewandte Chemie International Edition*, 2014, 53, 789-792.
11. T. C. Eisenschmid and R. Eisenberg, *Organometallics*, 1989, 8, 1822-1824.
12. S. N. Riduan, Y. Zhang and J. Y. Ying, *Angewandte Chemie International Edition*, 2009, 48, 3322-3325.
13. B. Aurian-Blajeni, in *Electrochemistry in Transition: From the 20th to the 21st Century*, eds. O. J. Murphy, S. Srinivasan and B. E. Conway, Springer US, Boston, MA, 1992, pp. 381-396.
14. C. C. Chong and R. Kinjo, *Angew. Chem., Int. Ed. Engl.*, 2015, 54, 12116-12120.
15. S. Bontemps and S. Sabo-Etienne, *Angewandte Chemie International Edition*, 2013, 52, 10253-10255.
16. F. Huang, G. Lu, L. Zhao, H. Li and Z.-X. Wang, *Journal of the American Chemical Society*, 2010, 132, 12388-12396.
17. V. P. Taori and M. R. Buchmeiser, *Chemical Communications*, 2014, 50, 14820-14823.
18. P. Schärringer, T. E. Müller and J. A. Lercher, *Journal of Catalysis*, 2008, 253, 167-179.
19. K. A. Nolin, J. R. Krumper, M. D. Pluth, R. G. Bergman and F. D. Toste, *Journal of the American Chemical Society*, 2007, 129, 14684-14696.
20. I. Knopf, T. Ono, M. Temprado, D. Tofan and C. C. Cummins, *Chemical Science*, 2014, 5, 1772-1776.
21. O. Jacquet, X. Frogneux, C. Das Neves Gomes and T. Cantat, *Chemical Science*, 2013, 4, 2127-2131.
22. O. Santoro, F. Lazreg, Y. Minenkov, L. Cavallo and C. S. J. Cazin, *Dalton Transactions*, 2015, 44, 18138-18144.
23. U. B. S. L. V. Ondrus, *Arkivoc*, 2005, 2005, 147.
24. Y. Li, X. Fang, K. Junge and M. Beller, *Angewandte Chemie International Edition*, 2013, 52, 9568-9571.
25. X. Frogneux, E. Blondiaux, P. Thuéry and T. Cantat, *ACS Catalysis*, 2015, 5, 3983-3987.
26. S. Bontemps, L. Vendier and S. Sabo-Etienne, *Journal of the American Chemical Society*, 2014, 136, 4419-4425.
27. L. González-Sebastián, M. Flores-Alamo and J. J. García, *Organometallics*, 2015, 34, 763-769.

28. L. W. Chung, H. G. Lee, Z. Lin and Y.-D. Wu, *The Journal of Organic Chemistry*, 2006, 71, 6000-6009.
29. M. Drees and T. Strassner, *Inorganic Chemistry*, 2007, 46, 10850-10859.
30. P. J. Costa, C. C. Romão, A. C. Fernandes, B. Royo, P. M. Reis and M. J. Calhorda, *Chemistry – A European Journal*, 2007, 13, 3934-3941.
31. S. K. Tahmassebi, R. R. Conry and J. M. Mayer, *Journal of the American Chemical Society*, 1993, 115, 7553-7554.
32. A. C. Fernandes, R. Fernandes, C. C. Romao and B. Royo, *Chemical Communications*, 2005, 213-214.
33. A. C. Fernandes, J. A. Fernandes, F. A. Almeida Paz and C. C. Romao, *Dalton Transactions*, 2008, 6686-6688.
34. T. T. Metsänen and M. Oestreich, *Organometallics*, 2015, 34, 543-546.

3. Deoxydehydration of Polyols

In the search for renewable chemicals, much attention has been drawn towards biomass as a potential source for feedstocks and fuels. However, the high oxygen content of products derived from biomass is a barrier in their use for these purposes. As such, new synthetic transformations must be developed in order to overcome the difficulties involved. One such transformation is the deoxydehydration (DODH) reaction which converts polyols to alkenes.

The first example of this reaction was shown by Cook and Andrews in 1996 who used [Cp*ReO_3] to catalyse the reduction of 1-phenyl-1,2-ethanediol (styrene diol) using PPh_3 as the reducing agent (Scheme 1).[1] They showed full conversion of the diol to styrene after 25 h at 90 °C with $OPPh_3$ and water as byproducts. An acid co-catalyst (*p*-toluenesulfonic acid (pTsA), 27.5 mol %) accelerated the reaction to give a 91 % yield after 13 h. It was presumed that this prevented deactivation of the catalyst through reduction to Re^{III} by accelerating formation of the glycolate.

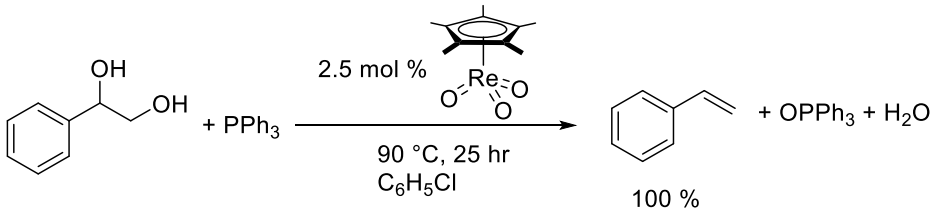

Scheme 1 DODH of styrene diol using [Cp*ReO_3].[1]

This is not the only time that an acid has been shown to accelerate the DODH reaction, Abu-Omar reported the disproportionation of glycerol where glycerol is the reducing agent for itself in a transfer hydrogenation reaction. Addition of 2 mol % of both the catalyst methyltrioxorhenium (MTO) and HCl at 165 °C reduced the reaction time from 2 h (in the absence of HCl) to 1 h with full conversion.[2] NH_4Cl was also shown to give the same results which were also similar to those of [NH_4][ReO_4], presumably also acting as a proton source under the high temperature conditions. Bergman also found that catalytic amounts of either pTsA or H_2SO_4 showed a reduction in reaction time using either [$Re_2(CO)_{10}$] or [$BrRe(CO)_5$] even at lower temperatures which is vital as polyols often decompose at high temperatures.[3]

Protic Perrhenate Salts

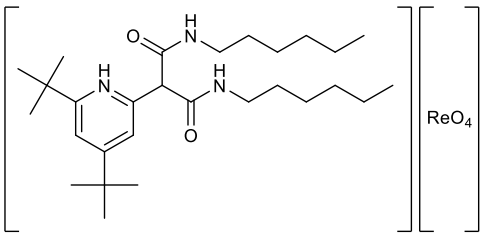

Figure 1 The pyridinium perrhenate salt [HL][ReO_4].

The pyridinium perrhenate salt [(4,6-$Bu^t_2C_5H_2NH$-2-CH{(CO)NH(C_6H_{13})}$_2$][ReO_4] ([HL][ReO_4], Figure 1) has previously been synthesised and has been shown to significantly enhance the catalytic behaviour of perrhenate as an epoxidation catalyst, exploiting the effect of the hydrophobic organic phase.[4] Due to the organic soluble protic counterion, [HL][ReO_4] was investigated as a catalyst for the DODH reaction of styrene diol with triphenylphosphine. With a 2.0 mol % loading, the salt catalysed the reaction in C_6D_6 to give 91 % of styrene after 15 h at 80 °C.

Exhibiting a faster conversion of styrene diol than previously reported in the work of Cook and Andrews and at a lower temperature, it was important to understand what the cause of this was. The $[HL]^+$ cation was originally developed as a chlorometalate extractant,[5] therefore certainly is responsible for improving the solubility of the perrhenate anion in the hydrophobic reaction medium. As the previously studied perrhenates that have been screened as catalysts ([NH_4][ReO_4] and [N(butyl)$_4$][ReO_4]) exhibit low solubilities, even at 80 °C in C_6D_6, it may appear that this is an effect of the solubility of the salt but it is unclear whether the protonated counterion plays a larger role than solubility. In order to understand this, a number of ammonium salts of perrhenate were prepared.

For the synthesis of [H_3N(hexyl)][ReO_4] and [H_2N(hexyl)$_2$][ReO_4], 75 % perrhenic acid in H_2O was added to the neat amine, immediately affording the solid salt which was suspended in hexane before filtering. [HN(hexyl)$_3$][ReO_4] was synthesised by adding the perrhenic acid to a toluene solution of the amine, drying with $MgSO_4$ and removing the solvent under reduced pressure to afford an oil. The synthesis of [N(hexyl)$_4$][ReO_4] was previously described in Chapter 2.

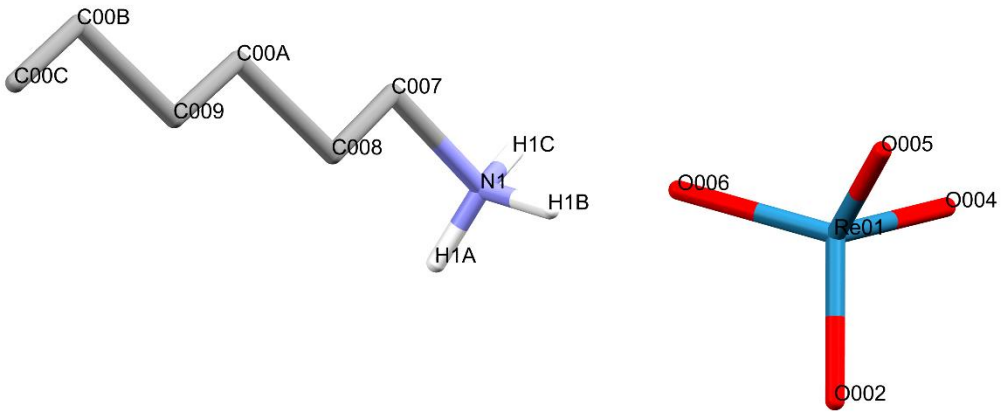

Figure 2 Solid state structure of $[H_3N(hexyl)][ReO_4]$. For clarity hydrogen atoms on the carbon backbone have been omitted.

Crystals of $[H_3N(hexyl)][ReO_4]$ suitable for X-ray diffraction were grown by the slow diffusion of hexane into a benzene solution and the solid state structure is shown in Figure 2. The rhenium-oxo bond lengths are 1.718(2)-1.724(2) Å and form a tetrahedron with angles between 111.75(11)-107.50(11) °. These bond lengths and angles are comparable to those of $KReO_4$.[6] The packing of the ion pair in the crystal is a ladder-type stacking with hexylammonium cations alternating in direction, facing channels of perrhenate anions (Figure 3).

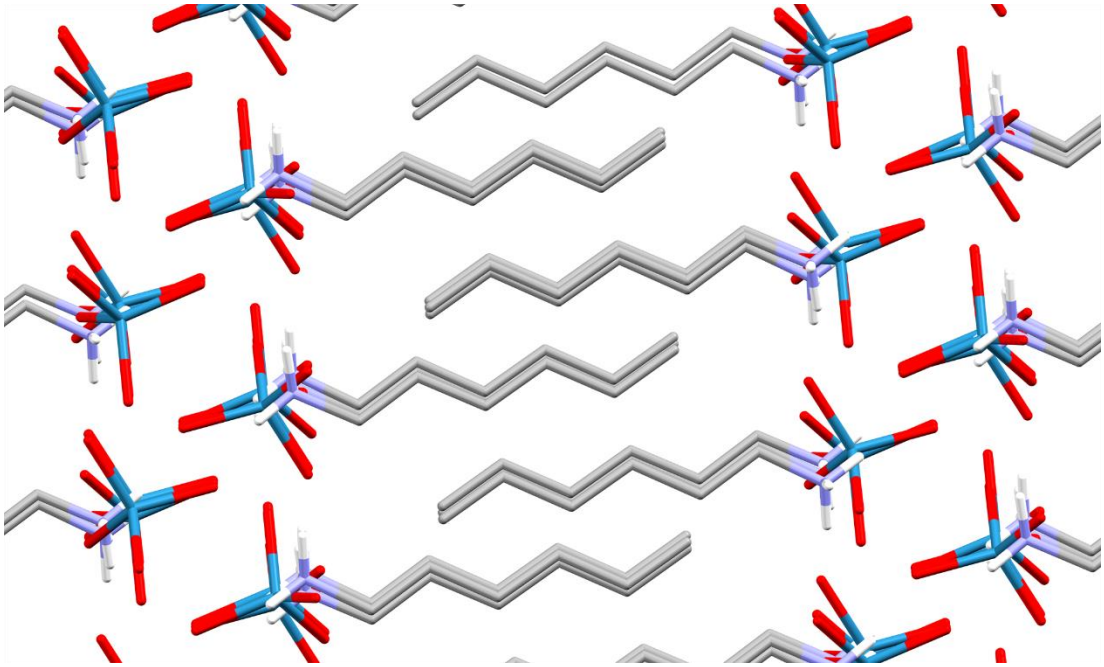

Figure 3 Packing of $[H_3N(hexyl)][ReO_4]$. For clarity hydrogen atoms on the carbon backbone have been omitted.

As catalysts for the DODH reaction there is not a large difference in performance between $[H_3N(hexyl)][ReO_4]$, $[H_2N(hexyl)_2][ReO_4]$ and $[HN(hexyl)_3][ReO_4]$ where yields of styrene are 46.6 %, 46.7 % and 53.2 % respectively are seen despite all of these compounds being highly soluble in C_6D_6 (Table 1). However, $[N(hexyl)_4][ReO_4]$ performed very poorly showing only 10.0 % conversion after 15 h at 80 °C. Additional experiments using $[N(butyl)_4][ReO_4]$ and $[NH_4][ReO_4]$ catalysts resulted in poor yields of 9.2 % and <1 % respectively, even at 5 mol % catalyst loading. As previously mentioned $[N(butyl)_4][ReO_4]$ and $[NH_4][ReO_4]$ both have poor solubilities in C_6D_6 therefore likely hindering their ability as catalysts, yet comparison with $[N(hexyl)_4][ReO_4]$ shows that solubility is only partially responsible for the effectiveness of the catalyst.

Certainly the protonated counterion appears highly important in the reaction, yet a considerable difference is still observed between the $[HL][ReO_4]$ and the alkylammonium perrhenates. All are soluble in the reaction solvent, C_6D_6, and evidently the number of alkyl chains has little to no effect on the catalyst efficacy. Therefore there must be a difference in how the counterions interact with the catalyst. $[HL]^+$ was initially designed for the extraction of chlorometallates and the bulky *t*-butyl substituents on the pyridinium block interaction of the pyridine nitrogen with the inner sphere of the metal anion it extracts from the aqueous phase and its success as a counterion for this reaction suggests the nucleophilicity of the counterion is important. It should also be noted that pyridines have a lower pKa than amines which may be beneficial towards acting as proton transfer sources. Bergman found alkylamines slowed the DODH reaction[3] and Nicholas observed the same but also that less basic additives slow the reaction less than the more basic additives.[7] This indicates that the free amines present due to deprotonation of the alkylammonium ions during catalysis are causing retardation of the reaction.

Table 1 Performance of various salts of perrhenate in the DODH reaction at 80 °C for 15 h in C_6D_6.

Catalyst	Loading (mol %)	Time (h)	Yield (%)	pKa
$[H_3N(hexyl)][ReO_4]$	2.0	16	44.6	10.56
$[H_2N(hexyl)_2][ReO_4]$	2.5	18	46.7	9.33[8]
$[HN(hexyl)_3][ReO_4]$	2.5	18	53.2	8.53[8]
$[N(hexyl)_4][ReO_4]$	2.0	15	10.0	-
$[N(butyl)_4][ReO_4]$	5.0	15	9.2	-
$[NH_4][ReO_4]$	5.1	15	< 1	9.25
$[HL][ReO_4]$	2.0	15	91.0	-
$[Lut][ReO_4]$	2.5	15	85.9	6.2[9]
$[Clpy][ReO_4]$	2.3	15	88.4	2.0[9]
$[DTBMP][ReO_4]$	1.7	15	100	4.41[10]

In order to test the effects of varying the basicity of the counterion, several pyridinium perrhenates were targeted. Using the same method as for the alkylammonium perrhenates, [2,6-dimethylpyridinium][ReO_4] [Lut][ReO_4] (Scheme 2) and [2-chloropyridinium][ReO_4] ([Clpy][ReO_4]) were synthesised. [2,6-di-*tert*-butyl-4-methylpyridinium][ReO_4] ([DTBMP][ReO_4]) was obtained by adding perrhenic acid to a toluene solution of 2,6-di-*tert*-butyl-4-methylpyridinie, isolating the precipitated solid and washing with hexane.

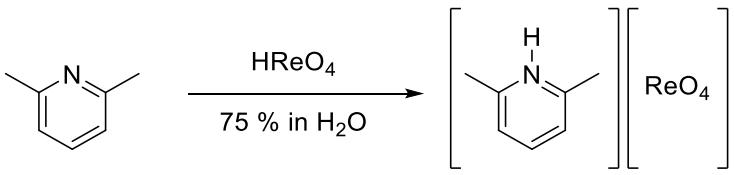

Scheme 2 Synthesis of [Lut][ReO_4] from lutidine and perrhenic acid.

These pyridinium catalysts demonstrated a much higher conversion of the styrene diol substrate (Table 1). [DTBMP][ReO_4] was the most capable, giving 100 % yield of styrene in 15 h at 80 °C, despite its poor solubility in C_6D_6. [Clpy][ReO_4] was the next best catalyst with 88.4 % yield, followed by [Lut][ReO_4] with 85.9 % yield. There are two explanations as to why these pyridinium perrhenates are significantly more active than the alkylammonium perrhenates, the first being the acidity of the proton. The more acidic counterions are more easily deprotonated by the catalyst which,

considering the relative lack of activity for $[N(hexyl)_4][ReO_4]$, appears to be important. A report by Wang proposing a similar role of alcohols as proton sources showed that when alcohols are used as the reducing agent, the alcohol also acts as a proton shuttle which often reduces the energies of the transition states involving the proton transfer.[11] Secondly, the bulky *t*-butyl groups on $[DTBMP]^+$ may prevent favourable interactions such as hydrogen bonding between the pyridinium proton and perrhenate anion catalyst that stabilise intermediates. Additionally the deprotonated "counterion" with steric bulk around the donor nitrogen will be less capable of coordination which has been suggested occurs when donor solvents are available due to the electron deficiencies of the rhenium complexes in question.[12]

Experiments designed in order to understand the effect of an excess of lutidinium cations, in the form of [Lut][Cl], would have on catalysis were conducted. To this end, 1 equivalent of [Lut][Cl] (with respect to the substrate) was added to a reaction with 2.5 mol % $[Lut][ReO_4]$ in $CDCl_3$ as $[Lut][ReO_4]$ was shown to be most effective in this solvent. Surprisingly, rather than increasing the reaction rate, no conversion of the styrene diol was observed after 2 or 4 h. In a control reaction where no [Lut][Cl] had been added, 13.3 % conversion of the substrate was seen after 2 h and 17.6 % after 4 h. Another reaction where only 0.1 equivalent of [Lut][Cl] was added showed a minimal conversion of 2.4 %. Evidently too much of the lutidinium cation impeded the reaction leading to the assumption that the counterions may be able to stabilise intermediates, impeding further reaction. This was surprising as Cook and Andrews added 11 equivalents of pTSA (with respect to the catalyst) and saw a large increase in the rate of catalysis in a polar solvent, THF.[1]

Another point of interest from the control reaction shows that the rate of conversion seems to significantly reduce between 2 and 4 h; compared with initial conversion of 13.3 % after 2 h, only an additional 4.3 % is converted after an additional 2 h. This suggests that the catalyst may be deactivated throughout the reaction. Cook and Andrews suggested that reduction to a Re^{III} species occurs and forms an inactive rhenium species and that this was a result of further reduction of the Re^{V} species. This would suggest that the presence of $[Lut]^+$ is not sufficient to accelerate the formation of the glycolate or that reduction of the glycolate may still occur to produce a Re^{III} product. Fristrup also identified, by *in situ* IR spectroscopy, a catalytically inactive Re^{VII} glycolate whose formation was reversible,[12] which offers another possibility.

With these results, a small solvent survey was conducted to find how the solvents $CDCl_3$ and CD_3CN affected the catalysis. Previously it has been shown that polar solvents such as THF and acetonitrile inhibit the DODH reaction.[1, 7] This is problematic as polyols are often insoluble in apolar solvents and therefore ability to use them as substrates for the DODH reaction is restricted. However, with a marked improvement of the efficiency of the catalysts the reaction may be able to proceed despite the polar interactions that appear to inhibit reaction.

Table 2 Results of a survey on the effects of solvent on the pyridinium perrhenates efficacy on the DODH reaction, 0.2 mmol styrene diol, 0.4 mmol PPh_3, 2 mol % catalyst at 80 °C for 15 h.

Catalyst	Solvent	Conversion (%)	Yield (%)
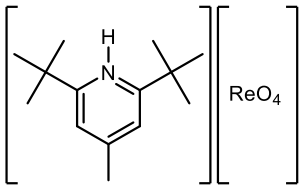	C_6D_6	100	92.6
	$CDCl_3$	58.0	48.1
	CD_3CN	13.2	13.2
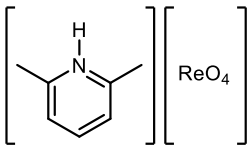	C_6D_6	87.0	87.0
	$CDCl_3$	88.5	92.5
	CD_3CN	< 1	< 1
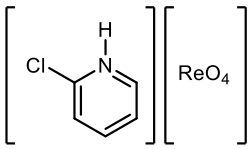	C_6D_6	88.8	90.7
	$CDCl_3$	18.7	18.7
	CD_3CN	8.0	12.0

Table 2 shows the results of this survey although in some cases the conversion appears lower than the yield which are likely due to integration errors. There is a strong preference for the apolar solvent. However, while very little conversion is seen for [Lut][ReO_4] in CD_3CN, it is interesting to note that it is not completely inhibited for [DTBMP][ReO_4] and [Clpy][ReO_4], both exhibiting ca. 12 % conversion. This is still a low conversion but we were pleased to see activity in the more polar solvents was not completely inhibited with these catalysts and higher conversion should be achieved by increasing the reaction temperature.

Mechanism

Two possible routes exist for the mechanism of the DODH reaction, starting with either initial coordination of the diol or initial reduction of the perrhenate with PPh_3. In an attempt to isolate the first intermediate and test the viability of initial coordination of the diol, a reaction between $[HL][ReO_4]$ (1.0 mol %) and styrene diol (0.14 mmol) (but no PPh_3) in C_6D_6 was investigated. Neither the alkoxide product nor the glycolate was observed although unexpectedly styrene was produced by heating this reaction. For this to occur the diol must be able to coordinate to perrhenate as heating styrene diol will not produce styrene in the absence of perrhenate. Furthermore this indicates that styrene diol is acting as both the substrate and reducing agent. Whilst this is not a clean conversion and likely proceeds through alcohol transfer hydrogenation, styrene does appear to be the major product with a 12.3 % yield. One of the byproducts, present in only a very small quantity is an aldehyde, which is visible by the C*H*O proton at 9.62 ppm. There are a number of additional resonances which presumably are the products of concurrent oxidation of styrene diol. Unfortunately, the identities of these compounds could not be identified by ^1H NMR spectroscopy.

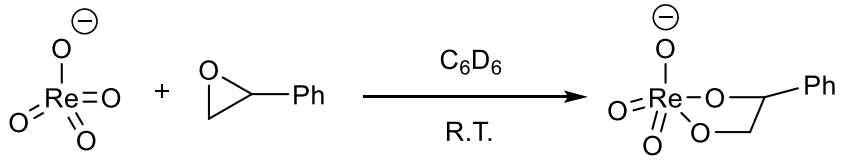

Figure 4 Reaction of perrhenate with styrene oxide to form the rhenium glycolate complex.To understand the mechanism some stoichiometric reactions were conducted. If the reaction proceeds by initial coordination of the diol with loss of water it could be expected that the rhenium-glycolate would be visible in these reactions. Nicholas showed that a glycolate could be synthesised by the reaction of styrene oxide with MTO at room temperature over 24 h.[7] Whilst the reaction rate appears to be slower, a similar reaction occurs with $[HL][ReO_4]$ and $[H_3N(hexyl)][ReO_4]$ at room temperature forming three new sets of resonances at 3.46, 3.56 and 4.60ppm for the former and 3.35, 3.44 and 4.45 ppm for the latter. Nicholas assigned these types of products as rhenium glycolates (Figure 4) and therefore we would suggest that these products are also glycolates.

Interestingly, Nicholas found that $[N(butyl)_4][ReO_4]$ did not react with styrene oxide (nor styrene diol) under similar conditions. Whilst this is likely due to the low solubility of $[N(butyl)_4][ReO_4]$ in C_6D_6, Nicholas presented DFT data showing that ΔH for the formation of the MTO glycolate was -22 kcal mol^{-1}, significantly lower than that for the perrhenate anion which was only -8 kcal mol^{-1}, suggesting that these thermodynamics play a role in the lack of activity for $[N(butyl)_4][ReO_4]$. Certainly, these computational results do explain the observations that $[HL][ReO_4]$ and $[H_3N(hexyl)][ReO_4]$ both form glycolates but much more slowly than MTO. Nonetheless, glycolates are not seen in catalytic reactions but heating these compounds leads to the formation of styrene as well as a number of unidentified byproducts.

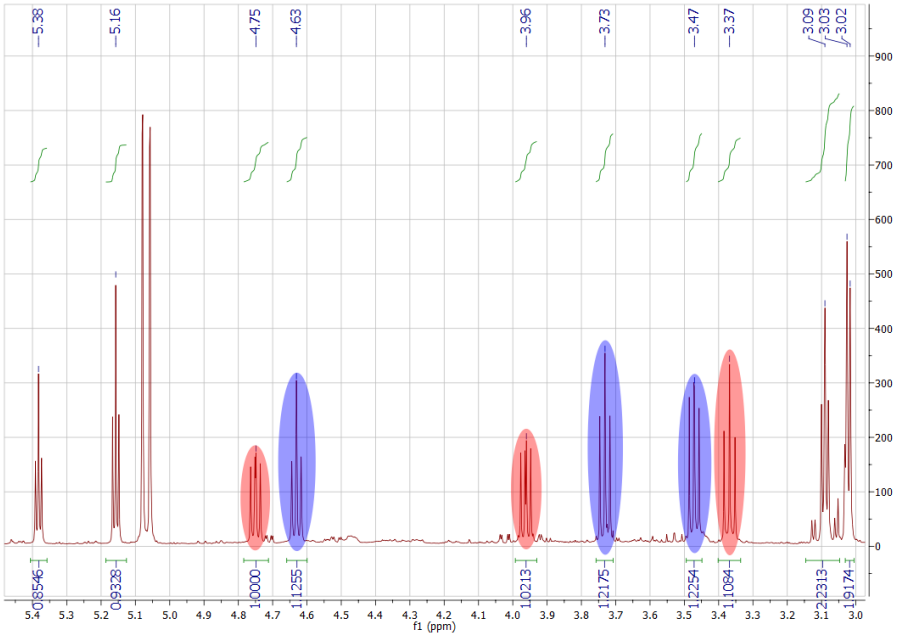

Figure 5 ^{1}H NMR spectrum showing the organic byproducts from the stoichiometric reaction of styrene diol and $[H_3N(hexyl)][ReO_4]$.

The stoichiometric reaction between $[H_3N(hexyl)][ReO_4]$ and styrene diol, heated at 80 °C for 14 h gives a mixture of products (Figure 5), one of which is styrene as seen before (although for clarity it is not shown in the above figure). Further analysis of the ^{1}H NMR and ^{1}H-^{1}H COSY spectra show a set of resonances at 3.37, 3.96 and 4.75 ppm (red) as well as another set at 3.47, 3.73 and 4.63 ppm (blue) which are both in a 1:1:1 ratio. A ^{1}H-^{13}C HSQC experiment confirms that the resonances at 3.36 and 3.95 ppm are attached to the same carbon at 72.77 ppm and those at 3.47 and 3.73 ppm are also attached to the same carbon at 72.05 ppm. Further heating up to 35 h shows full

conversion of styrene diol although significant quantities of the byproducts are still present.

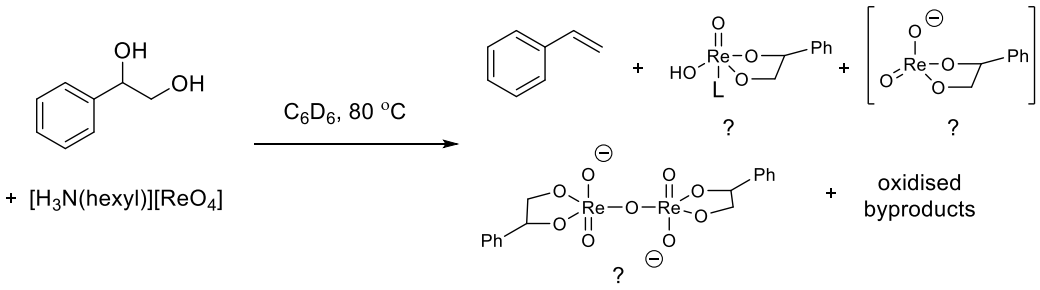

Scheme 3 Stoichiometric reaction between styrene diol and $[H_3N(hexyl)][ReO_4]$ with proposed Re^{V} glycolate and Re^{V}-Re^{VII} dimer products.

Possible identities of these products include the Re^{V} glycolate $[ReO_2(OCH_2CHOPh)]$ and a dimer between the Re^{V} and Re^{VII} glycolates (Scheme 3). An analogue of such a dimer has been spectroscopically identified *in situ* by Fristrup during a MTO catalysed reaction reducing 1,2-tetradecanediol with 3-octanol and is the product of a Re^{VII} glycolate and a Re^{V} glycolate.[12] Alternatively, an adduct of a glycolate and free amine may be present. In either case, the presence of glycolates may be explained by the extrusion of the alkene being slow, possibly the rate determining step as has been suggested for other catalytic systems,[13, 14] or a step with a high energy barrier.[11, 15]

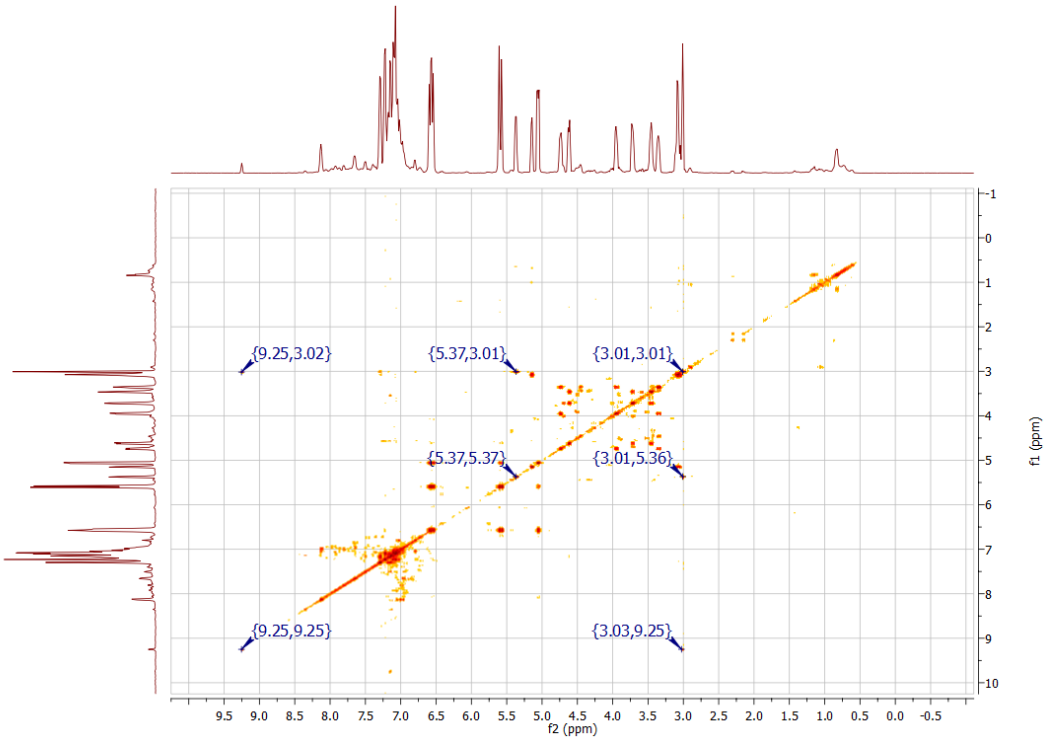

Figure 6 ^{1}H-^{13}C COSY spectrum with annotations marking aldehyde byproduct.

The identities of the organic byproducts from the concurrent oxidation of styrene diol are somewhat surprising. No definite identification of the products could be made and the expected products 2-hydroxy-2-phenylacetaldehyde, 2-hydroxyacetophenone or phenylglyoxal are not seen. Bergman reported that the vicinal diketones produced from reactions with diols and no additional reducing agent were unstable under catalytic conditions.[3] Indeed two aldehyde resonances can be seen in the ^{1}H NMR spectrum: a triplet at 9.26 ppm and a singlet at 9.64 ppm. The latter appears to be benzaldehyde, which suggests C-C bond cleavage has occurred. The former resonance is confirmed by a ^{1}H-^{1}H COSY experiment to be coupled to protons at 3.03 ppm which in turn are coupled to those at 5.38 ppm (Figure 6).

While no obvious product could be assigned to these resonances, due to the three distinct proton environments and the presence of benzaldehyde it could be a C_3 alkyl chain attached to a phenyl group; this would correspond to the second half of a molecule from which benzaldehyde has cleaved. Possibly the parent molecule is a product of an aldol reaction and the C-C bond cleavage is due to a subsequent retro-aldol reaction. Indeed there are similar resonances at 3.09 and 5.16 ppm with very similar chemical shifts, indicating that this may be the parent molecule. It should be noted that these unidentified organic products are seen in the reaction of $[H_3N(butyl)][ReO_4]$ with styrene oxide after heating, furthering the assumption that these are oxidised byproducts.

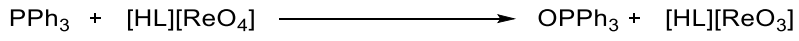

Scheme 4 Proposed reduction of $[HL][ReO_4]$ with PPh_3 to $[HL][ReO_3]$.

Alternatively, reduction of perrhenate with PPh_3 also appears to be possible (Scheme 4). When $[HL][ReO_4]$ is heated with one equivalent of PPh_3 at 80 °C for 25 h under N_2 a brown solution is produced. The ^{31}P NMR spectrum shows a large amount of $OPPh_3$ in a 91 % yield. There is a small shift of resonances for the counterion in the ^{1}H NMR spectrum and they are significantly broader. Presumably the product is a reduced rhenium species, possibly $[ReO_3]^-$ although no evidence of the identity of the anion is available. However, upon exposure to air, the brown solution slowly loses its colour and returns to the colourless solution, suggesting oxidation back to perrhenate.

Considering that [Lut][Cl] was suspected of interfering in the mechanism (perhaps by stabilising certain intermediates) yet no such intermediates were identified in the ^{1}H

NMR spectra, a stoichiometric reaction was undertaken with 1 equivalent of both [Lut][ReO_4] and styrene diol and 5 equivalents of [Lut][Cl] in $CDCl_3$. Heating for 2.5 h at 80 °C shows new resonances at 3.81 and 4.87 ppm in a 2:1 ratio suggesting mono-coordination of the diol to the rhenium centre. It is not possible to confirm whether the coordinating oxygen is deprotonated at this stage in the reaction but as there are only two resonances in the aliphatic region it can be concluded that this is not a glycolate. The presence of the [Lut][Cl] may in fact be preventing deprotonation and coordination of the second OH which would explain the slow rate of reaction in the presence of additional $[Lut]^+$ cations.

Both mechanistic routes (initial reduction or initial coordination of the diol) appear to be feasible from these reactions; under the standard conditions reaction of perrhenate with PPh_3 is observed as is reaction of the diol with perrhenate. Yet from the work presented, it is difficult to discern with which route the reaction proceeds. The ability of styrene diol to act as a reducing agent is of interest as it indicates that alternative reducing agents, specifically alcohols, may be used to reduce polyols.

DFT Mechanism Studies

Due to the questions raised by the above stoichiometric reactions, DFT calculations were undertaken in order to gain more insight into the mechanism. Calculations were performed using Gaussian 09. All geometries were optimised using the B3LYP functional and 6-31+G(d) basis set for all atoms except rhenium for which SDD was used. Single point calculations were ran on the optimised geometries using the 6-311++G(d,p) basis set and GD3BJ empirical dispersion corrections to obtain more accurate energies. Styrene diol was used as the substrate and $[H_3N(butyl)]^+$ or $[Lut]^+$ as the counterion but PMe_3 was used as a model for the reducing agent.

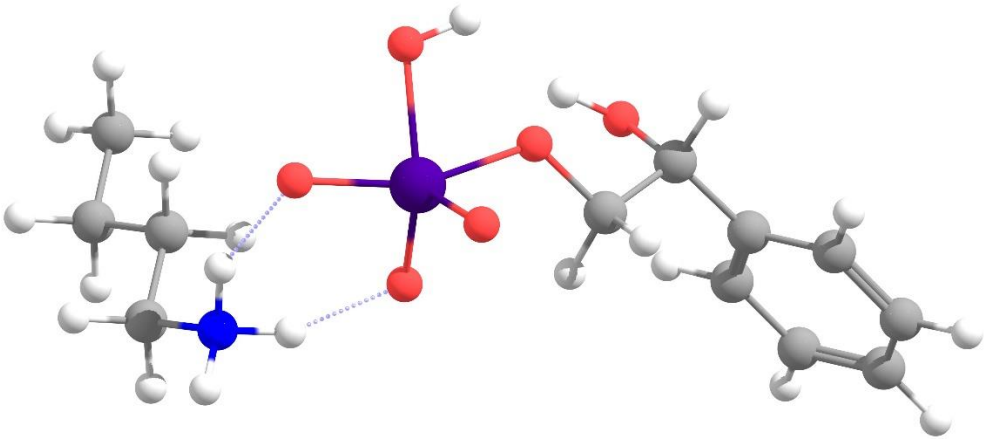

Figure 7 Initial coordination of styrene diol to $[H_3N(butyl)][ReO_4]$.

As previously mentioned the likely mechanism may proceed by first reducing the perrhenate with the phosphine or by coordination of the diol to perrhenate. Initially we considered coordination of the diol to $[H_3N(butyl)][ReO_4]$ (Scheme 5) which led to a relatively high energy trigonal bipyramidal product $[H_3N(butyl)][ReO_3(OH)(OCH_2CH\{OH\}Ph)]$ (Figure 7) where ΔG = +10.5 kcal mol^{-1}. The rhenium-alkoxide bond is 2.03 Å and the rhenium-hydroxide bond 1.96 Å, both significantly longer than the Re-O double bonds which are in the range of 1.72-1.78 Å, similar to those of $[H_3N(butyl)][ReO_4]$ (1.73-1.77 Å). The butylammonium NH protons are hydrogen bonded and bridging two oxo ligands with hydrogen bond lengths of 1.71 Å and 1.73 Å.

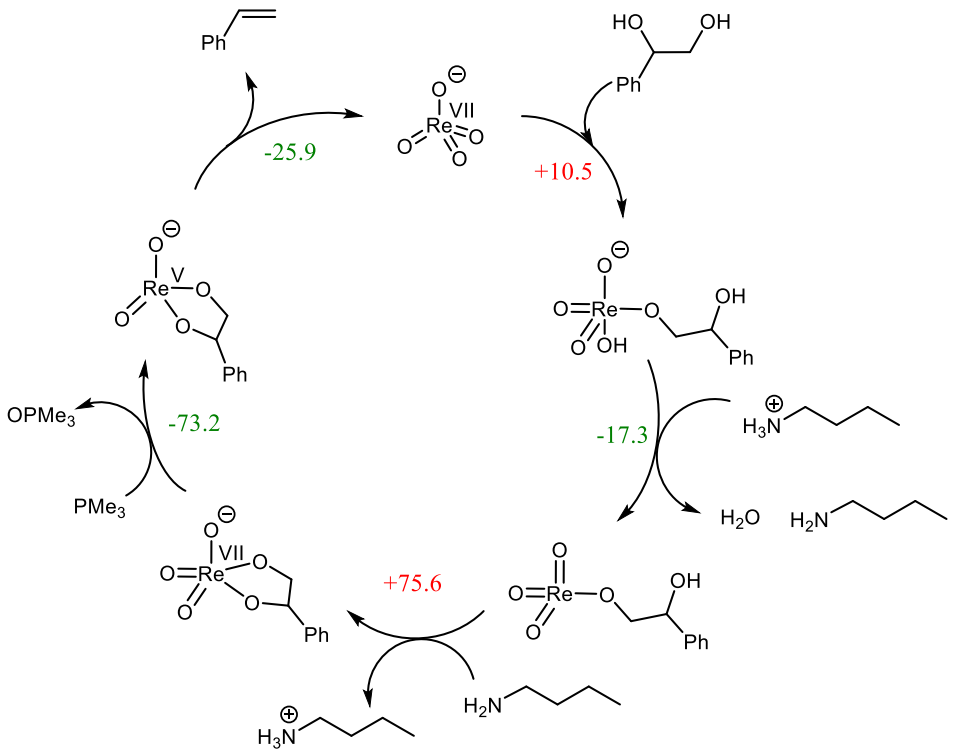

Scheme 5 Proposed catalytic cycle for the initial coordination of styrene diol to perrhenate, values are for ΔG in kcal mol^{-1}.

Protonation of the hydroxide ligand in order to remove water is exergonic; ΔG = -17.3 kcal mol^{-1} but subsequent coordination and deprotonation of the second hydroxide is highly endergonic with a large increase in free energy; ΔG = +75.6 kcal mol^{-1}. Subsequent intermediates are highly endergonic, although the large energies involved in this pathway suggest that it is not the correct mechanism. Such a large energy for the formation of the Re^{VII} glycolate is consistent with experimental results where $[H_3N(butyl)][ReO_3(OCH_2CHOPh)]$ is not seen in the ^1H NMR spectrum in stoichiometric reactions of styrene diol with the catalyst.

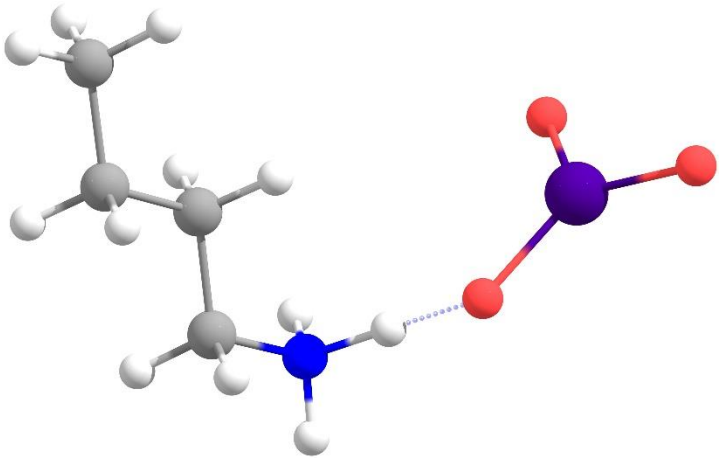

Figure 8 Product of the initial reduction of $[H_3N(butyl)][ReO_4]$.

Alternatively, the mechanism may initiate by reduction of $[H_3N(butyl)][ReO_4]$ with PMe_3 (Scheme 6). This has a much more thermodynamically favourable product (compared with coordinated diol) $[H_3N(butyl)][ReO_3]$ (Figure 8) where $\Delta G = +4.6$ kcal mol^{-1}. In this product the complex is in a trigonal planar geometry with Re-O bonds ranging 1.72-1.80 Å and with the counterion forming only one hydrogen bond to the longest oxo ligand. These rhenium-oxo bond lengths are not significantly different to those in $[H_3N(butyl)][ReO_4]$ which have a range of 1.73-1.77 Å. Subsequent coordination of the diol to give $[H_3N(butyl)][ReO_2(OH)(OCH_2CH\{OH\}Ph)]$ is favourable, $\Delta G = -3.8$ kcal mol^{-1}. This step reforms a tetrahedron, although there is an unusually small angle between the hydroxide and alkoxide ligands of 76.5 ° (Figure 9).

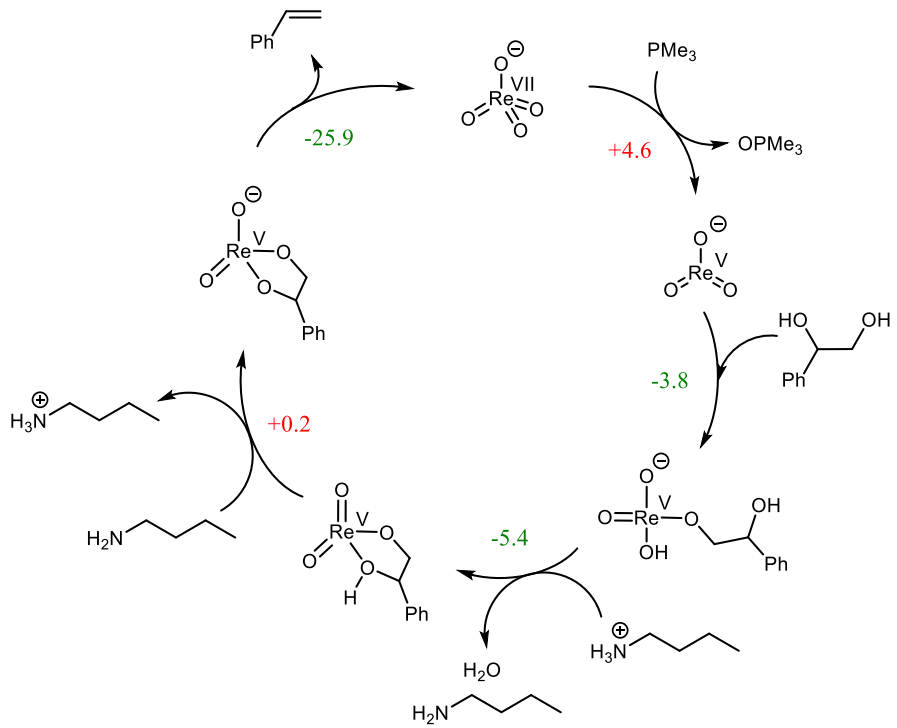

Scheme 6 Proposed catalytic cycle for the initial reduction of $[H_3N(butyl)][ReO_4]$ by PMe_3, values are for ΔG in kcal mol^1.

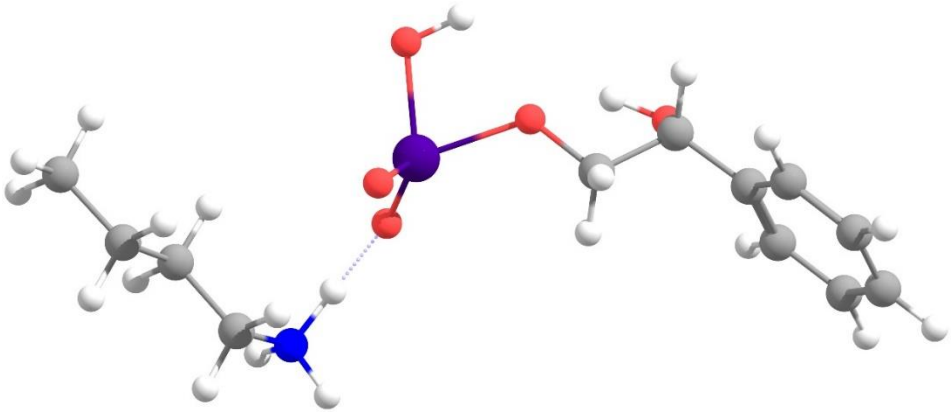

Figure 9 First coordination of styrene diol to $[H_7N(butyl)][ReO_3]$.

The second coordination of the diol to rhenium is also favourable with ΔG = -5.2 kcal mol^{-1} if the hydroxide ligand is protonated with the diol. An additional intermediate where the hydroxide ligand is protonated with the butylammonium cation to lose water (Figure 10) is very slightly more favourable with ΔG = -5.4 kcal mol^{-1} and the butylamine can be seen hydrogen bonded to the coordinated alcohol ligand. Such an interaction may stabilise this step as the deprotonation of the alcohol is slightly uphill, ΔG = -0.2 kcal mol^{-1}. Release of the styrene and reformation of perrhenate is highly exergonic with an increase in free energy of -25.9 kcal mol^{-1}.

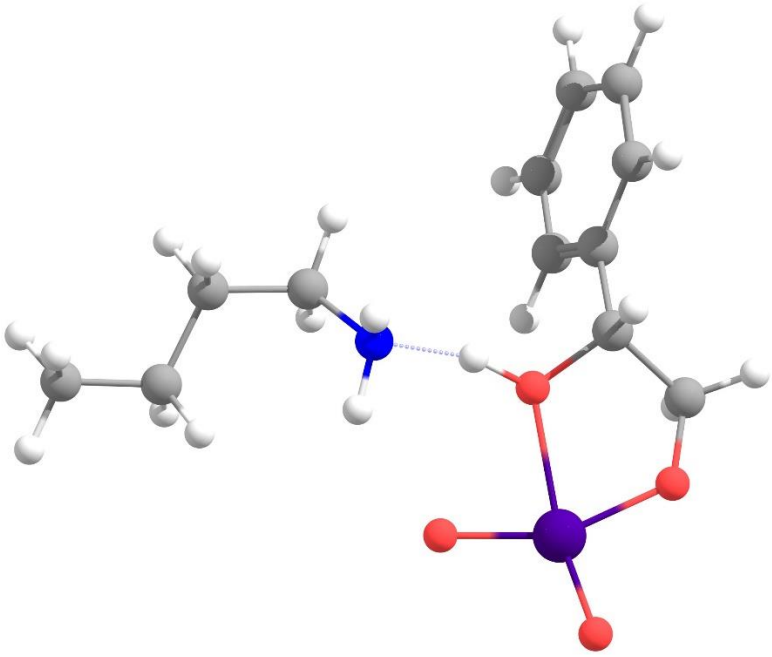

Figure 10 Second coordination of styrene diol after loss of H_2O.

It can be seen that structures of the rhenium intermediates following reduction of perrhenate with PMe_3 are often distorted, for example the aforementioned small angle between the hydroxide and alkoxide ligands in $[H_3N(butyl)][ReO_2(OH)(OCH_2CH\{OH\}Ph)]$ distorts the tetrahedral geometry. In DFT calculations reported by Chen and co-workers, the HOMO of $[ReO_3]^-$ is a nonbonding orbital, mainly composed of rhenium's d_z^2 orbital.[16] In this work the same is observed for $[H_3N(butyl)][ReO_3]$. Indeed, a similar HOMO exists that also appears to have significant d_z^2 character for $[H_3N(butyl)][ReO_2(OH)(OCH_2CH\{OH\}Ph)]$, apparently forcing the hydroxide ligand towards the alkoxide. Again, in $[H_3N(butyl)][ReO_2(OCH_2CH\{OH\}Ph)]$, the complex is square planar due to the HOMO occupying the plane above and below the rhenium atom. The nonbonding nature of this orbital may also explain why the rhenium-oxo bonds do not differ strongly from perrhenate as the extra electron density is not being shared amongst them. The HOMOs of these complexes are shown in Figure 11.

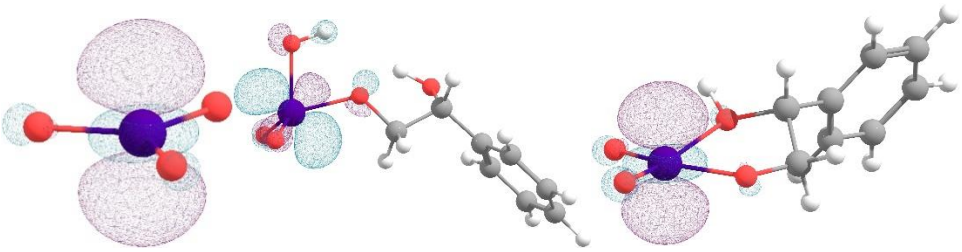

Figure 11 HOMOs for proposed Re^{V} intermediates in the DODH reaction.

Reduction of the rhenium complexes appears to be a requirement before the second hydroxyl group can coordinate to the complex. Therefore in the reactions where styrene diol is seen to reduce itself, after the initial coordination of the diol, another likely has to coordinate in order to act as the reducing agent. Indeed, the coordination of an additional styrene diol to $[H_3N(butyl)][ReO_2(OH)(OCH_2CH\{OH\}Ph)]$ giving $[H_3N(butyl)][ReO_2(OCH_2CH\{OH\}Ph)_2]$ is exergonic with ΔG = -7.1 kcal mol^{-1}, which helps explain why styrene diol can act as a reducing agent. Alternatively, the diol is oxidised before coordination of another diol as is proposed by studies on alcohol transfer hydrogenation DODH reactions[11, 12] although this pathway has not been explored further.

These results are consistent with mechanisms proposed in the literature. Nicholas presented DFT calculations showing that when sodium sulfite is used as the reducing agent, initial attack of $NaSO_3^-$ on one of the rhenium-oxos of MTO forming the Re^{V} species is exergonic.[13] Release of $NaSO_4^-$ is prohibitively endergonic and therefore this step is proceeded by coordination of the diol. While no rhenium catalyst has been modelled using a phosphine as the reducing agent, the vanadium complex $[N(butyl)_4][V(O)_2(dipic)]$ (dipic = 2,6-pyridinedicarboxylate) reported to catalyse the DODH reaction by Nicholas[17] was studied using DFT calculations by Galindo[18] who found that initial reduction by PPh_3 resulted in a more favourable pathway for the reduction of the diol.

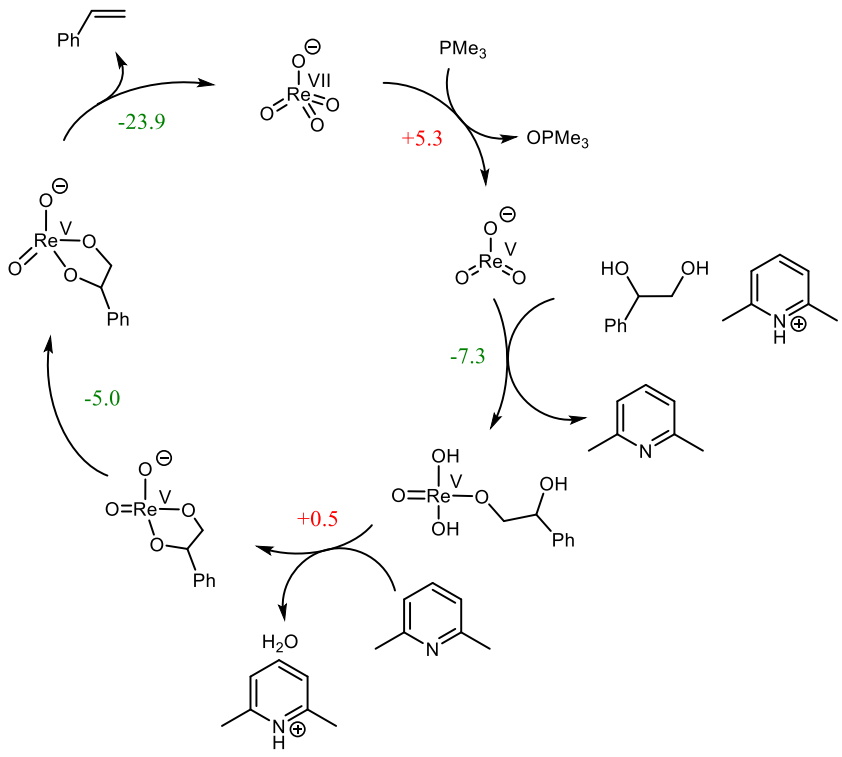

Scheme 7 Proposed catalytic cycle following the initial reduction pathway with $[Lut]^+$ counterion, values are for ΔG in kcal mol^{-1}.

Examining the initial reduction pathway with the lutidinium counterion shows some small differences (Scheme 7). Coordination of the diol to $[Lut][ReO_3]$ is more exergonic than in $[H_3N(butyl)][ReO_4]$; ΔG = -7.3 kcal mol^{-1}. However, in this case the lutidinium has been deprotonated by an oxo ligand and remains hydrogen bonded to the proton. The Re-O-H bond angle is much greater (125.7 °) than the hydroxide ligand, showing there is still a strong interaction (Figure 12). Rather than protonation of the hydroxide ligand by lutidinium, this suggests an alternate mechanism may be available for the loss of water from an intramolecular protonation rather than by lutidinium. Protonation of the hydroxide ligand to remove water is in fact slightly endergonic, with a decrease in free energy of +0.5 kcal mol^{-1}, yet in contrast to calculations with butylammonium the diol is deprotonated at this stage, perhaps explaining the endergonic reaction. Reorganisation of the square planar glycolate to afford the tetrahedral glycolate is significantly exergonic, in contrast to butylammonium, ΔG = -5.0 kcal mol^{-1}.

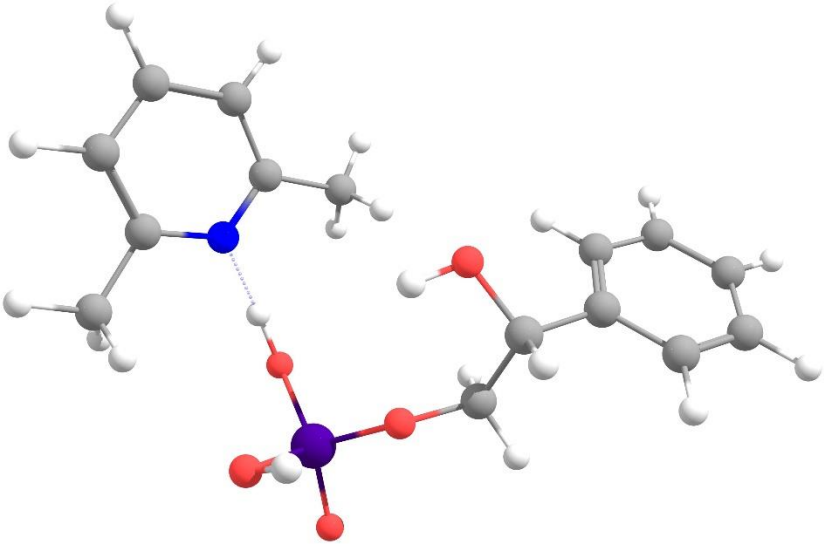

Figure 12 Geometry of intermediate after first coordination of diol to [Lut][ReO_3] with 2 OH ligands.

Interestingly, these results shows similarities to the results of Wang's DFT study on the MTO catalysed reaction using secondary alcohols as the reducing agent.[11] Rather than initial reduction to give [$CH_3Re(O)_2$] or initial coordination of the diol, a third pathway was found where MTO is reduced to [$CH_3Re(OH)_2O$] with the sacrificial alcohol. To this complex, the diol can coordinate in a stepwise manner, producing an equivalent of water with each coordination. In the case of [Lut][ReO_4], the diol has already coordinated once and apparently only deprotonates the second time after the loss of water (and coordination of the second hydroxyl group), suggesting a difference in the mechanism, although the presence of two OH ligands may lower the energy required to access the second deprotonation and indeed the second OH ligand is closer to the coordination site of the second alkoxide.

There is the possibility of free lutidine being present after the loss of water if it acts as a proton shuttle. The product was modelled and found that the lutidine coordinated to the rhenium complex and provides a significant increase in free energy: ΔG = -20.6 kcal mol^{-1}. Such a product (Figure 13 a.) is likely to stabilise the intermediate sufficiently to significantly reduce the rate of reaction. This does support the presence of a Re^V glycolate adduct in the ^1H NMR spectrum for the stoichiometric reaction between [H_3N(hexyl)][ReO_4] and styrene diol. A similar adduct was modelled with butylamine as the donor (Figure 13 b.) and despite similar Re-N bond lengths (2.21 and 2.19 Å respectively) was found to be significantly more exergonic with ΔG = -32.4 kcal mol^{-1}. Due to the stronger donor properties of the alkylamine, it presumably

forms a stronger bond and stabilises the complex more than lutidine. Furthermore, this explains the importance of protecting the donor nitrogen with bulky substituents to prevent such an interaction.

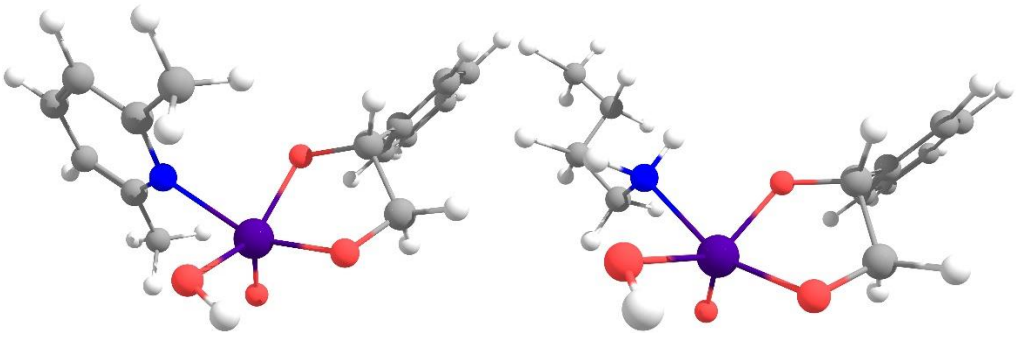

Figure 13 a. Lutidinium adduct of Re^{V} glycolate and b. corresponding butylammonium adduct.

Alternative Reducing Agents

Substituting the reducing agent for a more environmentally benign reducing agent is a requirement for any practical application of this reaction. Nicholas has reported success with sodium sulfite although due to the low solubility of sodium sulfite in non-polar solvents, high temperatures (150 °C) are required.[7] Abu-Omar has shown that H_2 can reduce MTO allowing reduction of epoxides and diols.[2] Interestingly, alcohol transfer hydrogenation has been shown to work and alcohols, due to the ability to reduce their oxidation products to alcohols again, are seen as a recyclable reducing agent. Toste reported that sugars and sugar alcohols could be reduced using 3-pentanol, 1-butanol and 3-octanol.[15] For example, using MTO as the catalyst and 3-pentanol as the reducing agent, D-allose was reduced to 2-vinylfuran and furan in a 40 % yield after 3 h at 155 °C (Scheme 8).

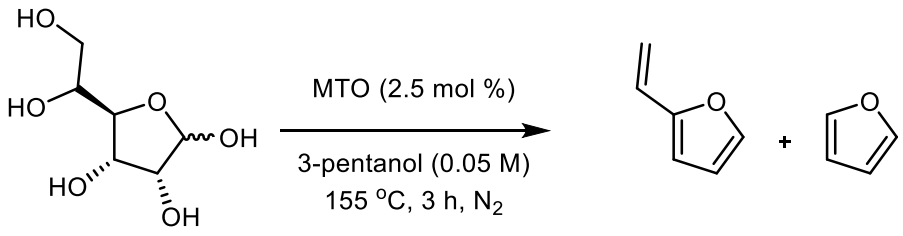

Scheme 8 DODH of D-allose with MTO and 3-pentanol giving 2-vinylfuran and furan as products.[15]

Simply by changing the reducing agent, Toste has shown that the DODH reaction can be applied to several biomass derived feedstocks. Using this inspiration, paired with the knowledge that the perrhenate system can use alcohols as reducing agents (i.e. styrene diol), some reactions were carried out in an attempt to replace PPh_3 as the reducing agent.

In an NMR scale reaction, styrene diol (0.2 mmol), 3-octanol (1.8 mmol) and $[HL][ReO_4]$ (2.0 mol %) in C_6D_6 were heated for 22 h at 80 °C. Whilst styrene is present in the products of this reaction, no 3-octanone can be seen in the ^1H NMR spectrum. Indeed, the products seen previously on reaction of styrene diol with the catalyst are seen here, including benzaldehyde. Therefore, here it appears that the 3-octanol is not involved in this reaction.

Noting that many reactions utilising alcohol transfer hydrogenation, in the context of the DODH reaction, are conducted at high temperatures and with the alcohol acting as solvent, another reaction was carried out. At 125 °C styrene diol (9.4 mmol) and 3-octanol (12.6 mmol) were stirred with $[DTBMP][ReO_4]$ (1.0 mol %). After 8 h, the total conversion of the diol was observed with 28.5 % yield of styrene and although large amounts of the oxidised styrene diol product are present, a small amount of 3-octanone is also observed (9.5 %) confirming that alternative alcohols are capable of acting as the reductant.

Unfortunately, no further reactions using 3-octanol as the reducing agent were carried out; however, this does show that by using a similar system, biomass derived feedstocks such as sugars may potentially be reduced this way. It also appears here that styrene diol is not a good model as unless a suitable reducing agent is present (e.g. PPh_3), it will compete and often supersede the abilities of other reducing agents.

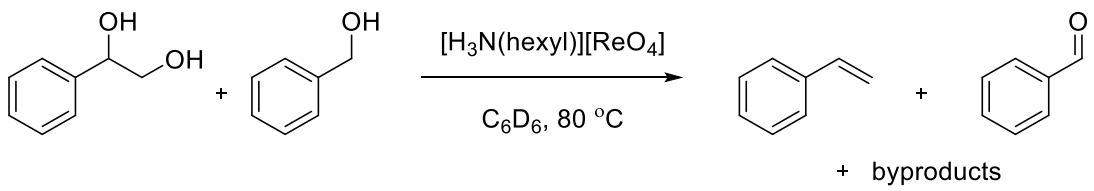

Scheme 9 DODH of styrene diol using benzyl alcohol as the reducing agent and $[H_3N(hexyl)][ReO_4]$ as the catalyst.

A further reaction attempting to use benzyl alcohol as the reducing agent, as was previously explored by Nicholas,[19] was conducted (Scheme 9). In a reaction of styrene diol (1.3 mmol) and benzyl alcohol (1.6 mmol) with $[H_3N(hexyl)][ReO_4]$ (2.8 mol %) heated at 80 °C in C_6D_6, similar issues with the styrene diol disproportionating are still obvious from the ^1H NMR spectrum but excitingly 5 % of the benzyl alcohol has been oxidised to benzaldehyde after heating for 56 h and full conversion of the diol is achieved with a 51.0 % yield of styrene. Whilst within the margin of error, a yield of more than 50 % does indicate an alternative reductant is also present. This conversion at much lower temperatures than required for 3-octanol indicates primary aromatic alcohols may be much more suitable reducing agents than long-chained alcohols. Along with conversion at lower temperatures, Nicholas explains that aldehyde byproduct could be separated and either used or recycled more easily than a ketone such as 3-ocanone.

Alternative Substrates

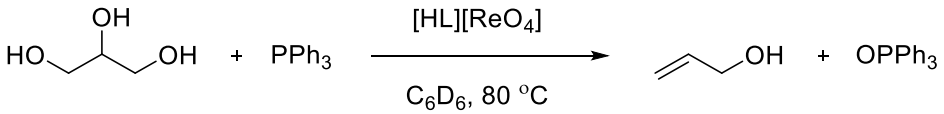

Scheme 10 DODH of glycerol with PPh_3 as reductant and $[HL][ReO_4]$ as catalyst.

Seeking to apply these catalysts to some alternate polyols, attention turned to glycerol. This polyol is produced in large quantities as a byproduct from the biofuel industry with significant quantities remaining unused.[2] A reaction with glycerol (0.29 mmol), PPh_3 (0.3 mmol) and $[HL][ReO_4]$ (2.0 mol %) in C_6D_6 was heated at 80 °C for 35 h (Scheme 10). Whilst glycerol has poor solubility in C_6D_6 the conversion of PPh_3 could be monitored, showing a 60.5 % conversion to $OPPh_3$ based on the ^{31}P NMR.

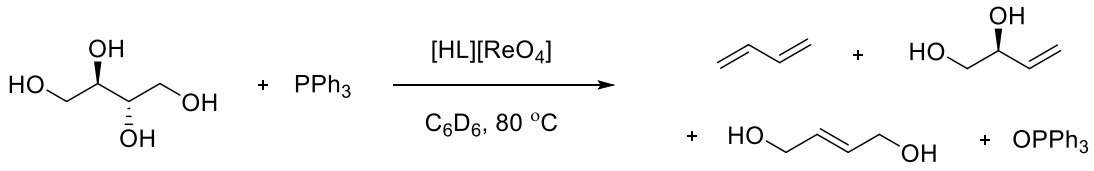

Scheme 11 DODH of reythritol with PPh_3 as reductant and $[HL][ReO_4]$ as catalyst.

Similarly, the sugar alcohol erythritol (0.23 mmol) was heated at 80 °C with PPh_3 (0.29 mmol) and $[HL][ReO_4]$ (1.2 mol %) in C_6D_6 for 35 h (Scheme 11). This gave

conversion of 11.7 % of the PPh_3. After 17 h the ^1H NMR spectrum shows butadiene and additional diol products from the partial deoxydehydration of erythritol.

Conclusions

The protic counterions of perrhenate have been shown to be non-innocent in the DODH reaction, significantly enhancing the activity of the catalyst at lower temperatures and catalyst loading than similar non-protic salts of perrhenate. Through experimental and computational studies, it appears that the most likely mechanism proceeds through the initial reduction of the catalyst. The role of the protic counterions appears to be facilitation of proton transfers. From stoichiometric reactions there appear to be a number of glycolates, which suggests that the deprotonated amine or pyridine is capable of coordinating to the glycolate. As DFT calculations indicate that the Re^{VII} glycolate is inaccessible starting from styrene diol and the experimental results do not show this product, it is reasonable to assume these are Re^{V} glycolates.

However, the stark difference between the rate of catalysis between alkylammonium perrhenates and pyridinium perrhenates may be due to the stabilisation of the Re^{V} glycolate through the formation of an adduct; DFT results suggest that alkylamines stabilise the glycolate more than pyridines. This mechanism for the stabilisation of such an intermediate would rationalise the improvement in catalysis seen using [DTBMP][ReO_4] whose donor nitrogen atom is sterically protected by *t*-butyl substituents, which would make coordination to a metal centre very difficult, perhaps preventing stabilisation of the glycolate.

Throughout this study, perrhenate has been shown to catalyse the alcohol transfer hydrogenation reaction in order to reduce styrene diol, often through the disproportionation of styrene diol itself. Promising results from the presence of 3-octanone in the ^1H NMR spectrum of the reaction using 3-octanol as the reducing agent suggest that alcohols other than styrene diol will react as reducing agents. Furthermore the primary alcohol benzyl alcohol was also observed to undergo oxidation but at lower temperatures indicating it may be a better choice of reductant. While the styrene diol proved to be a poor model in reactions, the catalyst has been shown to work for the real example polyols glycerol and erythritol and therefore it may be possible to explore these systems directly rather than using further models. These are exciting

results as both exhibit low solubilities in apolar solvents, yet nonetheless undergo conversion using the pyridinium perrhenate catalysts, providing an interesting starting point for the study of the DODH reaction on biomass derived polyols.

References

1. G. K. Cook and M. A. Andrews, *Journal of the American Chemical Society*, 1996, 118, 9448-9449.
2. J. Yi, S. Liu and M. M. Abu-Omar, *ChemSusChem*, 2012, 5, 1401-1404.
3. E. Arceo, J. A. Ellman and R. G. Bergman, *Journal of the American Chemical Society*, 2010, 132, 11408-11409.
4. M. Cokoja, I. I. E. Markovits, M. H. Anthofer, S. Poplata, A. Pothig, D. S. Morris, P. A. Tasker, W. A. Herrmann, F. E. Kuhn and J. B. Love, *Chemical Communications*, 2015, 51, 3399-3402.
5. R. J. Ellis, J. Chartres, K. C. Sole, T. G. Simmance, C. C. Tong, F. J. White, M. Schroder and P. A. Tasker, *Chemical Communications*, 2009, 583-585.
6. C. J. L. Lock and G. Turner, *Acta Crystallographica Section B*, 1975, 31, 1764-1765.
7. I. Ahmad, G. Chapman and K. M. Nicholas, *Organometallics*, 2011, 30, 2810-2818.
8. E. T. Borrows, B. M. C. Hargreaves, J. E. Page, J. C. L. Resuggan and F. A. Robinson, *Journal of the Chemical Society (Resumed)*, 1947, 197-202.
9. A. Krogul, J. Skupińska and G. Litwinienko, *Journal of Molecular Catalysis A: Chemical*, 2011, 337, 9-16.
10. E. Deutsch and N. K. V. Cheung, *The Journal of Organic Chemistry*, 1973, 38, 1123-1126.
11. S. Qu, Y. Dang, M. Wen and Z.-X. Wang, *Chemistry – A European Journal*, 2013, 19, 3827-3832.
12. J. R. Dethlefsen and P. Fristrup, *ChemCatChem*, 2015, 7, 1184-1196.
13. P. Liu and K. M. Nicholas, *Organometallics*, 2013, 32, 1821-1831.
14. S. Raju, J. T. B. H. Jastrzebski, M. Lutz and R. J. M. Klein Gebbink, *ChemSusChem*, 2013, 6, 1673-1680.
15. M. Shiramizu and F. D. Toste, *Angewandte Chemie International Edition*, 2012, 51, 8082-8086.
16. W.-J. Chen, H.-J. Zhai, X. Huang and L.-S. Wang, *Chemical Physics Letters*, 2011, 512, 49-53.
17. G. Chapman and K. M. Nicholas, *Chemical Communications*, 2013, 49, 8199-8201.
18. A. Galindo, *Inorganic Chemistry*, 2016, 55, 2284-2289.
19. C. Boucher-Jacobs and K. M. Nicholas, *ChemSusChem*, 2013, 6, 597-599.

4. Epoxidation of Alkenes with Oxo-Anions

Since 1991, methytrioxorhenium (MTO) has been known as an effective oxidation catalyst using hydrogen peroxide as an oxidant (Scheme 1).[1] Mechanistic studies have shown that reaction of MTO with hydrogen peroxide forms the metal peroxide [$CH_3Re(O)_2(\eta\text{-}O_2)$] and, when hydrogen peroxide is in excess, [$CH_3Re(O)_2(\eta\text{-}O_2)(H_2O)$]; both of which are catalytically competent.[2, 3] One of the important oxidations MTO catalyses is the epoxidation of alkenes. Indeed, from the first report of MTO's activity as an epoxidation catalyst, it has been shown that a wide variety of substrates are suitable for conversion including gaseous alkenes such as propene.[1] The catalyst has been shown to be highly efficient and recently turnover frequencies of 39000 h^{-1} have been reported by modification of the reaction conditions and inclusion of Lewis base additives.[4] Importantly, MTO was immediately proven to be very versatile, capable of epoxidising a range of substrates (including gaseous) in a variety of solvents over a range of temperatures.[1]

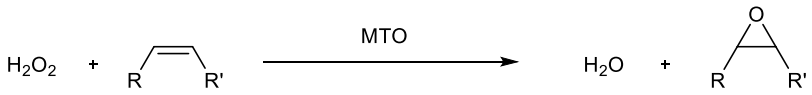

Scheme 1 General scheme for the epoxidation of alkenes with MTO and H_2O_2.[1]

Unfortunately, despite the successful application of MTO as an oxidation catalyst, it is known to decompose to methanol and perrhenate in the presence of hydrogen peroxide.[5, 6] Given the high cost of rhenium, such a limit on the catalyst lifetime is hugely problematic for this industrially relevant process and renders large scale applications impractical. Under the same catalytic conditions, the decomposition product perrhenate has previously been found to be catalytically inactive although perrhenic acid was shown to be capable of epoxidising alkenes but only in the presence of tertiary arsines was the rate of reaction reasonable.[7] These arsines were shown to immediately oxidise to the arsine oxide, which are known to form hydrogen bonded adducts with acids[8] and therefore the activity of perrhenic acid was attributed to its transfer into the organic phase.

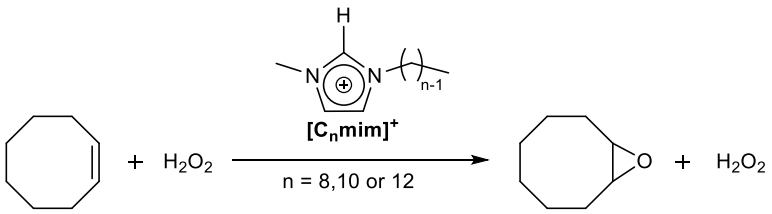

Scheme 2 Epoxidation of cyclooctene with stoichiometric quantities of perrhenate containing ionic liqudis.[9]

Kühn and co-workers have suggested that the hydration shell renders perrhenate inactive in aqueous solutions, which prompted them to synthesise perrhenate-containing ionic liquids in order to provide an environment in which no solvent shell is present (Scheme 2).[9] Resultantly, stoichiometric amounts of the perrhenate containing ionic liquids were shown to convert cyclooctene to cyclooctene oxide using hydrogen peroxide as the oxidant. Labelling studies observed no ^{17}O incorporation in the cyclooctene oxide product when ^{17}O labelled perrhenate was used, indicating that the peroxo complex was not formed as with MTO. Mechanistic studies involving a combination of *in situ* IR and Ramen spectroscopy and DFT calculations suggest that hydrogen peroxide is activated by forming hydrogen bonds with perrhenate (Figure 1), where a decrease in the symmetry of perrhenate from T_d to C_{2v} can be seen which is in agreement with the formation of hydrogen bonded complex between perrhenate and hydrogen peroxide. Clearly the use of the oxidant stable perrhenate as an epoxidation catalyst offers a significant advantage over MTO, in addition to the transfer of the polar hydrogen peroxide to an apolar reaction medium increasing the reactivity of the oxidant. Indeed, consistent yields of 98-99 % cyclooctene oxide were achieved in reactions recycling the ionic liquid $[C_8mim][ReO_4]$ at least eight times.

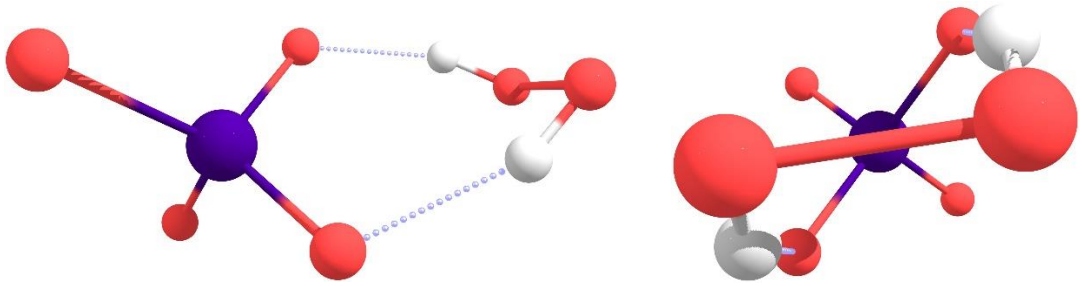

Figure 1 Structure of hydrogen peroxide hydrogen bonded to perrhenate and view down the C_2 axis.

Following this success, we studied (in collaboration with the Kühn group) the use of extractants to form outer-sphere complexes with perrhenate.[10] The three extractants (or here: receptors, Figure 2) used to synthesise these supramolecular ion pairs (SIPs) were chosen due to the resultant complexes' solubility in organic solvents such as toluene and the ability to retain perrhenate in the organic phase, therefore allowing hydrogen bonding with the oxidant to be enhanced without interference from an aqueous solvation shell. Furthermore their synthesis is straightforward, simply by adding an equivalent of perrhenic acid to a toluene solution of the receptor allows its protonation and transfer of perrhenate from the aqueous phase (Scheme 3).

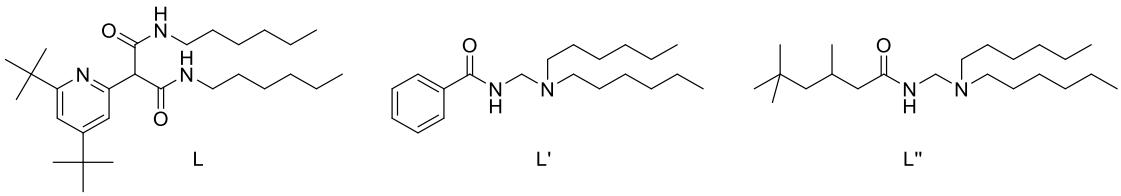

Figure 2 The three receptors used in this work.

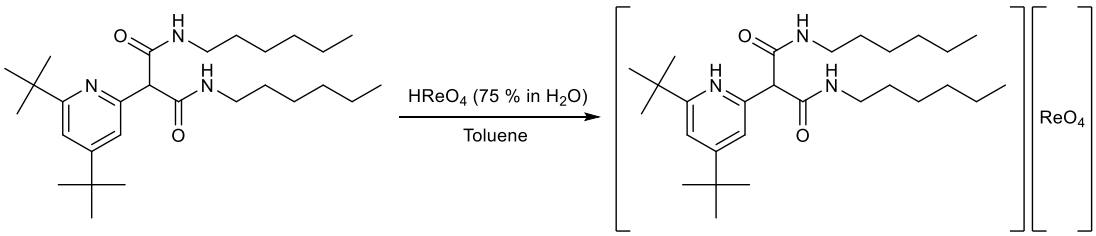

Scheme 3 Synthesis of SIP [HL][ReO_4].[10]

Using 5 mol % of the SIPs and 2.5 equivalents of aqueous hydrogen peroxide (50 %) at 70 °C, cyclooctene is almost quantitatively converted to cyclooctene oxide after 8 h with all three SIPs and with no evidence of the ring opened 1,2-cyclooctanediol present, thereby exhibiting high selectivity. These results were obtained without the addition of solvent, yet no difference was observed when toluene was also added. Recycling of the catalyst was shown to be possible with the catalyst being reused in catalytic reactions five times with no loss of activity. A labelling study with ^{17}O labelled perrhenate showed that (as with the ionic liquid labelling experiment) the cyclooctene oxide product contained no ^{17}O; therefore a rhenium peroxo species is also unlikely to form in this system. As such it is probable that the activation of hydrogen peroxide proceeds in a similar method suggested by the DFT calculations for perrhenate in the ionic liquid study; it appears clear that by the transfer of the perrhenate anion into the organic phase (and in this case the formation of SIPs) the catalytic activity is "turned on", presumably by enhancing the hydrogen peroxide/ perrhenate contacts in a hydrophobic medium.

It should be noted that all work described so far was conducted by the Kühn group.

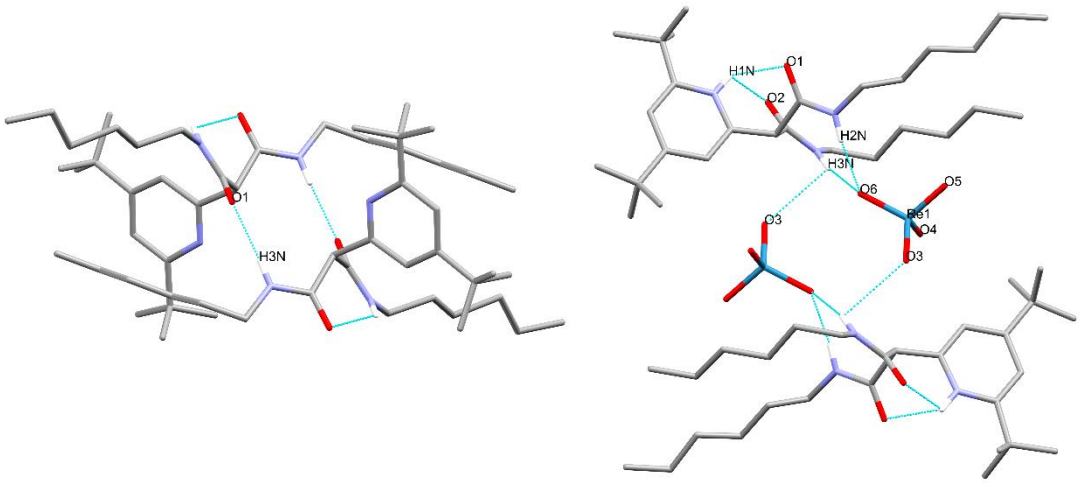

Figure 3 X-ray crystal structures of L and $[HL][ReO_4]$[10], both showing the hydrogen bonding resulting in dimers.

The reported solid state structure of $[HL][ReO_4]$ consists of two perrhenate anions encapsulated by two of the protonated receptors (Figure 3). Hydrogen bonds between the amide H2N and H3N with O6 as well as an additional hydrogen bond between H3N and O3 appear to hold this dimer together. The bifurcated hydrogen bond between H1N and amid oxygens O1 and O2 is also visible. We also found a dimeric structure in the solid state structure for L, with hydrogen bonds between the amide oxygen O1 and the amide H3N of the second receptor. We were curious as to whether this dimer exists in solution as well. If the reaction occurs within these supramolecular structures, it could be argued that they are necessary for the activation of perrhenate. Using a combination of electrospray ionisation mass spectrometry (ESI-MS) and diffusion-ordered spectroscopy (DOSY), the solution structure was probed.

ESI-MS Studies on Perrhenate SIPs

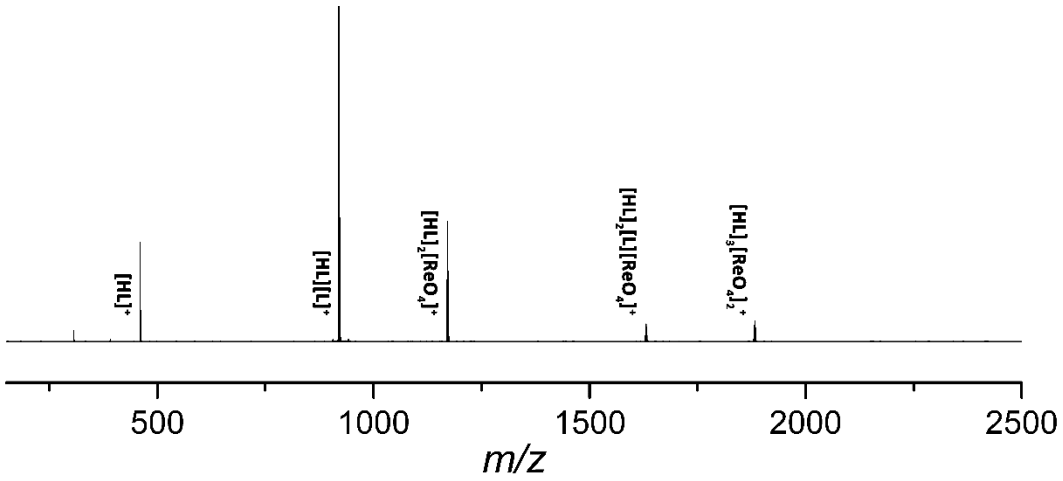

Figure 4 ESI-MS of [HL][ReO_4] in MeCN.

Dupont and Eberlin noted that ionic liquids retain their solution aggregate structures when studied by ESI-MS.[11] In their report they found that the soft ionisation technique was ideal for studying the weak intermolecular hydrogen bonds holding together the aggregates. In our case, using ESI-MS with a low inlet nozzle temperature of 50 °C for an acetonitrile solution of [HL][ReO_4] did not show an ion corresponding to the dimer seen in the solid state, although a neutral species would not be expected to be seen for ESI-MS. There are, however, a number of ions corresponding to aggregation of the receptor and perrhenate (Figure 4). For example at 1883 amu an ion for $[HL]_3[ReO_4]_2^+$ is found and ions for smaller aggregates with alternating loss of $HReO_4$ and L appear until $[HL]^+$ is reached.

This indicates that dimers may exist in solution, with $[HL]_2[ReO_4]^+$ and $[HL]L^+$ both seen, but in combination with higher order aggregates. Similar ions are seen for [HL′][ReO_4] (Figure 5) and [HL″][ReO_4] (Figure 6) under the same conditions, although both spectra are more complex as fragmentation of the receptor is evident. Some decomposition is also evident in the ^{1}H NMR spectrum for [HL″][ReO_4] with resonances corresponding to the amide and dihexylammonium ($[DHA]^+$) fragments of the receptor.[10] This fragmentation of [HL′][ReO_4] and [HL″][ReO_4] both show significant amounts of $[DHA]^+$, with all of the aggregates for both receptors showing sequential loss of the respective amide to give aggregates of the formula $[DHA]_n[ReO_4]_{n-1}$.

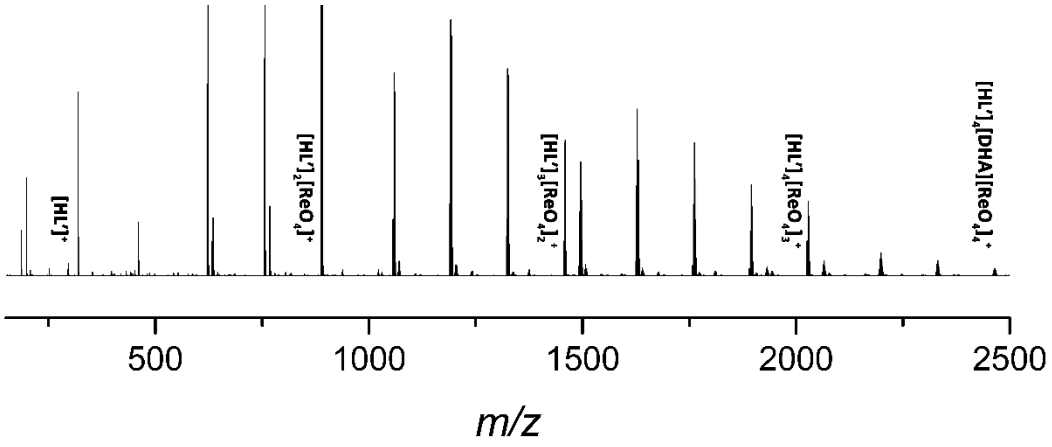

Figure 5 ESI-MS of [HL']$[ReO_4]$ in MeCN. $[DHA]^+$ = dihexylammonium. Fragmentation of each parent aggregate is seen to give the $[DHA]^+$ aggregate.

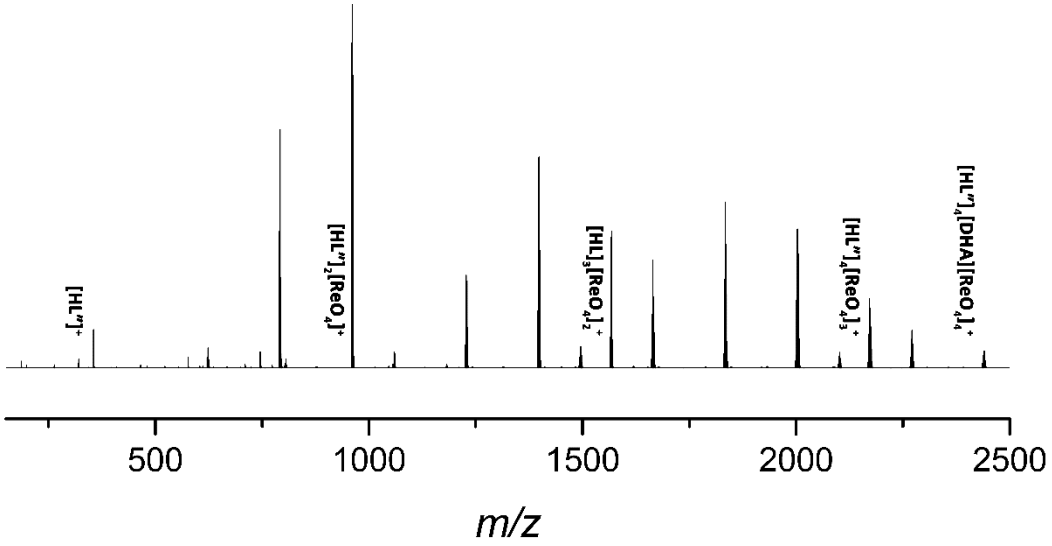

Figure 6 ESI-MS of [HL"]$[ReO_4]$ in MeCN. Similar fragmentation patterns as with [HL']$[ReO_4]$ are present.

DOSY Studies on Perrhenate SIPs

The DOSY spectrum for [HL]$[ReO_4]$ show a single species present (Figure 7), with a hydrodynamic radius of 4.5 Å in CD_3CN and 6.3 Å in C_6D_6. In comparison L in C_6D_6 has a hydrodynamic radius of 5.3 Å. These radii correspond to spherical volumes of 624 $Å^3$ and 1047 $Å^3$ for L and [HL]$[ReO_4]$ respectively, therefore indicating possible aggregation of [HL]$[ReO_4]$ in solution as the volume is much larger than that which may be expected for simple the ion pair. Whilst the volume would not be expected to be exactly double that of L, the ^1H NMR spectrum supports an organisation of the $[HL]^+$ cation with the hexyl chains split into two which is visible by the NCH_2 protons at 3.40 and 3.26 ppm. This is consistent with retaining the six-membered proton-chelate ring between the pyridinium NH and amide

oxygens seen in the solid state structure. Such an organisation of the $[HL]^+$ cation may contribute to the smaller volume of an aggregate. Hoffmann also reported an association between ion pairs for the ionic liquid $[C_6mim][NTf_2]$ (NTf_2 = bis(trifluoromethylsulfonyl)amide) at low concentrations in a study using ^1H and ^{19}F DOSY spectroscopy and although aggregates were seen at higher concentrations, some suggestion of aggregates were also discussed for the lowest concentrations studied.[12]

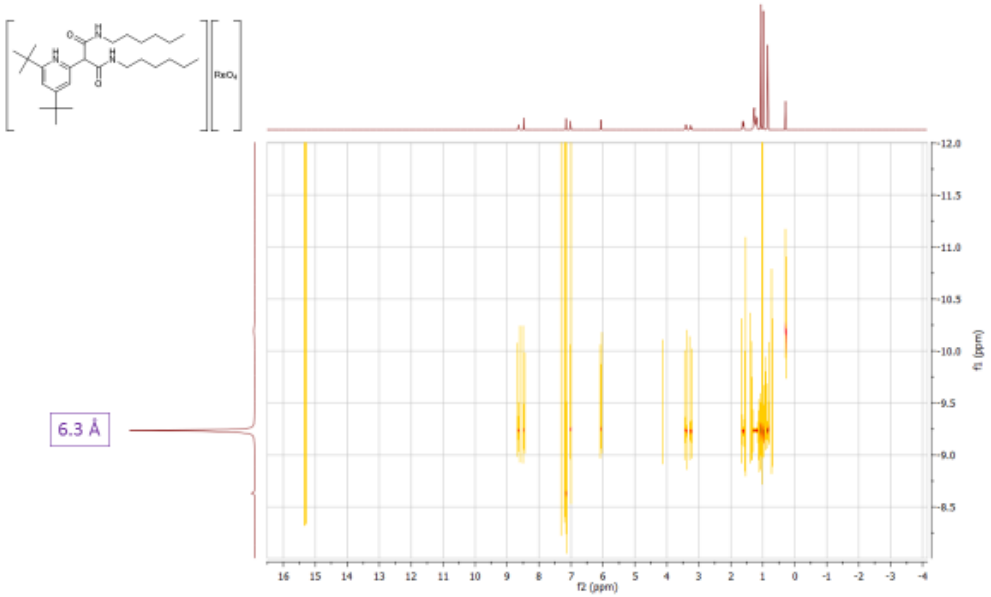

Figure 7 DOSY spectrum for [HL][ReO4] in C6D6.

Whether this supramolecular structure is necessary for the activation of hydrogen peroxide is not obvious; simply by transferring the perrhenate into the organic phase may be sufficient to make it catalytically active. This would appear to be consistent with the ability of the tertiary arsine/ perrhenic acid system to catalyse the epoxidation of cyclooctene where there is no indication of the formation of an encapsulated perrhenic acid supramolecular structure.

DOSY spectra for [HL′][ReO_4] and [HL″][ReO_4] show hydrodynamic radii of 6.6 Å and 6.7 Å respectively in C_6D_6, also consistent with aggregation. However in CD_3CN, numerous species are seen with hydrodynamic radii between 4.1 Å and 2.8 Å. This indicates that some separation of the ion pair occurs in more polar solvents for [HL′][ReO_4] and [HL″][ReO_4], which is consistent with DFT studies of ionic liquids by Hu and Wu;[13] they showed that solvents had a significant effect on the binding energy of the anion and cation and increased distances between the two in solvents with higher dielectric constants. Hydrogen bonded aggregates are also likely broken up due to increased solvent interactions and the ability of CD_3CN to act as a hydrogen bond donor.

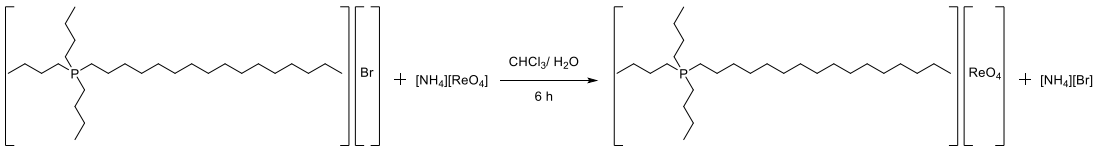

Scheme 4 Synthesis of the catalyst [P(4,4,4,16)][ReO_4].

From these results an alternative counterion was selected on the basis of its hydrophobicity and resistance to decomposition by hydrogen peroxide, tributyldodecylphosphonium ([P(4,4,4,16]$^+$), in order to retain perrhenate in the organic phase. [P(4,4,4,16)][Br] has commonly been used as a phase transfer agent, suggesting that the cation may be a suitable commercially available alternative to the receptors.[14] The perrhenate salt was synthesised by stirring an aqueous solution of ammonium perrhenate with a chloroform solution of [P(4,4,4,16)][Br] for 6 h (Scheme 4). Isolation of the organic phase and removal of the solvent yielded a white solid.

However, with a 5 % catalyst loading, only 20.5 % conversion of cyclooctene was achieved after 8 h at 80 °C. Even after 24 h only 70.6 % conversion was seen, although it is only at this point that a small amount (1.4 %) of the diol is seen in the ^{1}H NMR spectrum showing good selectivity. As [P(4,4,4,16)]$^+$ is significantly different to [HL]$^+$, [HL′]$^+$ and [HL″]$^+$ in that it is aprotic and is not a source of hydrogen bond donors, this implies the counterion is an important consideration. Furthermore, as the receptors are competent and selective extractants (extracting chlorometallates such as $CoCl_4^{2-}$ over anions such as chloride),[15] they may be more capable of retaining perrhenate in the organic phase whereas ion exchange with species such as HOO^- may occur with [P(4,4,4,16)]$^+$ thereby reducing its activity. This is likely a more important consideration than the formation of aggregates in solution.

Perrhenate-Containing Ionic Liquids

The Kühn group later synthesised a series of perrhenate containing ionic liquids (Figure 8) and studied them as catalysts for the epoxidation of alkenes.[16] By varying the C2 and *N*-wingtip substituents, the catalytic activity of the ionic liquids could be significantly altered as could their solubility in aqueous hydrogen peroxide. Out of the twelve ionic liquids studied, [C_8dmim][ReO_4] and [C_{10}dmim][ReO_4] exhibited the highest conversions of 88 % and 85 % respectively after 4 h with a 5 mol % catalyst loading, cyclooctene (10 mmol) and hydrogen peroxide (50 wt %, 25 mmol). Under the same conditions [C_8mim][ReO_4] and [C_{10}mim][ReO_4] gave moderate conversion of 44 % and 64 % but [C_8bumim][ReO_4] and [C_{10}bumim][ReO_4] gave poor conversions of 21 % and 2 %. This sensitivity to the C2 substituent was attributed to the hydrophilic or hydrophobic effect it has on the ionic liquid. Whilst [C_8mim][ReO_4] is completely miscible with aqueous hydrogen peroxide (50 wt %) and

[C_8dmim][ReO_4] is partially miscible (with 25 wt % of the ionic liquid dissolving), neither [C_8bumim][ReO_4] nor [C_{10}bumim][ReO_4] dissolved in the aqueous phase but formed a third layer during catalytic reactions.

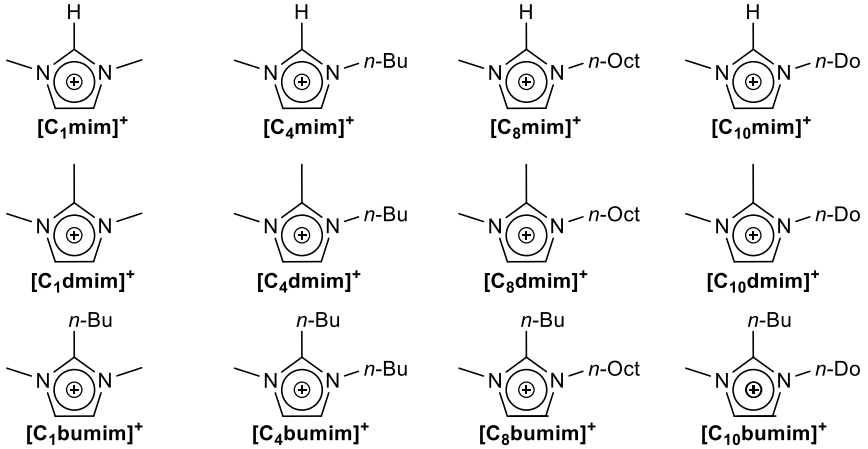

Figure 8 The series of ionic liquid cations used to synthesise the perrhenate-containing ionic liquids with abbreviations below.

Considering this solubility in the aqueous hydrogen peroxide, Kühn and coworkers investigated whether the ionic liquid catalyses the reaction in the aqueous phase or the organic cyclooctene phase. [C_8mim][ReO_4], [C_8dmim][ReO_4] and [C_8bumim][ReO_4] were all found to be poorly soluble in cyclooctene (less than 100 ppm) whereas the presence of cyclooctene in aqueous hydrogen peroxide (50 wt %) was increased from 50 ppm in the absence of ionic liquids to at least 50 times this in the presence of [C_8mim][ReO_4] and even more with [C_8dmim][ReO_4] at room temperature (as to avoid conversion of the substrate during measurement). These results strongly indicated that the reaction occurs in the aqueous phase, with the solubility of the ionic liquid being very important as it allows increased concentration of the substrate in the aqueous phase.

In addition to the low solubility of the ionic liquids in cyclooctene, we found the quantity of oxidant has a strong effect on the activity of [C_8dmim][ReO_4] (Figure 9a.). With a 5 mol % catalyst loading, aqueous hydrogen peroxide (50 wt %, 10 mmol) and cyclooctene (10 mmol), only 56.9 % conversion of the alkene was seen after 4 h (compared with 88 % with 2.5 equivalents of oxidant). No change was seen for [C_8mim][ReO_4] (Figure 9b.) and this can be attributed to its miscibility with aqueous hydrogen peroxide, whereas [C_8dmim][ReO_4] is not as soluble and a reduction of the quantity of oxidant affects its ability to dissolve into the aqueous phase and catalyse the epoxidation. However, [C_8mim][ReO_4] does also show ring opening of the epoxide to the diol after 5 h, steadily increasing over the reaction whilst [C_8dmim][ReO_4] is selective for the epoxide.

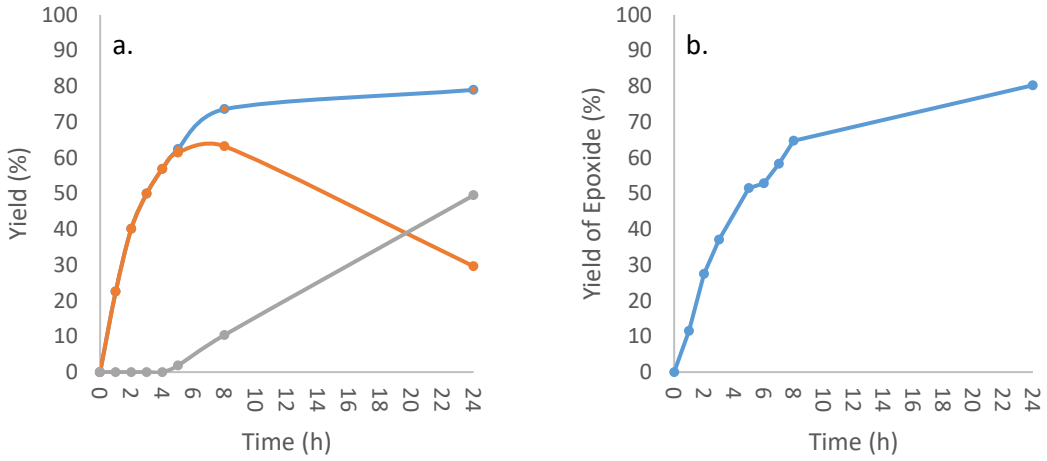

Figure 9 Graphs for the epoxidation of cyclocotene with a. [C_8mim][ReO_4] and b. [C_8dmim][ReO_4] in the presence of only 1 equivalent of hydrogen peroxide (50 wt %). 6a. shows the yield of epoxide in orange and the yield of diol in grey, with the total conversion in blue. 6b. only shows yield of epoxide as no diol was observed.

Decomposition of hydrogen peroxide in the presence of cyclooctene was found to be negligible for [C_8mim][ReO_4] and [C_8dmim][ReO_4] (less than 1 %). However, qualitative tests measuring gas (oxygen) produced by syringe show that in the absence of substrate [C_8mim][ReO_4] produced 73 cm^3 of gas after 1.5 h at 70 °C and [C_8dmim][ReO_4] only 17 cm^3 (Table 1). We noted with interest that [C_8dmim][Br] does not cause any decomposition of hydrogen peroxide under the same conditions, but [C_8mim][Br] also produced 73 cm^3 of gas, implying that the counterion is involved in the decomposition of hydrogen peroxide. As such, this may be advantageous as by selecting an appropriate ionic liquid decomposition of remaining hydrogen peroxide at the end of a reaction will facilitate in the separation of the ionic liquid from the aqueous phase in order to easily recycle the catalyst as these ionic liquids are not soluble in water.

Table 1 Volumes of gas produced after heating ionic liquids with aqueous hydrogen peroxide (50 wt %) after 1.5 h at 70 °C.

Ionic Liquid	Volume of Gas (cm^3)
[C8dmim][ReO_4]	17
[C8mim][ReO4]	73
[C8dmim][Br]	0
[C8mim][Br]	73

ESI-MS Studies of Perrhenate Containing Ionic Liquids

Considering that the SIPs were hypothesised to encourage hydrogen bonding between hydrogen peroxide and perrhenate in the organic phase (as perrhenate does not activate hydrogen peroxide in the aqueous phase), it was considered that as the reaction with these ionic liquids occurs in the aqueous phase micelles may form, providing a hydrophobic environment in which the reaction may occur. To probe this, ESI-MS was used to study $[C_8mim][ReO_4]$, $[C_4dmim][ReO_4]$ and $[C_8dmim][ReO_4]$ in hydrogen peroxide (50 wt %) using high concentrations of ionic liquid (0.7 M), similar to that used in catalytic reactions.

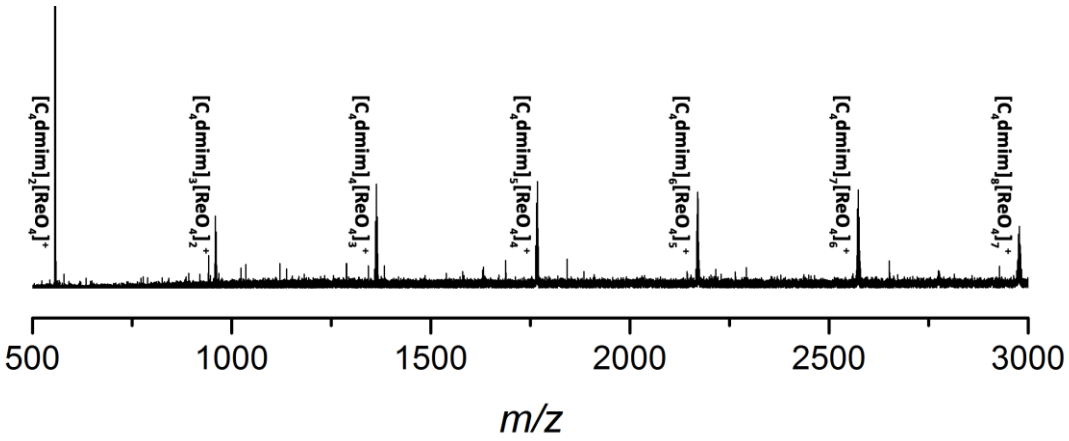

Figure 10 ESI-MS spectrum of $[C_4dmim][ReO_4]$ 0.7 M in H_2O_2 (50 wt %).

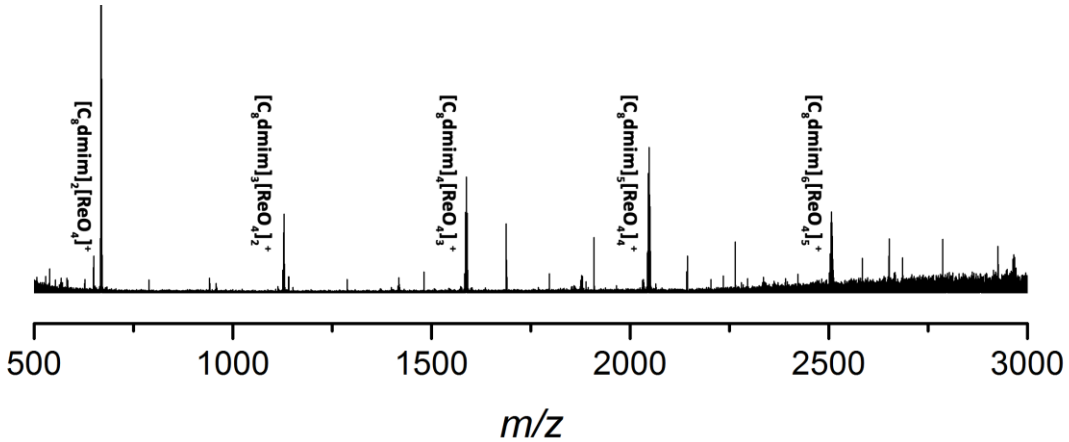

Figure 11 ESI-MS spectrum of $[C_8dmim][ReO4]$ 0.7 M in H2O2 (50 wt %).

Similarly to the SIPs, aggregates were seen for all three ionic liquids in hydrogen peroxide as has been reported with other ionic liquids.[11] The aggregates seen for $[C_4dmim][ReO_4]$ are larger (Figure 10) with the highest being $[C_4dmim]_8[ReO_4]_7^+$ whereas the largest for $[C_8dmim][ReO_4]$ is $[C_8dmim]_6[ReO_4]_5^+$ (Figure 11). Interestingly, for $[C_8dmim][ReO_4]$, the "magic number" $[C_8dmim]_5[ReO_4]_4^+$ ion was seen to be more abundant than larger and smaller aggregates (with the exception of $[C_8dmim]_2[ReO_4]^+$), which was noted by Dupont and Eberlin

as a feature of their ionic liquid ESI-MS studies.[11] They proposed that the abundance of these ions of formula $[IL]_5[A]_4^+$ (IL = ionic liquid, A = anion) in comparison to smaller aggregates was due to an increased stability for this ion; however no further details describing the origin of this stability have been reported subsequently. As ESI-MS is able to show supramolecular structures with intact hydrogen bonding, it might be expected that hydrogen peroxide should be seen within these aggregates but this does not appear to be the case for these two ionic liquids.

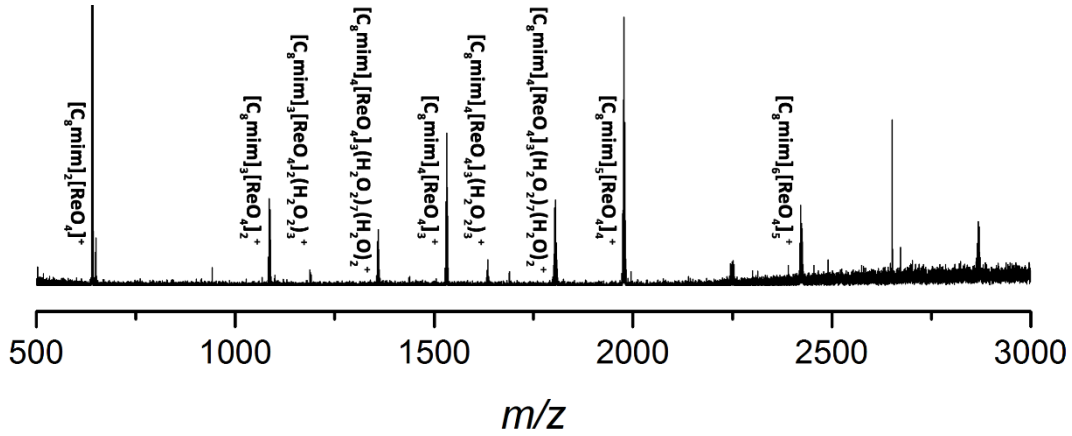

Figure 12 ESI-MS spectrum of $[C_8mim][ReO_4]$ 0.7 M in H2O2 (50 wt %).

The largest aggregate for $[C_8mim][ReO_4]$ is $[C_8mim]_7[ReO_4]_6^+$ (Figure 12), but whilst no incorporation of hydrogen peroxide is seen for the other two ionic liquids studied, this ionic liquid shows several. At 1805 and 1633 amu ions corresponding to $[C_8mim]_4[ReO_4]_3(H_2O_2)_7(H_2O)_2^+$ and $[C_8mim]_4[ReO_4]_3(H_2O_2)_3^+$ are seen. Additionally at 1359 and 1187 amu ions for $[C_8mim]_3[ReO_4]_2(H_2O_2)_7(H_2O)_2^+$ and $[C_8mim]_3[ReO_4]_2(H_2O_2)_3^+$ are present. These aggregates with hydrogen peroxide incorporation may only be visible with $[C_8mim][ReO_4]$ due to its higher solubility in aqueous hydrogen peroxide than $[C_8dmim][ReO_4]$ (no solubility measurements were taken for $[C_4dmim][ReO_4]$), therefore enabling a higher number of hydrogen bonds with hydrogen peroxide. Certainly the inclusion of up to seven hydrogen peroxide molecules in these aggregates indicates that its solubility in aqueous hydrogen peroxide is due to the ability to form a large number of hydrogen bonds. As to whether the formation of hydrophobic aggregates in the aqueous phase results in an environment for activation of hydrogen peroxide is less clear. However, considering the inactivity of perrhenate in the aqueous phase, this would appear to be a sensible mechanism through which a hydrated shell around perrhenate can be avoided to favour hydrogen bonding with hydrogen peroxide.

Other Oxo-Anion SIPs

As the high cost of rhenium makes catalytic processes based on rhenium compounds very expensive, alternatives have been sought. Considering that the perrhenate SIPs are thought to activate hydrogen peroxide through hydrogen bonds, we investigated whether the transfer of alternate oxo-anions into the organic phase (by the formation of SIPs) could achieve similar results.

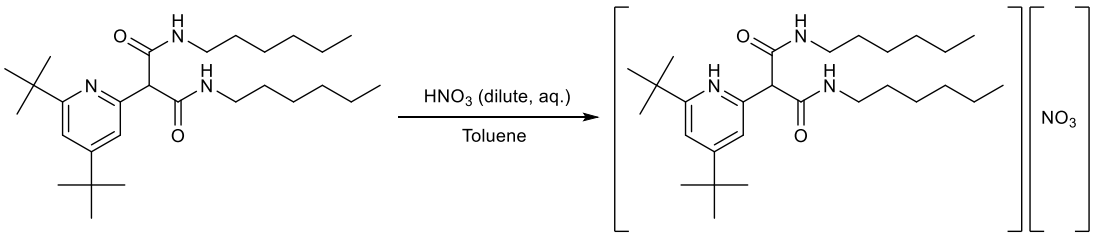

Scheme 5 Synthesis of [HL][NO_3] with dilute nitric acid.

The synthesis of [HL][NO_3] was performed by contacting a toluene solution of L with dilute nitric acid and isolating the organic phase (Scheme 5). In order to prevent exchange of ions when drying the toluene solution, $NaNO_3$ was used instead of $MgSO_4$ which did not give the same product. [HL][HSO_4] was synthesised in the same way but dried with $MgSO_4$. The solvent was removed under reduced pressure and the product dried for 16 h under high vacuum. Kühn and coworkers also attempted this synthesis of [HL][NO_3] (but not [HL][HSO_4]) although they followed the isolation of the organic phase by washing with water and found that it causes stripping of the nitric acid back into the aqueous phase.[17] As such, no washing of the product was attempted in our synthesis of [HL][NO_3].

The ^{1}H NMR spectrum (Figure 13) shows similar features to those seen for [HL][ReO_4] with two resonances for the NCH_2 protons showing the hexyl chains are split into two. Before drying under a high vacuum, the DOSY spectrum shows one species corresponding to a hydrodynamic radius of 7.0 Å which gives a spherical volume of 1437 Å^3. This volume is larger than seen for [HL][ReO_4] suggesting that water may still be present in the SIP, still strongly bound to the nitrate anion. After drying under a high vacuum, the radius of the species in the DOSY spectrum shows a reduction in size to 6.6 Å which gives a spherical volume of 1204 Å^3. Furthermore, it was discovered that when the product is left for several weeks a solid is formed, with a slight shift for the resonances in the ^{1}H NMR spectrum and presumably all of the water removed. However, due to the time taken for this process to occur and the contact the SIP would have with aqueous solutions, the SIPs were used for catalytic reactions without fully drying the product.

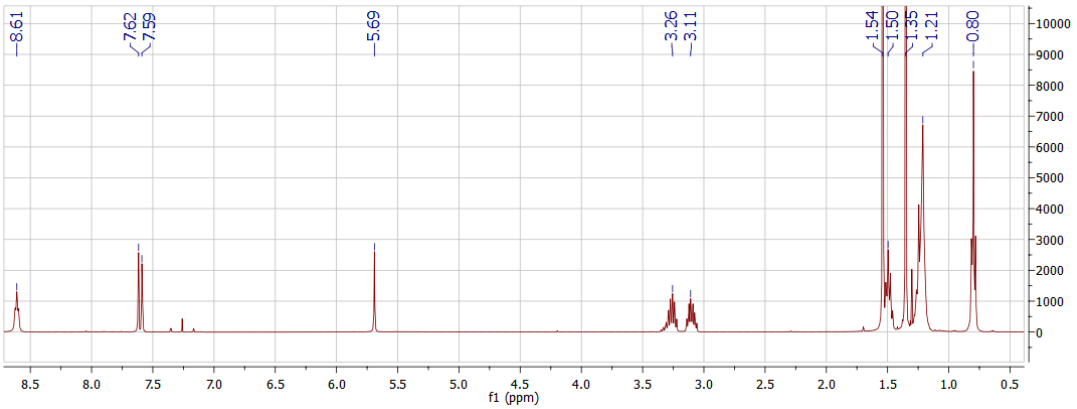

Figure 13 ^{1}H NMR spectrum of solid [HL][NO_3] product, after presumed loss of water.

Unfortunately, only a limited number of reactions were possible due to the difficulty in synthesising L on a large scale and the large quantities required for catalysis. A reaction of cyclooctene (10 mmol), aqueous hydrogen peroxide (50 % wt, 25 mmol) in the presence of [HL][NO_3] (20 mol %) with toluene (1 cm^3) showed slow conversion of the substrate into cyclooctene oxide, with 29.1 % conversion after 8 h (20.6 % epoxide and 8.5 % diol). A reaction with only 8.8 mol % catalyst loading and with less toluene (0.25 cm^3) showed a faster conversion of cyclooctene to give a conversion of 21.9 % after 5 h (17.4 % epoxide and 4.5 % diol) compared with 12.5 % with toluene with over double the catalyst loading. No further measurements for this reaction were taken but this suggests a strongly adverse effect from the addition of solvent. The large quantities of the diol are likely due to free acid catalysing the ring opening of the epoxide since washing is known to strip the receptor of nitric acid and this likely occurs under the biphasic reaction conditions as well.

Table 2 Conversion of cyclooctene using [HL][NO_3] and [HL][SO_4] SIPs at 80 °C with H_2O_2 (50 wt %).

SIP	Mol %	Toluene (cm^3)	Time (h)	Conversion (%)	Yield of Epoxide (%)	Yield of Diol (%)
[HL][NO_3]	20	1	8	29.1	20.6	8.5
[HL][NO_3]	8.8	0.25	5	21.9	17.4	4.5
[HL][SO_4]	10	1.75	7	31.5	22.4	9.1

A reaction using [HL][HSO_4] (10 mol %), cyclooctene (10 mmol) and hydrogen peroxide (50 wt %, 25 mmol) in toluene (1.75 cm^3) at 80 °C showed higher conversion after 7 h to 31.5 % (22.4 % epoxide, 9.1 % diol). As the charge on the anion is the same as $[NO_3]^-$, the difference in activity may be due to the tetrahedral anion activating the hydrogen bond more strongly than a trigonal planar anion. Results using the $[SO_4]^{2-}$ anion from our work and Kühn and

coworkers appeared to be more effective at catalysing the epoxidation and so was focussed on as the oxo-anion for all further reactions.

Whilst no mechanistic investigations were performed, we were aware that hydrogen peroxide is capable of oxidising sulfuric acid to give H_2SO_5, itself a strong oxidising agent.[18] Therefore, oxidation of the sulfate anion may also occur in this case giving $[HSO_5]^-$. $KHSO_5$ is known to oxidise ketones to dioxiranes, which subsequently are capable of oxidising alkenes to epoxides.[19] Whilst ketones are not present in these reactions to act as an oxygen transfer agent, it is worth considering direct oxidation from $[HSO_5]^-$ due to the well documented use of peroxyacids as epoxidation agents such as *meta*-chloroperoxybenzoic acic. However, given the lack of evidence for direct epoxidation by $KHSO_5$, this may be unlikely. Indeed, Redlich notes that whilst organic acids may be used to catalyse rections with hydrogen peroxide sulphuric acid does not react similarly despite H_2SO_5 being a highly reactive acid.[18]

SIP Alternatives

Similarly to $[HL''][ReO_4]$, Kühn and coworkers noticed that nitrate, sulfate and phosphonium SIPs of $[HL']^+$ and $[HL'']^+$ undergo decomposition to the corresponding amide and dihexylammonium.[17] The catalyst was therefore found to contain a mixture of the receptor and its decomposition products, although this mixture was still capable of transferring the anion into the organic phase and catalysing the epoxidation reaction. They noted that it was possible that under these conditions formaldehyde (another presumed decomposition product) may be oxidised to performic acid, itself a strong oxidising agent capable of epoxidising alkenes.[20] Therefore, the individual components of L′ and L″ (the respective amide and dihexylammonium salt) were considered as possible substitutes for the receptors that would remove the possibility of contamination with formaldehyde and so the effects of the anion could be studied. As these components are commercially available this would be an attractive simplification of the system.

$[DHA]_2[SO_4]$/$(benzamide)_2$ was found to be more active than $[DHA]_2[SO_4]$/$(3,5,5\text{-trimethylhexanamide})_2$ showing 63 % yield of cyclooctene oxide after 12 h with 20 mol % of the catalyst mixture and 2.5 equivalents of hydrogen peroxide (50 wt %) at 80 °C.[17] After 24 h the yield increased to 94 %. $[DHA]_2[SO_4]$/3,5,5-trimethylhexanamide gave a yield of 58 % after 12 h and 87 % after 24 h under the same conditions. Comparatively the mixtures of decomposed $[HL']_2[SO_4]$ and $[HL'']_2[SO_4]$ gave yields of >95 % after only 8 h, which is likely due to the involvement of performic acid.

We attempted to repeat these results, but using an alternative synthesis of $[DHA]_2[SO_4]$ was used to avoid the possibility of the presence of $[HSO_4]^-$ anions in the mixture. This was

achieved by stirring Ag_2SO_4 with two equivalents of [DHA][Br] in methanol for 6 h in the dark. The methanol solution was isolated from the precipitate and solvent removed under reduced pressure to give an off-white waxy solid. This method removes the need for washing of the material with water to remove acidic residues. Using this material under identical conditions to those mentioned above, the reaction mixture separated into three layers within 1 h. Unfortunately, this makes it difficult to take measurements during the reaction; one of the layers is largely cyclooctene and the other cyclooctene oxide/catalyst. However, there were only two layers after 24 h and could therefore be seen that a yield of 60.3 % of the epoxide was present. Further heating until 48 h gave a yield of 95.2 %. It was hoped that by adding toluene (2 cm^3) that the catalyst, substrate and product would form one phase but this was not the case. Cyclooctene oxide and the catalyst appeared to be more soluble in the central phase, with toluene present in both phases. As with $[HL][NO_3]$, toluene appears to have a retarding effect on the catalysis, with only 37.2 % yield of the epoxide after 24 h (at which point only one organic phase was present again).

Interestingly the use of $[DHA][HSO_4]$/benzamide under the same conditions gave a higher yield of 71.9 % epoxide albeit after a slightly longer reaction time of 26 h. This catalyst mixture also formed three layers after 1 h but again the two organic layers became miscible again by 26 h of heating. As both the $[DHA]_2[SO_4]$/benzamide and $[DHA][HSO_4]$/benzamide mixtures both formed two organic layers initially, the higher yield using $[DHA][HSO_4]$/benzamide may be due to the re-combination of these into one phase earlier than with $[DHA]_2[SO_4]$/benzamide. The Kühn group did find an induction period when measuring the kinetics of the $[DHA]_2[SO_4]$/benzamide catalysed epoxidation, with a steep increase in yield of cyclooctene oxide between 5 h and 6 h and a yield increase from 10 % to 41 %. This was a result of the water solubility of $[DHA]_2[SO_4]$/benzamide which switched into the organic phase due to the increase in cyclooctene oxide after 5 h.

Again, we decided to use the $[P(4,4,4,16)]^+$ counterion as the strongly hydrophobic counterion although $[P(4,4,4,16)][ReO_4]$ has cast doubt on the ability of the cation to retain the anion in the organic phase. Both $[P(4,4,4,16)][NO_3]$ and $[P(4,4,4,16)]_2[SO_4]$ were synthesised according to literature methods.[21] However, with 20 mol % catalyst loading, cyclooctene (10 mmol) and hydrogen peroxide (25 mmol, 50 wt %) at 80 °C, neither catalyst performed well with only 13.5 % conversion after 24 h for $[P(4,4,4,16)][NO_3]$ and 16.2 % for $[P(4,4,4,16)]_2[SO_4]$ after the same amount of time. After 74 h, $[P(4,4,4,16)][NO_3]$ achieved conversion of 80.9 % of the substrate but in the presence of toluene, only 38.5 % conversion was achieved after 71 h. Again this could be due to poor selectivity of anions by $[P(4,4,4,16)]^+$, with exchange occurring during the reaction.

Conclusions

Perrhenate containing SIPs show similarities to ionic liquids in solution, forming aggregates that could be studied by ESI-MS. DOSY experiments also show species sufficiently large to suggest aggregates have a relatively long lifetime in solution, although it appears that the use of more polar solvents such as acetonitrile breaks them up, possibly only showing the ion pair or more likely the organic cation separated from the ion pair. Unfortunately, even though it seems highly likely that aggregation of the SIPs occurs during the reaction, it is not clear whether this is a requirement for the activation of hydrogen peroxide. However, the use of [P(4,4,4,16)][ReO_4] shows that the cation is highly important in the reaction although no experiments were conducted to understand whether this also formed aggregates in solution. Therefore it is possible that the supramolecular structure of the SIPs is partially responsible for the activation of hydrogen peroxide.

The aggregate behaviour of the perrhenate-containing ionic liquids has also been studied in aqueous hydrogen peroxide. Work from Kühn and co-workers make it clear that the reaction occurs in the aqueous phase but previously it has been shown that perrhenate is inactive as an epoxidation catalyst in the aqueous phase. Our work shows aggregates of the ionic liquids are observed by ESI-MS, yet only in the case of [C_8mim][ReO_4] were aggregates with incorporation of hydrogen peroxide seen. This would appear to suggest that a different environment exists in the aqueous phase and hydrogen peroxide can exist within it. However, as only [C_8mim][ReO_4] shows hydrogen peroxide/ ionic liquid aggregates and is known to significantly decompose hydrogen peroxide in the absence of cyclooctene, stronger hydrogen bonding between the ionic liquid and oxidant may explain why these aggregates are seen only for [C_8mim][ReO_4] as would its higher solubility in aqueous hydrogen peroxide than [C_8-dmim][ReO_4]. Given that perrhenate is usually inactive in the aqueous phase it seems likely that these aggregates help prevent the aqueous solvation shell yet encourage hydrogen bonding with hydrogen peroxide but solvation of cyclooctene may also be important.

Efforts to replace the expensive perrhenate constituent of these catalysts has been met with mixed results. Whilst both nitrate and sulfate both show conversion of the cyclooctene substrate to cyclooctene oxide when made organic soluble by the receptor L or for sulfate the simplified hexylammonium/ benzamide system, the catalyst loadings required were very high, i.e. 20 mol %. Additionally, conversion was not high after 8 h when, in comparison, many of the perrhenate catalysts had achieved almost quantitative conversion. However, both of these systems show higher conversion than a more traditional phase transfer agent $[P(4,4,4,16)]^+$ which may not be as capable of keeping the oxo-anions in the organic phase and preventing anion exchange. Yet these metal-free catalysis results are nonetheless interesting, specifically

for the possibility they offer in replacing the expensive metal rhenium which makes these processes too expensive for large scale applications. If stripping of the anions from the organic phase can be prevented and recycling shown possible, they may prove to be a viable alternative to perrhenate systems.

References

1. W. A. Herrmann, R. W. Fischer and D. W. Marz, *Angewandte Chemie International Edition in English*, 1991, 30, 1638-1641.
2. W. A. Herrmann, R. W. Fischer, W. Scherer and M. U. Rauch, *Angewandte Chemie International Edition in English*, 1993, 32, 1157-1160.
3. M. M. Abu-Omar and J. H. Espenson, *Journal of the American Chemical Society*, 1995, 117, 272-280.
4. P. Altmann, M. Cokoja and F. E. Kühn, *European Journal of Inorganic Chemistry*, 2012, 2012, 3235-3239.
5. M. M. Abu-Omar, P. J. Hansen and J. H. Espenson, *Journal of the American Chemical Society*, 1996, 118, 4966-4974.
6. J. H. Espenson, *Chemical Communications*, 1999, 479-488.
7. M. C. A. van Vliet, I. W. C. E. Arends and R. A. Sheldon, *Journal of the Chemical Society, Perkin Transactions 1*, 2000, 377-380.
8. U. Boehner and G. Zundel, *The Journal of Physical Chemistry*, 1985, 89, 1408-1413.
9. I. I. E. Markovits, W. A. Eger, S. Yue, M. Cokoja, C. J. Münchmeyer, B. Zhang, M.-D. Zhou, A. Genest, J. Mink, S.-L. Zang, N. Rösch and F. E. Kühn, *Chemistry – A European Journal*, 2013, 19, 5972-5979.
10. M. Cokoja, I. I. E. Markovits, M. H. Anthofer, S. Poplata, A. Pothig, D. S. Morris, P. A. Tasker, W. A. Herrmann, F. E. Kuhn and J. B. Love, *Chemical Communications*, 2015, 51, 3399-3402.
11. F. C. Gozzo, L. S. Santos, R. Augusti, C. S. Consorti, J. Dupont and M. N. Eberlin, *Chemistry – A European Journal*, 2004, 10, 6187-6193.
12. N. T. Scharf, A. Stark and M. M. Hoffmann, *The Journal of Physical Chemistry B*, 2012, 116, 11488-11497.
13. X. Hu, Q. Lin, J. Gao, Y. Wu and Z. Zhang, *Chemical Physics Letters*, 2011, 516, 35-39.
14. C. M. Starks, *Journal of the American Chemical Society*, 1971, 93, 195-199.
15. R. J. Ellis, J. Chartres, K. C. Sole, T. G. Simmance, C. C. Tong, F. J. White, M. Schroder and P. A. Tasker, *Chemical Communications*, 2009, 583-585.
16. M. Cokoja, R. M. Reich, M. E. Wilhelm, M. Kaposi, J. Schäffer, D. S. Morris, C. J. Münchmeyer, M. H. Anthofer, I. I. E. Markovits, F. E. Kühn, W. A. Herrmann, A. Jess and J. B. Love, *ChemSusChem*, 2016, 9, 1773-1776.
17. S. Poplata, Masters, Technischen Universität München, 2014.
18. J. M. Monger and O. Redlich, *The Journal of Physical Chemistry*, 1956, 60, 797-799.
19. H. Tian, X. She, L. Shu, H. Yu and Y. Shi, *Journal of the American Chemical Society*, 2000, 122, 11551-11552.
20. G. Goor, in *Catalytic Oxidations with Hydrogen Peroxide as Oxidant*, ed. G. Strukul, Springer Netherlands, Dordrecht, 1992, pp. 13-43.
21. G. Cerichelli, C. La Mesa, L. Luchetti and G. Mancini, *Langmuir*, 2000, 16, 166-171.

5. Experimental

General Procedures

NMR spectra were recorded on a Bruker AVA400 spectrometer for ^{1}H (399.90 MHz); a Bruker AVA500 spectrometer ^{1}H (500.12 MHz), ^{13}C (125.76 MHz), ^{1}H DOSY, ^{1}H COSY, ^{1}H-^{13}C HMQC; a Bruker PRO500 spectrometer ^{1}H (500.23 MHz), ^{11}B (160.49 MHz), ^{29}Si (99.38 MHz), ^{31}P (202.50 MHz) or a Bruker AVA600 spectrometer ^{1}H (599.81 MHz). All chemicals were purchased from Sigma-Aldrich and used as supplied without further purification. Deuterated solvents were purchased from Cambridge Isotopes. CO_2 was supplied by BOC gases UK, labelled $^{13}CO_2$ from Cambridge Isotopes. Elemental analysis was carried out by Mr. Stephen Boyer at the London Metropolitan University, measured in duplicate.

DFT calculations were carried out using the Gaussian09 package[1] on the Edinburgh Compute and Data Facility and CompChem server systems at the University of Edinburgh. Initial guess geometries were generated from a drawn molecule using Gabedit, images of optimised geometries were made with Chemcraft. All structures in this text were optimized and converged according to the criteria for maximum displacement and force. Frequency calculations were conducted to confirm that the optimised structures represented minimum energy geometries, which were supported by having no imaginary frequencies. Transition state geometries were calculated using QST2 and QST3 features or from geometries found from potential energy scans. Specific uses of basis sets and corrections for the work studied are mentioned in their respective chapters.

Hydrosilylation and Hydroboration with Perrhenate

Synthesis of $[N(hexyl)_4][ReO_4]$

An aqueous solution of ammonium perrhenate (1.26 g, 4.7 mmol) was added to a solution of tetrahexylammonium bromide (2 g, 4.6 mmol) in chloroform (35 cm^3) and stirred for 6 h at room temperature after which the two layers were separated and the aqueous layer extracted with chloroform (2 x 10 cm^3). The combined chloroform extracts were dried over magnesium sulfate and the solvent evaporated under reduced pressure to give 2.1 g (75.4 %) of tetrahexylammonium perrhenate as a colorless solid.

^{1}H NMR (500.12 MHz; CD_3CN): δ_H (ppm) 3.07 (m, 8H, NC*H*$_2$), 1.60 (m, 8H, C*H*$_2$), 1.33 (m, 24H, C*H*$_2$), 0.91 (t, 12H, C*H*$_3$); ^{13}C NMR (125.76 MHz; CD_3CN): δ_C (ppm) 59.48 (N*C*H$_2$), 31.84 (*C*H$_2$), 26.57 (*C*H$_2$), 26.57 (*C*H$_2$), 23.10 (*C*H$_2$), 22.34 (*C*H$_2$), 14.21 (*C*H$_3$); FTIR (ATR): υ_{max}/cm^{-1} 902 (Re=O); Analysis. Calculated for $C_{24}H_{52}NO_4Re$: C, 47.66 %; H, 8.67 %; N, 2.32 %. Found: C, 47.55 %; H, 8.72 %; N, 2.38 %.

General Experimental Procedure: [N(hexyl)$_4$][ReO$_4$] catalysed hydrosilylation of carbonyl compounds

[N(hexyl)$_4$][ReO$_4$] (3 mg, 0.005 mmol, 2.5 mol %) in 0.6 cm^3 of d-solvent, phenylsilane (26 mg, 0.24 mmol), carbonyl substrate (0.2 mmol) and trimethylphenylsilane (1.7 mg, 0.01 mmol) as an internal standard were added to a Teflon tapped NMR tube. The ^{1}H NMR spectrum was recorded and then the tube was placed in a preheated oil bath (80 °C) for 10 h. The ^{1}H NMR spectrum was recorded before the reaction was hydrolysed with water (10 mg, 0.56 mmol), heated for 2 h and the ^{1}H spectrum was recorded again.

NMR data for the hydrosilylation of carbonyl compounds, Chapter 2, Table 2.Benzaldehyde

^{1}H NMR (500.12 MHz; CD_3CN): δ_H (ppm) 7.35 (m, 4 H, Ar-*H*), 7.26 (m, 1 H, Ar-*H*), 4.58 (s, 2 H, C*H*$_2$); ^{13}C NMR (125.76 MHz; CD_3CN): δ_C (ppm) 143.1 (Ar-*C*), 129.1 (Ar-*C*), 127.8 (Ar-*C*), 127.6 (Ar-*C*), 64.4 (*C*HOH).

4-Methoxybenzaldehyde

^{1}H NMR (500.12 MHz; CD_3CN): δ_H (ppm) 7.27 (d, J_{HH} = 8.8 Hz, Ar-*H*), 6.90 (d, J_{HH} = 8.8 Hz, Ar-*H*), 4.50 (s, C*H*$_2$OH), 3.77 (s, OC*H*$_3$); ^{13}C NMR (125.76 MHz; CD_3CN): δ_C (ppm) 159.8 (Ar-*C*), 135.2 (Ar-*C*), 129.3 (Ar-*C*), 114.6 (Ar-*C*), 64.3 (O*C*H$_3$), 55.8 (*C*HOH).

4-Bromobenzaldehyde

^{1}H NMR (500.12 MHz; CD_3CN): δ_H (ppm) 7.49 (d, J_{HH} = 7.5 Hz, 2 H, Ar-*H*), 7.26 (d, J_{HH} = 7.3 Hz, Ar-*H*), 4.53 (s, 2 H, C*H*$_2$); ^{13}C NMR (125.76 MHz; CD_3CN): δ_C (ppm) 142.51 (Ar-*C*), 132.11 (Ar-*C*), 129.55 (Ar-*C*), 121.03 (Ar-*C*), 63.83 (*C*HOH).

Acetophenone

^{1}H NMR (500.12 MHz; CD_3CN): δ_H (ppm) 4.81 (q, J_{HH} = 6.4 Hz, 1 H) 1.39 (d, J_{HH} = 6.5 Hz, 3 H).

4-Methoxyacetophenone

^{1}H NMR (500.12 MHz; CD_3CN): δ_H (ppm) 7.28 (d, J_{HH} = 8.6 Hz, 2 H, Ar-*H*), 6.88 (d, J_{HH} = 8.6 Hz, 2 H, Ar-*H*), 4.75 (q, J_{HH} = 6.45 Hz, 1H, C*H*OH), 1.37 (d, J_{HH} = 6.45 Hz, 3 H, CH_3).

4-Bromoacetophenone

^{1}H NMR (500.12 MHz; CD_3CN): δ_H (ppm) 7.50 (d, J_{HH} = 8.3 Hz, 2 H, Ar-*H*), 7.31 (d, J_{HH} = 8.3 Hz, 2 H, Ar-*H*), 4.81 (q, J_{HH} = 6.6 Hz, 1 H, C*H*OH), 1.39 (d, J_{HH} = 6.6 Hz, 3 H, CH_3).

Benzophenone

^{1}H NMR (500.12 MHz; CD_3CN): δ_H (ppm) 7.41 (d, J_{HH} = 7.4 Hz, 4 H, *o*-Ar-*H*), 7.33 (t, J_{HH} = 7.6 Hz, 4 H, *m*-Ar-*H*), 7.24 (t, J_{HH} = 7.6 Hz, 2 H, *p*-Ar-*H*), 5.79 (s, 1 H).

General Experimental Procedure: $[N(hexyl)_4][ReO_4]$ catalysed hydroboration of carbonyl compounds

$[N(hexyl)_4][ReO_4]$ (3 mg, 0.005 mmol, 2.5 mol %) in 0.6 cm^3 of d-solvent, carbonyl substrate (0.2 mmol) and trimethylphenylsilane (1.7 mg, 0.01 mmol) as an internal standard were added to a Teflon tapped NMR tube. The ^{1}H NMR spectrum was recorded and then the HBpin (31 mg, 0.24 mmol) was added. The ^{1}H NMR spectrum was recorded periodically to follow the reaction. The ^{1}H spectrum was recorded when the reaction showed no further signs of change.

NMR data for the hydrosilylation of carbonyl compounds, Chapter 2, Table 5.Benzaldehyde

^{1}H NMR (500.12 MHz; C_6D_6): δ_H (ppm) 7.31 (m, 2 H, *o*-Ar-*H*), 7.13 (m, 2 H, *m*-Ar-*H*), 7.00 (m, 1 H, *p*-Ar-*H*), 4.94 (s, 2 H, C*H*OB).

4-Methoxybenzaldehyde

^{1}H NMR (500.12 MHz; C_6D_6): δ_H (ppm) 7.25 (d, J_{HH} = 8.7 Hz, 2 H, Ar-*H*), 6.75 (d, J_{HH} = 8.7 Hz, 2 H, Ar-*H*), 4.92 (s, 2 H, CH_2OB), 3.29 (s, 3 H, CH_3O).

4-Bromobenzaldehyde

^{1}H NMR (500.12 MHz; C_6D_6): δ_H (ppm) 7.22 (d, J_{HH} = 8.6 Hz, 2 H, Ar-*H*), 6.93 (d, J_{HH} = 8.6 Hz, 2 H, Ar-*H*), 4.73 (s, 2 H, C*H*OB).

Acetophenone

^{1}H NMR (500.12 MHz; C_6D_6): δ_H (ppm) 7.36 (m, 2 H, Ar-*H*), 5.40 (q, J_{HH} = 6.5 Hz, 1 H, C*H*OB), 1.45 (d, J_{HH} = 6.5 Hz, 3 H, CH_3),

4-Methoxyacetophenone

^{1}H NMR (500.12 MHz; C_6D_6): δ_H (ppm) 7.29 (d, J_{HH} = 8.7 Hz, 2 H, Ar-*H*), 6.75 (d, J_{HH} = 8.7 Hz, 2 H, Ar-*H*), 5.39 (q, J_{HH} = 6.5 Hz, 1 H, C*H*OB), 3.30 (s, 3 H, CH_3O), 1.48 (d, J_{HH} = 6.5 Hz, 3 H, CH_3).

4-Bromoacetophenone

^{1}H NMR (500.12 MHz; C_6D_6): δ_H (ppm) 7.22 (d, J_{HH} = 8.5 Hz, 2 H, Ar-*H*), 6.99 (d, J_{HH} = 8.5 Hz, 2 H, Ar-*H*), 5.21 (q, J_{HH} = 6.5 Hz, 1 H, C*H*OB), 1.32 (d, J_{HH} = 6.5 Hz, 3 H, CH_3).

Benzophenone

^{1}H NMR (500.12 MHz; C_6D_6): δ_H (ppm) 7.44 (d, J_{HH} = 7.5 Hz, 2 H, *o*-Ar-*H*), 7.09 (t, J_{HH} = 7.5 Hz, 2 H, *m*-Ar-*H*), 7.01 (t, J_{HH} = 7.5 Hz, 1 H, *p*-Ar-*H*), 6.42 (s, 1 H, C*H*OB).

General Procedure for Catalytic Reactions of Hydrosilanes with CO_2

[N(hexyl)$_4$][ReO_4] (3 mg, 0.005 mmol, 2.5 mol %) in 0.6 cm^3 of d-solvent, hydrosilane (0.2 mmol) and trimethylphenylsilane (1.7 mg, 0.01 mmol) as an internal standard (unless otherwise stated) were added to a Teflon tapped NMR tube. The solution was freeze-pump-thaw degassed three times before being refilled with 1 bar CO_2. The ^{1}H NMR spectrum was recorded and then the tube was placed in a preheated oil bath (80 °C). The reactions were monitored by ^{1}H NMR spectroscopy until the hydrosilane was consumed. At this point the reaction was quenched with water (10 mg, 0.56 mmol), heated for 2 h and the ^{1}H NMR spectrum recorded.

General Procedure for Catalytic Methylations of Amines with Hydrosilanes and CO_2

$[N(hexyl)_4][ReO_4]$ (3 mg, 0.005 mmol, 2.5 mol %) in 0.6 cm^3 of CD_3CN, diphenylsilane (147 mg, 0.8 mmol), amine (0.2 mmol) and trimethylphenylsilane (1.7 mg, 0.01 mmol) as an internal standard (unless otherwise stated) were added to a Teflon tapped NMR tube. The solution was freeze-pump-thaw degassed three times before being refilled with 2 bar CO_2. The ^1H NMR spectrum was recorded and then the tube was placed in a preheated oil bath (80 °C). The reactions were heated for 2 h followed by assessment of conversion and yield of the methylated product by ^1H NMR spectroscopy.

NMR data for methylation of amines:

$CH_3N^iPr_2$: ^1H NMR (599.81 MHz; CD_3CN): δ_H (ppm) 2.94 (sept, J_{HH} = 6.5 Hz, 2 H, C*H*$(CH_3)_2$), 2.16 (s, 3 H, NC*H*$_3$), 1.04 (d, J_{HH} = 6.5 Hz, 12 H, CH(C*H*$_3)_2$).

$(CH_3)_2N^iPr$: ^1H NMR (599.81 MHz; CD_3CN): δ_H (ppm) 2.59 (spet, J_{HH} = 6.5, 1 H, C*H*$(CH_3)_2$), 2.20 (s, 6 H, NC*H*$_3$), 1.02 (d, J_{HH} = 6.5 Hz, 6 H, CH(C*H*$_3)_2$).

$CH_3N(CH_2)_4$: ^1H NMR (599.81 MHz; CD_3CN): δ_H (ppm) 2.41 (m, 4 H, NC*H*$_2$,), 2.30 (s, 3 H, NC*H*$_3$), 1.74 (m, 4 H, C*H*$_2$).

$CH_2(PhNH)_2$: ^1H NMR (500.12 MHz; CD_3CN): δ_H (ppm) 7.24 (m, 4 H, *m*-Ar-*H*), 6.87 (m, 4 H, *o*-Ar-*H*), 6.76 (m, 2 H, *p*-Ar-*H*), 4.78 (s, 2 H, C*H*$_2$), 2.86 (s, 6 H, NC*H*$_3$); ^{13}C NMR (125.76 MHz; CD_3CN): δ_C (ppm) 123.0 (*m*-Ar), 118.6 (*p*-Ar), 114.8 (*o*-Ar), 70.9 (*C*H$_2$), 37.0 (N*C*H$_3$).

$PhN(CH_3)_2$: ^1H NMR (500.12 MHz; CD_3CN): δ_H (ppm) 2.91 (s, 6 H, NC*H*$_3$); ^{13}C NMR (125.76 MHz; d_3-MeCN): δ_C (ppm) 40.9 (N*C*H$_3$).

NMR data for Hydroboration of CO_2

^1H NMR (500.12 MHz; C_6D_6): δ_H (ppm) 8.13 (s, *H*C(O)OBpin), 7.41 (s, 1 H, *H*C(O)OCH$_2$OBpin) 5.48 (s, C*H*$_2${OBpin}), 5.39 (s, 2H, HC(O)OC*H*$_2$OBpin), 3.51 (s, *H*$_3$COBpin).

Single crystals were grown by slow diffusion of hexane into a C_6D_6 solution of $[N(hexyl)_4][ReO_4]$

	j15075_twin_twin1_hklf4
Crystal data	
Chemical formula	$ORe_{0.25}{\cdot}C_6H_{12.73}N_{0.25}$
M_r	151.22
Crystal system, space group	Monoclinic, *C*2/*m*
Temperature (K)	170
a, *b*, *c* (Å)	10.1264 (3), 11.2062 (4), 13.0777 (10)
β (°)	101.892 (5)
V (Å^3)	1452.19 (13)
Z	8
Radiation type	Mo *K*α
μ (mm^{-1})	4.21
Crystal size (mm)	0.72 × 0.39 × 0.02
Data collection	
Diffractometer	Xcalibur, Eos
Absorption correction	Multi-scan *CrysAlis PRO*, Agilent Technologies, Version 1.171.37.35 (release 13-08-2014 CrysAlis171 .NET) (compiled Aug 13 2014,18:06:01) Empirical absorption correction using spherical harmonics, implemented in SCALE3 ABSPACK scaling algorithm. Empirical absorption correction using spherical harmonics, implemented in SCALE3 ABSPACK scaling algorithm.
T_{min}, T_{max}	0.339, 1.000
No. of measured, independent and observed [$I > 2\sigma(I)$] reflections	15481, 1913, 1453
R_{int}	0.088
$(\sin\theta/\lambda)_{max}$ (Å^{-1})	0.686
Refinement	
$R[F^2 > 2\sigma(F^2)]$, $wR(F^2)$, *S*	0.040, 0.079, 0.97
No. of reflections	1913
No. of parameters	136
H-atom treatment	H-atom parameters constrained
$\Delta\rangle_{max}$, $\Delta\rangle_{min}$ (e Å^{-3})	1.00, -0.39

Deoxydehydration

General Procedure for the DODH reaction

Styrene diol (27.6 mg, 0.2 mmol) was added to a 0.6 cm^3 C_6D_6 solution of the catalyst (2.5 mol %), PPh_3 (76 mg, 0.29 mmol) and 2-methylnaphtalene (8.5 mg, 0.06 mmol) as an internal reference in a Teflon tapped NMR tube. A ^1H NMR spectrum was recorded before placing the NMR tube in a pre-heated oil bath (80 °C) for 16 h after which another ^1H NMR spectrum and ^{31}P spectrum would be recorded.

Synthesis of $[H_3N(hexyl)][ReO_4]$

Perrhenic acid (76.5 %, 0.3 cm^3) was added to neat hexylamine (204 mg, 2 mmol) which immediately reacted to give a solid. This product was suspended in hexane (10 cm^3), filtered, washed with hexane (3 x 5 cm^3) and dried under reduced pressure to give the white solid (551 mg, 77.6 %).

^1H NMR (500.12 MHz; CD_3CN): δ_H (ppm) 6.35 (t, J = 53 Hz, 3 H, H_3N), 2.95 (m, 2 H, NCH_2), 1.61 (quint, 2 H, CH_2), 1.31 (m, 6 H, $\{CH_2\}_3$), 0.90 (t, 3 H, CH_3); ^{13}C NMR (125.76 MHz; CD_3CN): δ_C (ppm) 41.3 (NCH_2), 31.3 (CH_2), 27.6 (CH_2), 26.4 (CH_2), 23.0 (CH_2), 14.1 (CH_3); FTIR (ATR): υ_{max}/cm^{-1} 889 (Re=O); Analysis. Calculated for $C_6H_{16}NO_4Re$: C, 20.45 %; H, 4.58 %; N, 3.97 %. Found: C, 20.51 %; H, 4.62 %; N, 4.01 %.

Synthesis of $[H_2N(hexyl)_2][ReO_4]$

Perrhenic acid (76.5 %, 0.15 cm^3) was added to neat dihexylamine (194 mg, 1 mmol) which immediately reacted to give a solid. This product was suspended in hexane (10 cm^3), filtered, washed with hexane (2 x 5 cm^3) and dried under reduced pressure to give the white solid (284 mg, 62.2 %).

^1H NMR (500.12 MHz; CD_3CN): δ_H (ppm) 6.59 (br, 2 H, H_2N), 2.96 (m, 4 H, NCH_2), 1.64 (quint, 4 H, CH_2), 1.32 (m, 12 H, $\{CH_2\}_3$), 0.90 (t, 6 H, CH_3); ^{13}C NMR (125.76 MHz; CD_3CN): δ_C (ppm) 49.2 (NCH_2), 31.8 (CH_2), 26.6 (CH_2), 26.58 (CH_2), 23.0 (CH_2), 14.2 (CH_3); FTIR (ATR): υ_{max}/cm^{-1} 888 (Re=O).

Synthesis of $[HN(hexyl)_3][ReO_4]$

Perrhenic acid (76.5 %, 0.15 cm^3) was added to neat trihexylamine (272 mg, 1 mmol) then dissolved in toluene (10 cm^3) and dried with $MgSO_4$. The solvent was removed under reduced pressure to afford the oil (352 mg, 67.8 %).

^{1}H NMR (500.12 MHz; CD_3CN): δ_H (ppm) 6.60 (br, 1 H, *H*N), 2.96 (m, 6 H, NC*H*$_2$), 1.64 (quint, 6 H, C*H*$_2$), 1.32 (m, 18 H, {C*H*$_2$}$_3$), 0.90 (t, 9 H, C*H*$_3$); ^{13}C NMR (125.76 MHz; CD_3CN): δ_C (ppm) 49.2 (N*C*H$_2$), 31.8 (*C*H$_2$), 26.6 (*C*H$_2$), 26.58 (*C*H$_2$), 23.0 (*C*H$_2$), 14.2 (*C*H$_3$); FTIR (Thin Film): υ_{max}/cm^{-1} 915 (Re=O).

Synthesis of [Lut][ReO_4]

Perrhenic acid (77 %, 0.15 cm^3) was added to neat 2,6-lutidine (122 mg, 1.1 mmol) and stirred for 1 h. The aqueous phase was removed, the oil dissolved in ethanol (10 cm^3) and the solvent removed under reduced pressure to give a white solid and dried under a high vacuum further for 16 h (295 mg, 78.4 %).

^{1}H NMR (599.81 MHz; $CDCl_3$): δ_H (ppm) 15.12 (br, 1 H, N*H*), 8.21 (t, J_{HH} = 7.9 Hz, 1 H, *p*-Ar-*H*), 7.56 (d, J_{HH} = 7.9 Hz, 2 H, *m*-Ar-*H*), 2.88 (s, 6 H, C*H*$_3$); ^{13}C NMR (125.76 MHz; $CDCl_3$): δ_C (ppm) 154.1 (*C*CH$_3$), 145.7 (*m*-Ar), 124.9 (*p*-Ar), 20.4 (*C*H$_3$).

Synthesis of [DTBMP][ReO_4]

Perrhenic acid (77 %, 0.15 cm^3) was added to a solution of 2,6-ditertbutyl-4-methylpyridine (225 mg, 1.1 mmol) in toluene (6 cm^3), from which a white precipitate formed. The solution was stirred for 1 h before filtering and washing with hexane (2 x 10 cm^3). The solid was dried under reduced pressure for 16 h to give the white product (370 mg, 73.9 %).

^{1}H NMR (500.12 MHz; CD_3CN): δ_H (ppm) 7.72 (s, 2 H, *m*-Ar-*H*), 2.61 (s, 3 H, C*H*$_3$), 1.50 (s, 18 H, ^{t}Bu); ^{13}C NMR (125.76 MHz; CD_3CN): δ_C (ppm) 163.0, 162.9, 124.1,37.3 (*C*H$_3$), 28.9 (^{t}Bu).

Synthesis of [ClPy][ReO_4]

Perrhenic acid (77 %, 0.15 cm^3) was added to neat 2-chloropyridine (126 mg, 1.1 mmol) and the mixture stirred for 1 h, over which time a white solid formed. The organic product was extracted into dichloromethane and dried with $MgSO_4$. The solvent was removed under reduced pressure to give a white solid (254 mg, 62.7 %).

^{1}H NMR (500.12 MHz; CD_3CN): δ_H (ppm) 8.53 (m, 1 H), 8.24 (m, 1 H), 7.80 (m, 1 H), 7.71 (m, 1 H).

Crystal Structure of $[H_3N(hexyl)][ReO_4]$

Single crystals of $[H_3N(hexyl)][ReO_4]$ were grown by slow diffusion of hexane into a C_6D_6 solution.

	j15022
Crystal data	
Chemical formula	$O_4Re{\cdot}C_6H_{16}N$
M_r	352.40
Crystal system, space group	Monoclinic, $P2_1/c$
Temperature (K)	100
a, b, c (Å)	14.9581 (4), 7.5570 (2), 9.3623 (3)
β (°)	107.339 (3)
V (Å^3)	1010.21 (5)
Z	4
Radiation type	Mo $K\alpha$
μ (mm^{-1})	12.01
Crystal size (mm)	0.81 × 0.11 × 0.06
Data collection	
Diffractometer	Xcalibur, Eos
Absorption correction	Analytical *CrysAlis PRO*, Agilent Technologies, Version 1.171.37.34 (release 22-05-2014 CrysAlis171 .NET) (compiled May 22 2014,16:03:01) Analytical numeric absorption correction using a multifaceted crystal model based on expressions derived by R.C. Clark & J.S. Reid. (Clark, R. C. & Reid, J. S. (1995). Acta Cryst. A51, 887-897) Empirical absorption correction using spherical harmonics, implemented in SCALE3 ABSPACK scaling algorithm.
T_{min}, T_{max}	0.950, 0.994
No. of measured, independent and observed [$I > 2\sigma(I)$] reflections	18942, 2314, 2147
R_{int}	0.044
$(\sin\theta/\lambda)_{max}$ (Å^{-1})	0.649
Refinement	
$R[F^2 > 2\sigma(F^2)]$, $wR(F^2)$, S	0.016, 0.038, 1.09

No. of reflections	2314
No. of parameters	111
H-atom treatment	H-atom parameters constrained
$\Delta\rangle_{max}$, $\Delta\rangle_{min}$ (e Å^{-3})	0.70, -1.02

Epoxidation of Alkenes with Oxo-Anions

The SIPs [HL][ReO_4], [HL′][ReO_4], [HL″][ReO_4] and ionic liquids [C_4dmim][ReO_4], [C_8dmim][ReO_4], [C_8mim][ReO_4], [C_8dmim][Br], [C_8mim][Br] were donated to us by the Kühn group for studies on their solution structure and preliminary studies on the hydrogen peroxide decomposition effected by the ionic liquids. L, [P(4,4,4,16)][NO_3] and [P(4,4,4,16)]$_2$[SO_4] were synthesised according to literature procedures.[2, 3]

General Catalysis Procedure

Cyclooctene (1.1 g, 10 mmol), hydrogen peroxide (50 wt. %, 1.42 cm^3, 25 mmol) and catalyst (2 mmol) were combined and heated at 80 °C with stirring. Samples were taken from the organic layer hourly to monitor by ^{1}H NMR spectroscopy. (In the cases where there are two organic layers, both were sampled.)

Synthesis of [HL][NO_3]

L (500 mg, 1.1 mmol) in toluene (5 cm^3) was stirred with dilute nitric acid (1 cm^3) for 16 h at room temperature. The organic layer was separated from the aqueous layer, dried with $NaNO_3$ and the solvent removed under reduced pressure to give an oil that was used without further purification (463 mg, 81.4 %).

^{1}H NMR (500.12 MHz; C_6D_6): δ_H (ppm) 9.45 (br, 1 H, pyridinium-N*H*), 8.36 (s, 1 H, Ar-*H*), 7.12 (s, 1 H, Ar-*H*), 6.37 (s, 1 H, C*H*(CO)$_2$), 3.49 (m, 1 H, amide-N*H*), 3.33 (m, 1 H, amide-N*H*), 1.66 (m, 4 H, NHC*H*$_2$), 1.21 (m, 12 H, {C*H*$_2$}$_3$), 1.07 (s, 9 H, ^{t}Bu), 1.06 (s, 9 H, ^{t}Bu), 0.83 (t, 6 H, C*H*$_3$).

Synthesis of [HL][HSO_4]

L (965 mg, 2.1 mmol) in toluene (10 cm^3) was stirred with sulfuric acid (0.4 cm^3, 6 M) for 16 h at room temperature. The organic layer was separated from the aqueous layer, dried with $MgSO_4$ and the solvent removed under reduced pressure to give an oil that was used without further purification (850 mg, 79.7 %).

^{1}H NMR (500.12 MHz; $CDCl_3$): δ_H (ppm) 8.42 (br, 1 H, pyridinium-N*H*), 8.11 (s, 1 H, Ar-*H*), 7.58 (s, 1 H, Ar-*H*), 5.59 (s, 1 H, C*H*$(CO)_2$), 3.29 (m, 1 H, amide-N*H*), 3.18 (m, 1 H, amide-N*H*), 1.57 (m, 4 H, NHC*H*$_2$), 1.57 (s, 9 H, ^{t}Bu), 1.43 (s, 9 H, ^{t}Bu), 1.26 (m, 12 H, {C*H*$_2$}$_3$), 0.84 (t, C*H*$_3$).

Synthesis of $[H_2N(hexyl)_2][HSO_4]$

Dihexylamine (6.5 g, 35 mmol) in toluene (100 cm^3) was stirred with sulfuric acid (10 cm^3, 7 M) for 16 h at room temperature. The organic layer was separated from the aqueous layer, dried with $MgSO_4$ and the solvent removed under reduced pressure to give an waxy solid (7.56 g, 76.3 %).

^{1}H NMR (500.12 MHz; $CDCl_3$): δ_H (ppm) 8.62 (br, 2 H, *H*$_2$N), 2.97 (m, 4 H, NC*H*$_2$), 1.78 (m, 4 H, C*H*$_2$), 1.31 (m, 12 H, {C*H*$_2$}$_3$), 0.89 (t, 6 H, C*H*$_3$).

Synthesis of $[H_2N(hexyl)_2]_2[SO_4]$

[DHA][Br] (10.2 g, 38.3 mmol) was stirred with $AgSO_4$ (16.76 g, 53.7 mmol) in methanol (300 cm^3) in the dark for 6 h at room temperature. The solids were filtered off and the solvent removed from the solution under reduced pressure to give an off white waxy solid (8.29 g, 93.7 %).

^{1}H NMR (500.12 MHz; $CDCl_3$): δ_H (ppm) 8.62 (br, 2 H, *H*$_2$N), 2.83 (m, 4 H, NC*H*$_2$), 1.80 (m, 4 H, C*H*$_2$), 1.27 (m, 12 H, {C*H*$_2$}$_3$), 0.86 (t, 6 H, C*H*$_3$).

Synthesis of $[P(4,4,4,16)][ReO_4]$

[P(4,4,4,16)][Br] (994 mg, 2 mmol) in chloroform (10 cm^3) was stirred with an aqueous solution (10 cm^3) of $[NH_4][ReO_4]$ (541 mg, 2 mmol) for 6 h at room temperature. The organic phase was separated from the aqueous and the aqueous phase extracted with chloroform (2 x 5 cm^3). The combined chloroform solutions were dried with $MgSO_4$ and the solvent removed under reduced pressure to give a white solid (858 mg, 63.2 %).

^{1}H NMR (599.81 MHz; $CDCl_3$): δ_H (ppm) 2.21 (m, 8 H, PC*H*$_2$), 1.54 (m, 16 H, C*H*$_2$), 1.25 (m, 24 H, C*H*$_2$), 0.9 (t, 9 H, C*H*$_3$), 0.87 (t, 3 H, C*H*$_3$).

Crystal Structure of L

Single crystals were grown by slow evaporation of a $CDCl_3$ solution of L.

	SHELX
Crystal data	
Chemical formula	$C_{28}H_{47}Cl_0N_3O_2$
M_r	457.68
Crystal system, space group	Triclinic, $P\bar{1}$
Temperature (K)	170
a, *b*, *c* (Å)	10.2025 (3), 11.0813 (4), 13.7978 (5)
α, β, γ (°)	103.506 (3), 91.764 (3), 104.334 (3)
V (Å^3)	1463.06 (9)
Z	2
Radiation type	Mo *K*α
μ (mm^{-1})	0.07
Crystal size (mm)	1.07 × 0.83 × 0.31
Data collection	
Diffractometer	Xcalibur, Eos
Absorption correction	Multi-scan *CrysAlis PRO*, Agilent Technologies, Version 1.171.37.34 (release 22-05-2014 CrysAlis171 .NET) (compiled May 22 2014,16:03:01) Empirical absorption correction using spherical harmonics, implemented in SCALE3 ABSPACK scaling algorithm. Empirical absorption correction using spherical harmonics, implemented in SCALE3 ABSPACK scaling algorithm.
T_{min}, T_{max}	0.547, 1.000
No. of measured, independent and observed [$I > 2\sigma(I)$] reflections	45821, 6693, 4636
R_{int}	0.047
$(\sin\theta/\lambda)_{max}$ (Å^{-1})	0.649
Refinement	
$R[F^2 > 2\sigma(F^2)]$, $wR(F^2)$, *S*	0.093, 0.273, 1.02
No. of reflections	6693
No. of parameters	298
H-atom treatment	H-atom parameters constrained
$\Delta\rangle_{max}$, $\Delta\rangle_{min}$ (e Å^{-3})	0.85, -0.43

References

1. M. J. Frisch, G. W. Trucks, H. B. Schlegel, G. E. Scuseria, M. A. Robb, J. R. Cheeseman, G. Scalmani, V. Barone, B. Mennucci, G. A. Petersson, H. Nakatsuji, M. Caricato, X. Li, H. P. Hratchian, A. F. Izmaylov, J. Bloino, G. Zheng, J. L. Sonnenberg, M. Hada, M. Ehara, K. Toyota, R. Fukuda, J. Hasegawa, M. Ishida, T. Nakajima, Y. Honda, O. Kitao, H. Nakai, T. Vreven, J. A. Montgomery Jr., J. E. Peralta, F. Ogliaro, M. J. Bearpark, J. Heyd, E. N. Brothers, K. N. Kudin, V. N. Staroverov, R. Kobayashi, J. Normand, K. Raghavachari, A. P. Rendell, J. C. Burant, S. S. Iyengar, J. Tomasi, M. Cossi, N. Rega, N. J. Millam, M. Klene, J. E. Knox, J. B. Cross, V. Bakken, C. Adamo, J. Jaramillo, R. Gomperts, R. E. Stratmann, O. Yazyev, A. J. Austin, R. Cammi, C. Pomelli, J. W. Ochterski, R. L. Martin, K. Morokuma, V. G. Zakrzewski, G. A. Voth, P. Salvador, J. J. Dannenberg, S. Dapprich, A. D. Daniels, Ö. Farkas, J. B. Foresman, J. V. Ortiz, J. Cioslowski and D. J. Fox, *Gaussian, Inc.*, Wallingford CT, 2009.
2. R. J. Ellis, J. Chartres, D. K. Henderson, R. Cabot, P. R. Richardson, F. J. White, M. Schröder, J. R. Turkington, P. A. Tasker and K. C. Sole, *Chemistry – A European Journal*, 2012, 18, 7715-7728.
3. G. Cerichelli, C. La Mesa, L. Luchetti and G. Mancini, *Langmuir*, 2000, 16, 166-171.